Dynamic analysis and characterization of a Desorption column for a continuous air capture process

Ved Shrivallabh Dubhashi

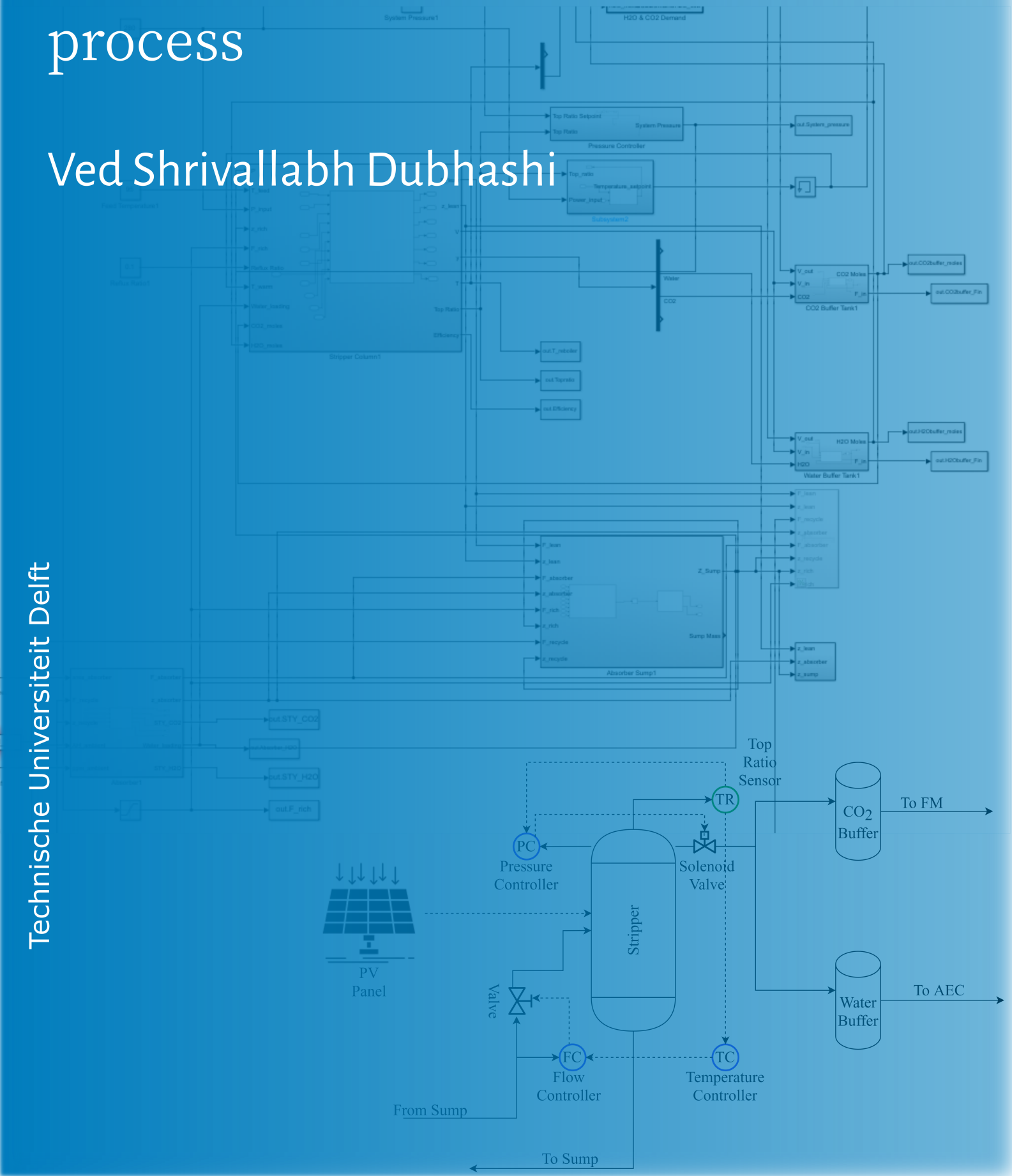

Technische Universiteit Delft

Delft University of Technology

Dynamic Analysis and Characterization of a Desorption column for a Continuous Air Capture process

Author:
Ved Shrivallabh Dubhashi

To obtain the degree of Master of Science
at the Delft University of Technology,
to be defended publicly on Monday, August 30, 2021 at 13:00.

Student Number:	5096995
Supervisor:	Prof. dr. ir. E. Goetheer, TU Delft
Daily supervisor:	Ir. M. Sinha, ZEF BV
Committee:	Prof. dr. ir. E. Goetheer, TU Delft, Chairman Prof. dr. ir. B. J. Boersma, TU Delft Prof. dr. ir. A. Urakawa, TU Delft Ir. M. Sinha, ZEF BV

This thesis is confidential and cannot be made public until August 30, 2023

TU Delft Delft University of Technology

विकृतिः एवम् प्रकृति

vikrtiḥ ēvam prakrti

What seems unnatural is also natural

Rig Veda

Abstract

The world is currently in the middle of an energy crisis, with a growing demand for energy playing catch up with an increasing population. The problem stems from the fact that we rely heavily on fossil fuels to meet our energy needs, and the combustion of these fuels are the primary source of greenhouse gas emissions. An accelerated rate of emissions of greenhouse gases has led and continues to lead to an increase in the average temperature of the planet, stated: Global Warming.

Shifting the balance in our favour requires arresting and lowering our emissions. Direct air capture of Carbon dioxide is one solution that has garnered massive traction in the global scientific community. Zero Emission Fuels is a visionary start-up operating out of Delft that aims to build a micro-plant capable of producing methanol using energy derived from the sun and raw material (CO_2 and H_2O) harnessed from the atmosphere. The heart of their concept is liquid amine-based direct air capture. ZEF has pioneered the continuous process that involves the simultaneous absorption and desorption of CO_2 and water as the amine circulates from the absorber to the desorption column.

The raw material and the energy to drive the process is harnessed from the environment. Thus these inputs remain outside the control of the ZEF system and are treated as external disturbances. This research aims to analyse the impact of the varying environmental conditions, i.e. the ambient temperature, absolute humidity and incident solar radiation, on the performance of the desorption column. Following which a control scheme is developed to ensure the system meets the requirements of ZEF, i.e. production of CO_2 and water in a 3:1 molar ratio and an energy consumption limit of 450 kJ/mol of CO_2 desorbed.

Firstly, a set of experiments with a trayed stripping column were performed to understand the start-up and shut-down behaviour of the column. Based on the observations, a simplistic model of the reboiler was developed to predict the transient behaviour of the column during start-up. A sensitivity analysis was carried out to gain insights into the parameters influencing start-up time and energy demand. Furthermore, different scenarios to start up a column were identified and based on the results, the batch mode is adopted as the efficient way to start up a column. The model predicts that start-up and shut-down account for less than 10% of the total operating time available. Moreover, start-up accounts for a maximum of 6% of the total available energy for production.

Secondly, a set of single-stage kinetic experiments were performed at different temperatures to understand the limitations of the desorption process inside the column. A vapour-liquid equilibrium based stage-by-stage model of a desorption column integrated with a varying space-time yield based absorber model. Design parameters of the integrated DAC model were tweaked, and a base case was developed, to understand the impact of a varying sorbent composition and PV panel output on the performance of the DAC subsystem. It was clear the open model was not capable of meeting the 3:1 top ratio specifications of ZEF. Which prompted the implementation of control structures.

Single loop mass-flow control, pressure control and cascade mass flow-temperature control schemes were individually tested with the aid of the integrated DAC model. Finally, based on the performance of the individual control schemes, a final parallel control scheme was developed. Wherein the temperature and the pressure of the system adjusts according to the varying power input and the absolute humidity conditions that impact the top ratio of products. The parallel control scheme was found to be adequate in maintaining the top ratio at desired levels.

Acknowledgements

Ineffable is perhaps the word to capture the nature of my emotions at the moment. The journey that began two years ago has been one of rediscovery—rediscovering my love for science, a thirst for knowledge rediscovering myself when all seemed lost. I made several mistakes; I learned lessons, friendships were forged, and some old ones were lost. Although overcoming these tribulations have helped me grow as a person, none of this would have been possible without the aegis of dear ones far and near.

Firstly, I thank Zero Emission Fuels for this opportunity of working on my thesis with them and for letting me be a part of the conducive learning environment that ensures no (wo)man is left behind. ZEF continues to accumulate a treasure trove of inspiring stories and knowledge that I shall always cherish.

This thesis would not be a reality if it weren't for the constant guidance from Mrigank Sinha. Your discipline inspired me to push myself beyond what I felt was possible. Your ability to articulate and break down complex problems helped me see beyond the obvious. Thank you for having faith in my abilities at a time where I lacked self-belief. Thank you for being a kind-hearted mentor and always having the perfect things to say for every moment.

A person with immense knowledge that is only surpassed by his humility is Jan van Kranendonk. Thank you for having the patience to clarify the innumerable doubts I've had during my thesis. You've taught me the importance of accountability and the need to take ownership. Debugging code with a cup of tea will not be the same without you.

Ulrich Starke, thank you for engaging with me in conversations not limited to my work at ZEF. Your work ethic and propensity for order motivated me to strive to carve a sense of rationality and punctuality in my life. Your advice has been a balanced source of reason and emotions that, has to date, held me in good stead.

Thank you, Hessel Jongebreur, for helping the entire ZEF team keep the ship steady and asking the most insightful questions during the sprint presentations. Your experience and insights are a stroke of brilliance.

Professor Earl Goetheer, you've been a beacon of enlightenment since the beginning of my thesis. Thank you for being my thesis chair and nudging me in the right direction on the occasions I was stuck. Your approach towards challenges has instilled a new belief in me that it is okay to have more questions than answers. Thank you for offering crucial feedback at every meeting that helped sharpen my focus and zeal to perform better than before.

I want to express gratitude to my blueprints- my parents. You are the reason I stand here today. Thank you for your unconditional love and support. Thank you for ensuring that I do not feel the lack of anything and imparting good values. I dedicate this thesis to you.

Ashna Ghosh, in this sea of variables, you've been my constant over the last two years. Thank you for your patience, understanding and companionship through thick and thin. Thank you for the endless conversations that helped me expand my perspective and made me strive to be a better version of myself.

Nikhil and Sharon, thank you for being my home away from home. Nishant, Teja, Abhirath Sowmya, thank you for having my back and convincing me that the glass is indeed half full. Life in Delft would have been incomplete without your companionship. Our relationship continues to age like fine wine to Judy, Vrushab, Maryam Radhesh; your unbridled support has helped me maintain my sanity in dark times.

In the end, I'd like to seek comfort in knowing that this is not the end but just the beginning of a new phase filled with challenges and adventure.

Contents

List of Figures

List of Tables

Nomenclature

General Parameters

A_{cross}	Cross flow passage area	m^2
A_c	Collector area	m^2
w	Mass fraction	wt%
x	Liquid phase mole fraction	-
y	Vapour phase mole fraction	-
c	Molar concentration	mol/m^3
C_p	Specific heat capacity	$J/kg{\cdot}K$
D	Diffusion coefficient	m^2/s
d	Diameter	m
d_i	Inner diameter	m
d_o	Outer diameter	m
F	Feed mass flow rate	mol/s
f	Friction coefficient	
G	Solar radiation intensity	W/m^2
h	Convective heat transfer coefficient	$W/m^2 \cdot K$
h	Molar enthalpy	J/mol
$H_{absorption}$	Heat of absorption	kJ/mol
H	Henry's constant	$mol/m^3 \cdot Pa$
I	Current	A
z	Feed mole fraction	-
k	Thermal conductivity	$W/m{\cdot}K$
A	Additional mass flow rate	mol/s
D	Distillate flow rate	mol/s
K	K value	-
L	Liquid mass flow rate	mol/s
l	Length	m

$\dot{m}$	Mass flow rate	kg/s
t	Time	s
N	Number of stages	-
V_B	Boil-up ratio	-
V	Volume flow rate	m^3/s
N	Number of moles	moles
P	Pressure	N/m^2
P_{abs}	Absolute pressure	N/m^2
p	Partial pressure	N/m^2
q	Heat flux	W/m^2
Q	Heat duty	Watts
R	Thermal resistance	$K{\cdot}m^2/W$
R	Reflux ratio	-
R	Universal gas constant	$J/mol{\cdot}K$
r	Reaction rate	$mol\ {\cdot}s/m^3$
T	Temperature	K
T_r	Reference temperature	K
u_{mean}	Mean velocity	m/s
V	Vapor mass flow rate	mol/s
V	Voltage	Volts
V	Volume	m^3
W	Power	Watt

Greek Letters

α	Relative volatility	
β	Fraction that is vaporised	
Δ	Difference	
δ	Thickness of layer	m
ϵ	Emissivity	
η	Efficiency	
η_{r}	Reference solar cell efficiency	
γ	Activity coefficient	
κ	Boltzmann constant	$1.381 \times 10^{-23}\ J/K$
Λ	Wilson's parameter	
μ	Viscosity	$Pa{\cdot}s$

ϕ	Fugacity	
ρ	Density	kg/m^3
σ	Stefan Boltzmann constant	$5.670 \times 10^{-8}\ W/(m^2 \cdot K^4)$
τ	Transmission coefficient	
θ	Angle in degrees	
φ	Volume fraction	

Dimensionless Numbers

Nu	Nusselt number
Pe	Peclet number
Pr	Prandtl number
Re	Reynolds number

Subscripts

absorber	Absorber stream
absorption	Absorption
ambient	Ambient
conv	Convection
desorption	Desorption
in	Input
isc	Short circuit
lean	Lean loading stream
load	Electric load
out	Output
panel	PV Panel
rad	Radiation
recycle	Recycle stream
ref	Reference coefficient
sensible	Sensible heating
stripper	Stripper stream
v	volumetric

Table 1: List of molecular structures used in this work including their description.

Molecular structure	Description
CaCO	Calcium Oxide
$CaCO_3$	Calcium Carbonate
$Ca(OH)_2$	Calcium Hydroxide
CH_3OH	Methanol
CO	Carbon Monoxide
CO_2	Carbon Dioxide
H_2	Hydrogen
HCO_3^-	Bicarbonate
H_2O	Water
K_2CO_3	Potassium Carbonate
KOH	Potassium Hydroxide
NaOH	Sodium Hydroxide
O_2	Oxygen
$R_1R_2NCOO^-$	Carbamate
R_1R_2NH	Secondary amine
$R_1R_2NH^+COO^-$	Zwitterion

Table 2: List of abbreviations used in this work including their description.

Abbreviation	Description
AEC	Alkaline Electrolysis Cell
ANN	Artificial Neural Network
CCS	Carbon Capture and Storage
CCU	Carbon Capture and Utilisation
DAC	Direct Air Capture
DEEA	Diethanolamine
DS	Distillation
FM	Fluid Machinery
FTIR	Fourier-transform infrared spectroscopy
HEX	Heat Exchanger
HT	High Temperature
LT	Low Temperature
MEA	Mono-ethanolamine
MeOH	Methanol
MS	Methanol Synthesis
SIT	Specific Ion Interaction Theory
PEG	Polyethylene Glycol TEPA
Tetraethylpentamine	
TSA	Temperature Swing Absorption
VLE	Vapor-liquid equilibrium
ZEF	Zero Emission Fuels

Chapter 1

Introduction

1.1 Global Warming

The world is currently in the middle of an energy crisis, with a growing demand for energy playing catch up with an increasing population. The problem stems from the fact that we rely heavily on fossil fuels to meet our energy needs [1]. This skewed dependence on petroleum and other fossil fuels as our primary energy sources puts our planet in jeopardy as we are consuming these resources at a pace much faster than nature can replace them. Moreover, fossil fuel combustion is the primary source of greenhouse gas (GHG) emissions. The scientific community has been aware of the heat-trapping abilities of GHGs since the industrial revolution; unfortunately, our lifestyles and the corporate greed necessary to sustain said lifestyle has led to an accelerated rate of emission of GHGs. This sustained release of greenhouse gases into the atmosphere traps an increasing amount of the terrestrial radiation emitted by the Earth at night, compounding the Greenhouse effect which leads to an overall increase in the average temperature of the planet or simply stated: Global warming.

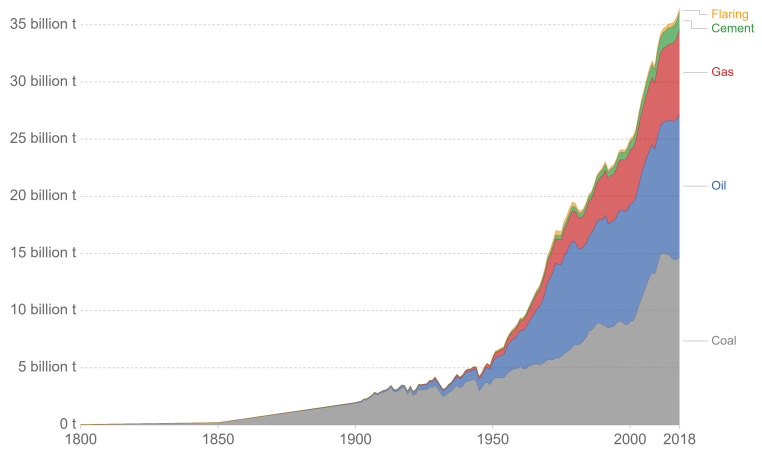

Figure 1.1: Global CO_2 emissions by source [1]

Historically the Earth has undergone shifts in its temperature in alternating warm and cold periods, primarily due to slight variations in the Earth's orbit. Nevertheless, these changes have occurred throughout a millennium not in a matter of decades as is the case today. Moreover, data suggests that human emissions add excess carbon dioxide to the atmosphere at an unprecedented rate , compared to natural sources while taking the last ice age as a reference [2].

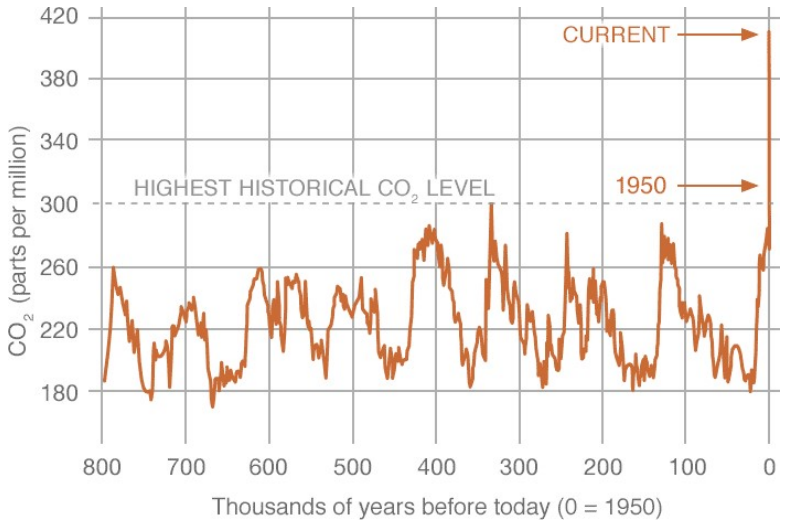

Figure 1.2: Historical variation of CO_2 levels [3]

1.1.1 Evidence

Since the industrial revolution, as a consequence of human activities, the concentration of carbon dioxide in the atmosphere has increased by 47% compared to pre-industrial levels with 1850 as the base year [4]. The Climate Action Tracker (CAT), is a collaboration between Climate Analytics and New Climate institute. They have estimated that our actions have increased the global average temperature by 1.1°C as of September 2020 [5]. This engenders the question, why are we so concerned with increasing temperatures, what are the consequences of global warming?

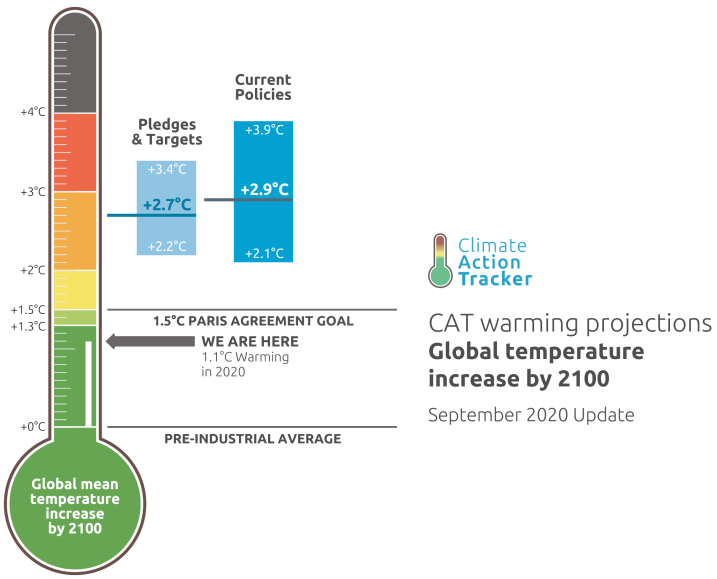

Figure 1.3: Current increase in average global temperature [5]

As temperatures increase the polar ice caps melt and release a large amount of freshwater into the oceans contributing to rising sea levels. Ecosystems in the polar regions are fragile, melting of icecaps has pushed flora and fauna in this region to endangerment. The rising sea levels are a significant cause of concern for island nations and coastal cities. The ocean currents are changing due to being inundated with ice-cold water; this has contributed to more potent weather phenomenon like the El

Nino and increased the strength of the Indian Ocean Dipole (IOD). The Australian bush fires resulted from lack of rainfall in the region due to the changing nature of the IOD. [6].

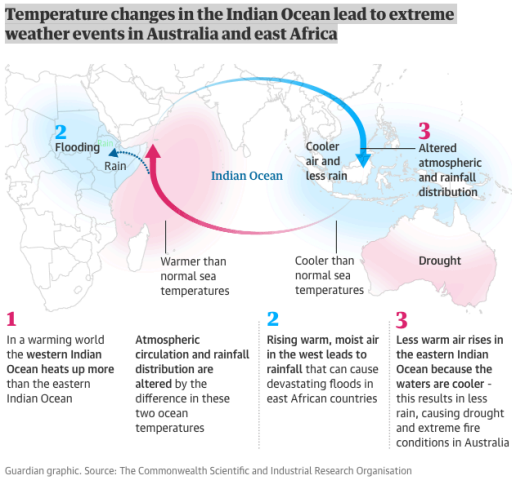

Figure 1.4: Schematic of the Indian ocean dipole

1.1.2 Mitigation

Firstly, a sincere and coordinated effort between all the nation-states of the world is necessary for combatting the effects of climate change. Half a decade ago, every nation on the planet decided to be a part of the collective effort to (ideally) stop climate change caused through anthropogenic emissions in its tracks by signing the Paris Agreement [7]. A landmark agreement, which was devoid of the usual haggling between developed and developing nations. Each country was given free rein to set their targets, and draw a road map to achieve those targets via legally binding INDCs or Intended Nationally Determined Contributions. The Paris agreement essentially aims at limiting global temperature increase to 2°C by the end of this century, and if possible, to within 1.5°C. The number of signatories today stands at 197 [5].

Secondly, to accomplish the Paris agreement goals, **the net CO_2 emissions need to be almost half of 2010 levels by the year 2030 and reach net zero emissions by 2050** [8]. Naturally this requires an overhaul of our economic system and our energy sources. Over the last few decades, there has been a steady shift towards adopting renewable sources of energy.

With the amount of incoming solar radiation we receive every hour greater than the annual consumption globally, harnessing solar power has received a lot of importance. It is primed to be a viable alternative source of energy. Manufacturers of wind turbines are pioneering better and bigger designs to harness the wind's power. The scientific community is moving towards identifying alternatives for space heating and cooling since a significant amount of energy in the residential sector is utilised for making our environment suitable for living. Ground-based heat pumps, thermal storage using phase change materials, vapour absorption-based refrigeration systems driven by solar energy are upcoming alternatives for space heating or cooling. **Currently, 24% of the global electricity demand is derived from sustainable forms of energy. To achieve net-zero emissions by 2050 this number has to go up to 86%, which requires a cumulative average growth rate of 3.8**% [9].

Electricity is a high-grade form of energy. Depending on the source, it is classified as a green alternative. We must increase the share of electricity use in consumer activities aiming for massive electrification at the grassroots level to minimise emissions. Unfortunately, some sectors of our economy at this stage cannot be electrified completely, for example, commercial aviation, shipping, road transport. [9].

1.2 Carbon Neutral Methanol

Conventionally methanol is manufactured from syngas (a combination of CO and hydrogen). Methanol is currently used as a feedstock for a large number of process industries [10]. A blend of methanol and conventional gasoline can be used as fuel for vehicles and other combustion-related processes. Ongoing research focuses on methanol production using greener alternatives for feedstock, such as direct air capture methods, and conversion of the captured CO_2 into methanol using the following reaction.

$$CO_2 + 3\,H_2 \longleftrightarrow CH_3OH + H_2O$$

This nascent technology currently requires a large amount of energy to produce methanol. Still, it is possible to design processes which source the raw materials needed, i.e., CO_2 and H_2 via renewable energy, thereby making it a reliable candidate as a green fuel. Some efficient methods of achieving this are :

- Photo-chemical [11] conversion of methane produced via microbial action or bio-methane.
- Electrochemical reduction [12] of CO_2 using electrical energy derived from renewable sources.

However, with current technology, the cost of methanol [13] synthesis using direct air capture methods makes it economically unviable. Ongoing research and improved regulations such as a carbon tax will exert a upward push on synthetic methanol's price over the next decade.

1.3 Zero Emission Fuels

Zero Emission Fuels B V (ZEF) is a visionary start-up operating out of Delft. ZEF focuses on building a micro-plant capable of producing methanol using energy derived from the sun and raw material harnessed from the atmosphere. The significant advantage of building micro plants is the ease of construction, lower capital cost and faster dynamics of the setup process. Photovoltaic panels, will convert the incident solar energy into electrical energy, the latter is used to supply power to the micro-plant. A large number of these micro-plants will work together to produce methanol during the day.

1.3.1 The ZEF Method

The methanol production at ZEF can be divided into six subsystems as shown in Figure 1.5 – Direct Air Capture (DAC) system, Fluid Machinery (FM), Alkaline Electrolysis Cell (AEC), Methanol Synthesis Reactor (MSR), Distillation unit and the solar panel. The DAC system is responsible for capturing the CO_2 & H_2O from the atmosphere. The DAC process can be divided into absorption and desorption components. In the former, atmospheric air is made to interact with a flowing sorbent, the CO_2 and H_2O are absorbed into the lean sorbent through chemical reactions. The loaded sorbent is pumped into the desorber. Here at high temperatures the CO_2 and H_2O are stripped from the rich sorbent. The lean sorbent is recirculated back to the absorber, while the lighter products from the system are sent to the FM and AEC systems respectively.

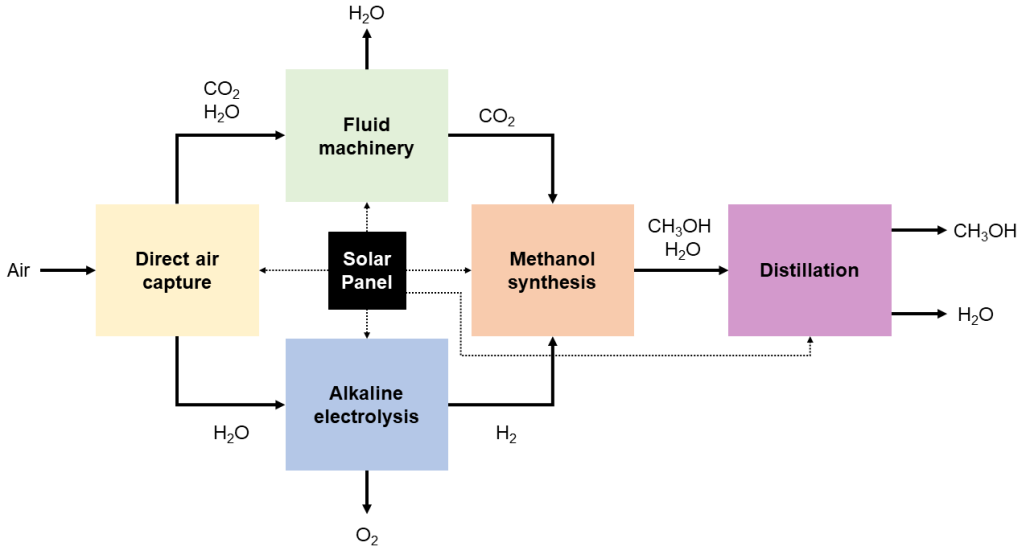

Figure 1.5: A schematic overview of the five subsystems in the ZEF process.

The CO_2 entering the FM system is dried first using a desiccant and then compressed to the desired pressure for use in the MSR. The water entering the AEC undergoes electrolysis and is split into hydrogen and oxygen gas. The former is sent to the MSR, and the latter is purged to the atmosphere. The MSR produces methanol from the aforementioned reaction, and the product is sent to the distillation unit to separate the methanol from water and enhance the purity.

1.3.2 ZEF:Key Performance Indicators

To evaluate the performance of the desorption column, a set of key performance indicators have been identified by ZEF, and are highlighted in Table 1.1

Table 1.1: Key performance indicators identified by ZEF

Key Performance Indicator	**ZEF Design Specification**	**Reason**
Optimal top ratio of stripper products	3:1 (P_{H_2O}:P_{CO_2})	The chemical reaction for the production of methanol , requires 3 Moles of Hydrogen (from H_2O) and 1 Mole of CO_2 to produce 1 mole of Methanol. Thus a 3:1 molar ratio requirement.
Operating pressure of the stripper column	Minimum 1 bar. Higher pressures possible.	Limit set by ZEF.
Operating temperature of the stripper column	Upper limit of 120 Celsius.	Upper limit is decided by the thermal degradation properties of the current sorbent.
Energy Consumption	<450 kJ/mol CO_2	Limit set by ZEF.
Production rate of CO_2	6.55e-4 mol/s	ZEF requirement : 600 grams of methanol per day. Assuming the plant operates for 8 hours a day, the system needs to produce 18.75 moles of CO_2.
Production rate of H_2O	1.965e-3 mol/s	56.25 moles of H_2O needed to meet production demand.

1.4 Aim of this thesis

The raw material and the energy to drive the process is harnessed from the environment. The inputs for the process are:

- **Solar radiation :** The incident solar radiation is converted into electrical energy by PV panels to run the micro-plant. The amount of solar radiation depends on the time of day, location and the season.
- **Atmospheric CO_2 :** The concentration of CO_2 in the atmosphere is 410 ppm on an average, although this is increasing slowly.
- **Atmospheric H_2O:** The absolute humidity indicates the water concentration in the atmosphere, and it varies significantly over short time intervals depending on the time of day, location and the season.

It is expected that **fluctuations in the concentration of H_2O and in the amount of incident solar radiation will impact the production capacity and the operation window of ZEF's system**.
Therefore, the focus of this research is to **analyse the impact of the varying environment conditions i.e. the ambient temperature, absolute humidity and incident solar radiation on the performance of the desorption column, following which a control scheme is developed to ensure the system meets the requirements of ZEF.** Stripping presents a multi-variable problem, which requires a keen analysis of external and internal parameters that will impact the performance of the stripper.

1.5 Research Objectives

This thesis's primary aim is to understand the dynamic response of a stripper column to fluctuations in the inputs. To tackle this, the task at hand has been sub-divided into a set of research questions.

1. What is the impact of varying environmental conditions (disturbances: relative humidity, temperature and solar radiation) **on the inputs to the desorption column**?.
2. What is the impact of start-up and shut-down on the operation window of the desorption column? What are the factors influencing the start-up of the column ?
3. What is the impact of varying environmental conditions (disturbances: relative humidity, temperature and solar radiation)on the performance (outputs) of the desorption column?
4. What is the limiting step for desorption of CO_2 from the TEPA-PEG sorbent mixture?
5. What are the optimal design conditions for a continuous desorption process that meets ZEF's requirements?

1.6 Scope of Thesis

The field of direct air capture and the work being done at ZEF is boundless, thus it is essential to create an outline that demarcates the extents of this thesis. The scope of the current work is elaborated as follows:

- The desorption experiments conducted make use of quaternary blend of TEPA-PEG-H_2O-CO_2. **This sorbent mixture is decided by the sorbent selection team of ZEF, based on specific criteria aligned with the objectives of ZEF.**
- **The experimental and modelling focus will be limited to the desorption process.** Although we will try to understand the desorption column's influence on other parts of the overall system, no experiments will be carried out related to absorption, distillation or electrolysis.
- The experimental work carried out is limited to the analysis of the start-up & shut down behaviour of the column, including insights on the chemical kinetics of the desorption process. **No experiments were carried out related to emulate the fluctuating dynamics of the environment.** This was achieved majorly through Simulink modelling.

An overview of the report is presented in Figure 1.6.

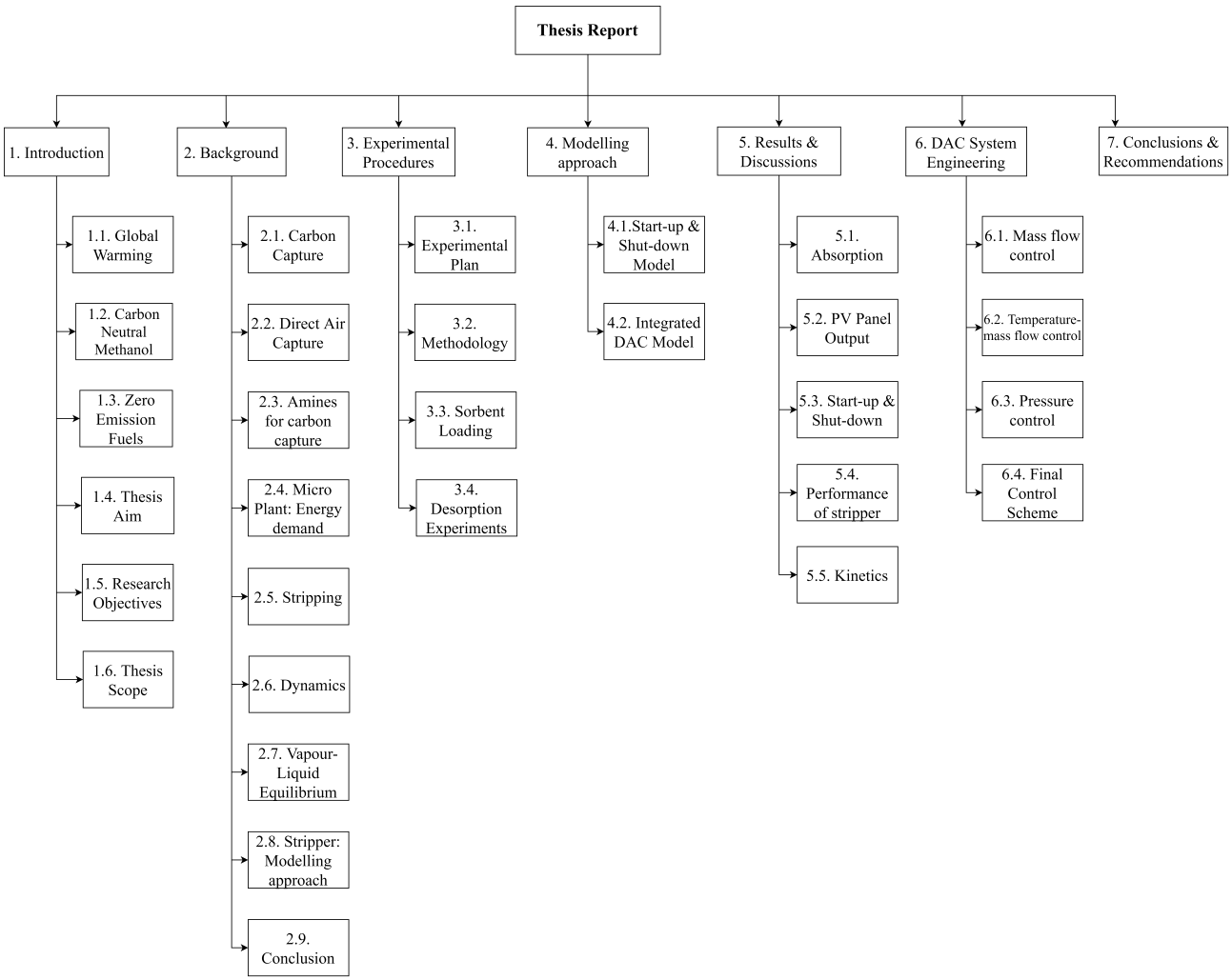

Figure 1.6: A schematic overview of the report.

Chapter 2

Background

This chapter provides a succinct overview of the background knowledge that ties in with this thesis's goals, the flow of the chapter is depicted in Figure 2.1. Firstly, a run-through of carbon capture technologies is provided coupled with insights on the state of the art of direct air capture. Next, the section dives into the chemistry and selection criteria associated with liquid amine sorbents and provides the basis for the sorbents used in this work. Third, stripper functioning is introduced, followed by an explanation of energy consumption in a stripper column and the importance of dynamics. Fourth, the process of desorption is explained by using essential vapour and VLE curve data. Also, kinetics' role in designing a stripper column is discussed. In the end, a concise summary is provided.

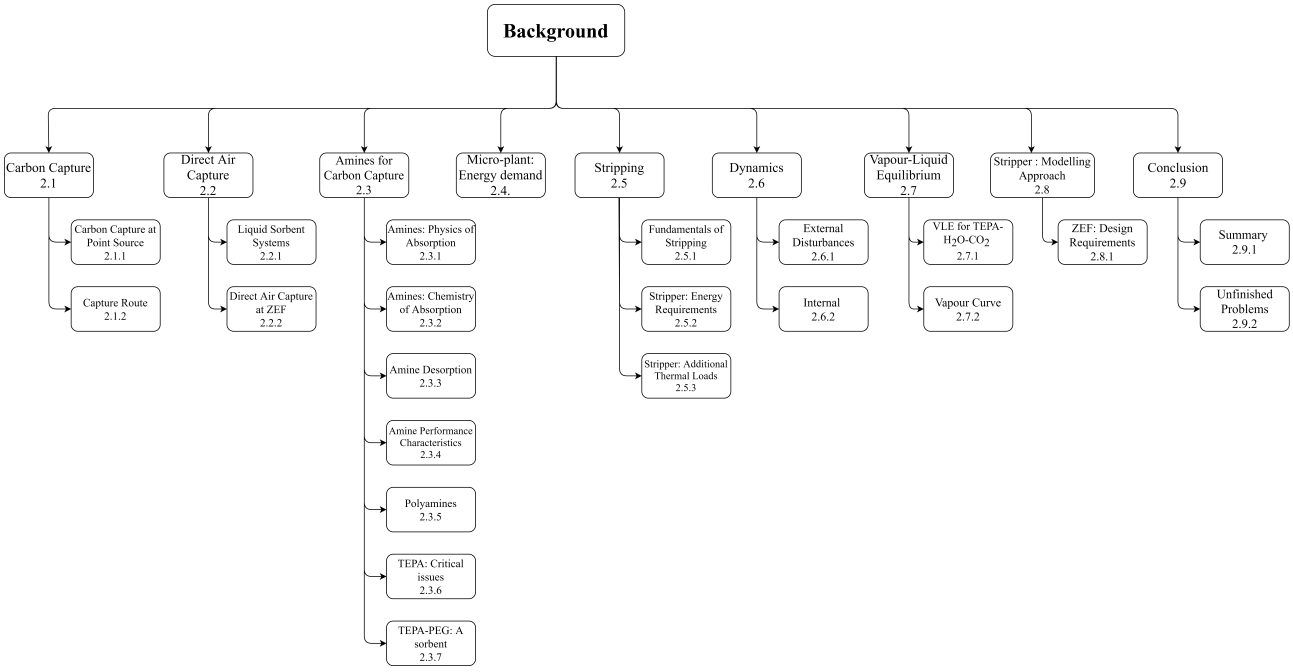

Figure 2.1: Schematic depicting the flow of the background chapter.

2.1 Carbon Capture

Carbon capture can be divided into two categories depending upon the purpose and end-use: Carbon Capture Storage (CCS) and Carbon Capture & Utilization (CCU) [14]. Recent studies have investigated the possibility of storing CO2 in depleted oil and gas fields [15]. The latter case deals with converting the captured carbon as an alternative input to carbon-based process industries.

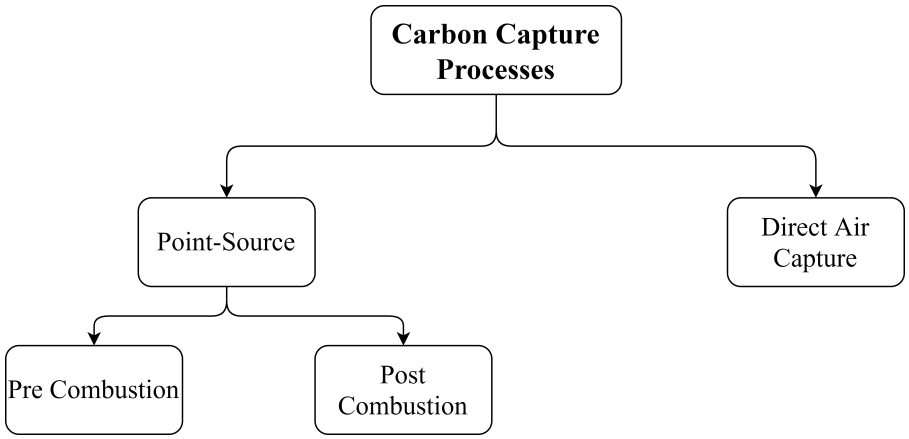

Figure 2.2: Schematic of different carbon capture methods currently being explored

Based on the source carbon capture is classified into point source and direct air capture as shown in Figure 2.2, discussed in the following sections.

2.1.1 Carbon Capture at Point Source

Capturing carbon dioxide from point sources with a relatively high concentration of CO_2 is economical [16]. Most of our CO_2 emissions result from combustion or gasification processes in cement manufacturing, oil refining, plastics moulding, and the treatment of natural gas and iron & steel making industries. Point source capture is further classified depending on the approach as:

Post Combustion Capture

When CO_2 is captured from a waste gas stream or flue gas generated due to combustion of carbon-based fuels such as oil, natural gas coal is referred to as post-combustion capture as shown in Figure 2.3. The primary advantage here is the ability to retrofit the carbon capture system to existing power plants. Naturally, this comes at the cost of efficiency [16].

Pre-Combustion Capture

Capturing the CO_2 before the fuel undergoes combustion is called pre-combustion capture. A carbon-based fuel (eg.coal) is subjected to gasification resulting in synthesis gas (CO+ H_2O). This product mixture is made to undergo the water gas shift reaction resulting in a gaseous mixture predominant in CO_2 and hydrogen. The CO_2 is captured and separated, while the hydrogen is used for combustion [17].

Oxy-Fuel Combustion

A carbon-based fuel undergoes combustion in the presence of a stream of pure oxygen instead of air. The flue gases are recycled to maintain the flame temperature to minimise NOx emissions. The resulting gaseous mixture contains CO_2 and H_2O, and the former is captured and separated while the H2O is condensed. The sourcing of pure oxygen via air separation is costly; thus, making this method prohibitively expensive with current separation technology [17] .

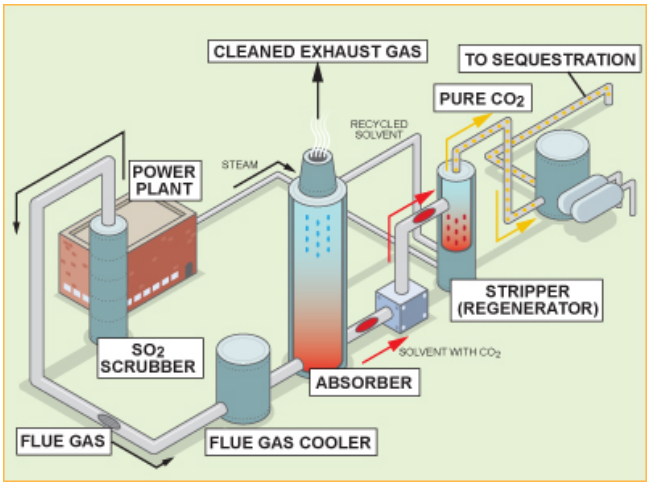

Figure 2.3: Schematic of conventional post combustion capture process [18]

2.1.2 Capture Route

Carbon capture can be achieved via absorption, adsorption, membrane separation or cryogenic separation as indicated in Figure 2.4. Albeit this work deals with desorption of CO2; it is vital to understand the absorption route for carbon capture [19].

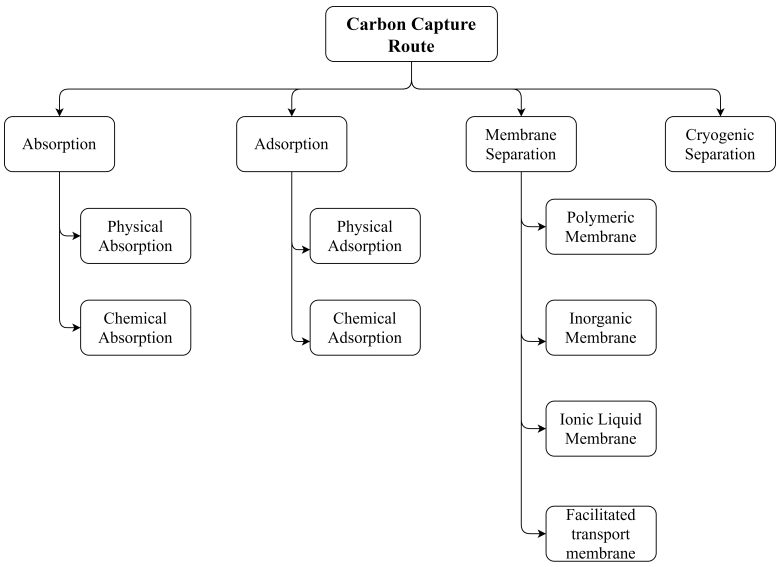

Figure 2.4: Schematic of carbon capture routes.

Absorption

Absorption is a bulk phenomenon; the absorbate diffuses into the absorbent bulk. It is a process by which a gas can be separated from a gaseous mixture using a solvent. Absorption is further classified into physisorption and chemisorption based on the nature of bonds made between the absorbent and absorbate.

- In physical absorption, the bonds are formed due to weak Van der Waals forces between the different molecules. The behaviour can be modelled using Henry's Law. The gas is absorbed at high partial pressures, and desorbed at lower partial pressures. The driving force for absorption is the partial pressure, thus the loading and unloading cycle can be established using pressure

swing methods (Figure 2.5), which requires lesser energy. But, it is not suitable for direct air capture, since the partial pressure of CO_2 in air is low.

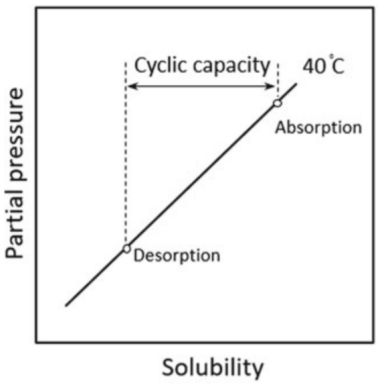

Figure 2.5: Relation between solubility and partial pressure for physical absorption [19]

- Chemisorption is a result of chemical bonds forming at reactive sites on the absorbent, independent of the component's pressure and is thus more suitable for low-pressure applications as in the case of direct air capture [20]. Recovering the sorbent entails shifting the vapour-liquid equilibrium by increasing the temperature as shown in Figure 2.6, or decreasing the pressure, or a combination of both. Naturally, this costs more energy. But, the chemical reactions are highly selective in nature, and thus a better separation of gases can be obtained as compared to physical absorption.

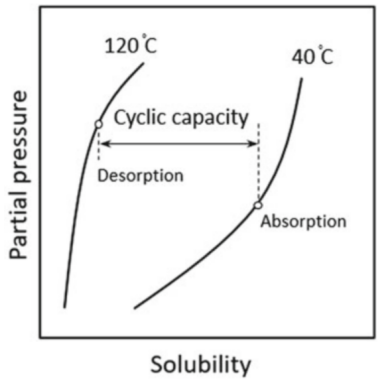

Figure 2.6: Relation between solubility and partial pressure for chemical absorption [19]

Note: Adsorption and membrane separation as carbon capture routes are briefly discussed in Appendix A.

2.2 Direct Air Capture

In some cases, point source carbon capture is not feasible for example, emissions from the agricultural and animal rearing industry, but it is essential to develop a method that can capture these emissions since food production accounts for 25% of the global greenhouse gas emissions [21]. Direct air capture, a novel technology focused on capturing carbon dioxide directly from the ambient air, is one way to reduce these emissions [22].

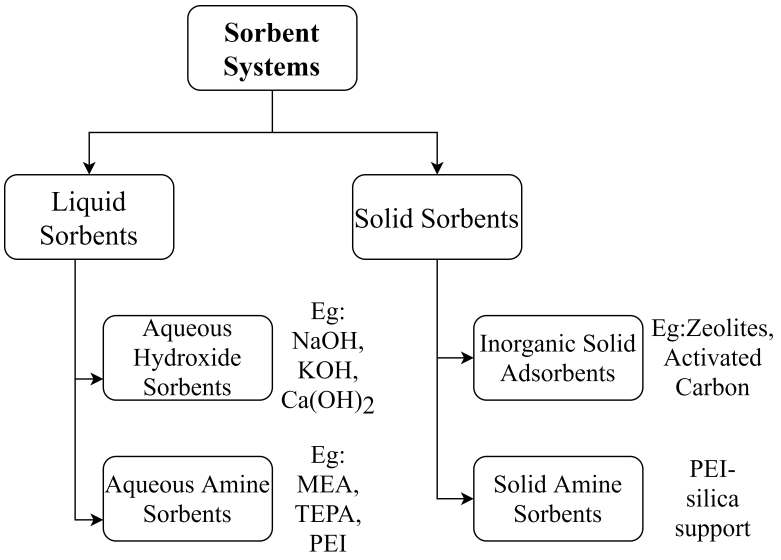

Figure 2.7: Classification of sorbent systems

2.2.1 Liquid Sorbent Systems

Liquid sorbent systems conventionally comprise two major components: an absorber and desorber [23]. In the absorber, incoming air contacts a flowing sorbent, which allows the CO_2 to react with the sorbent and absorb into the sorbent. **Before absorption, the sorbent has a low concentration of CO_2 and is referred to the as lean sorbent. Post absorption, the sorbent has higher concentrations of CO_2 it is called as rich or loaded sorbent.** The rich sorbent enters the desorber, where a change in temperature, pressure or a combination of the two shifts the VLE causing the CO_2 to desorb from the sorbent. This is called solvent regeneration.

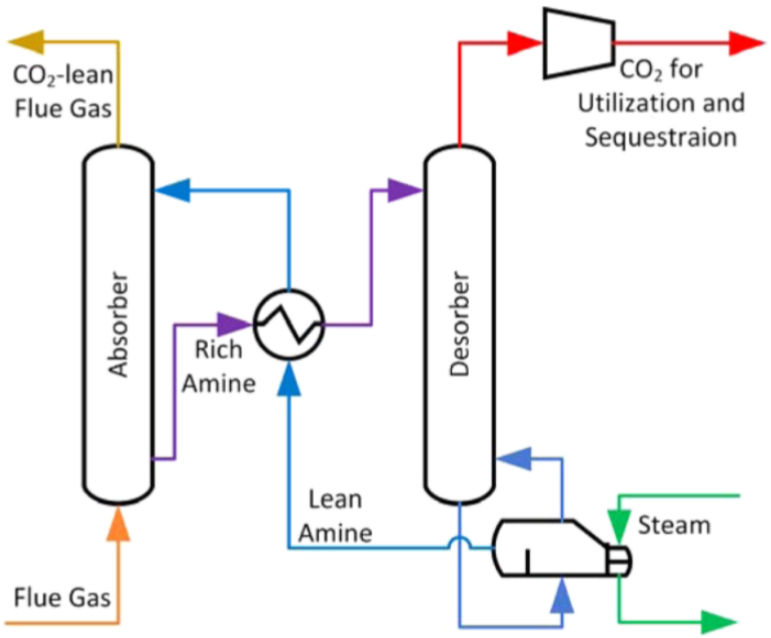

Figure 2.8: Flow sheet of a typical amine scrubbing process used in post-combustion capture of CO2

For direct air capture, solvent regeneration is usually done through temperature swing desorption. Monoethanolamine or MEA [24] has become synonymous with liquid sorbent-based carbon capture, some

other alternatives to MEA used commonly in the industry are diethanolamine (DEA), Sodium Hydroxide (NaOH), Potassium Hydroxide (KOH), at Zero Emission Fuels B V significant focus has been towards using less volatile and heavier amines as sorbents such as Tetraethylenepentamine (TEPA) [25] due to a host of properties discussed in subsequent sections.
Advantages:

- The air contactor or the absorber can be designed to operate continuously.
- Absorber design is economical and can be based on existing technology.
- The contact interface between the liquid and gas is continuously refreshed, allowing for better absorption, limiting the effect of external contaminants such as dust particles.
- It is easier to transfer the rich sorbent to the desorption column via pipes and pumps [26].

Disadvantages:

- Solvent regeneration demands high energy investment, tends to be the costliest part of the process.
- Depending on sorbent volatility, sorbent evaporation can be a significant concern. Life-cycle costs can go up.
- Some sorbents tend to be highly caustic; leakages can pose a serious threat to the environment and personnel [26].

Note: Solid sorbent systems are briefly discussed in section A.2

2.2.2 Direct Air Capture ability at ZEF

ZEF began their experiments with polyamines such as polyethyleneimine (PEI) and (TEPA) over conventional carbon capture amines like MEA [27]. Outdoor operations have a prerequisite of sorbents that do not evaporate quickly, decrease replacement costs, and extend life-cycle times. Volatility decreases with increasing molecular weight of the compound; naturally heavier polyamines are better choices than more volatile compounds like MEA.
Moreover, researchers [28] discovered that polyamines have better absorption characteristics for CO_2 than MEA because of the higher number of reaction sites available, naturally allowing for a more compact design for the same desired cyclic loading. Currently, ZEF is working with a blend of TEPA and PEG. The diluent is added to overcome the high viscosity issues experienced in the previous iterations of the prototype.

2.3 Amines for Carbon Capture

Amines are organic compounds or functional groups. They are derivatives of ammonia, containing a nitrogen atom with a base pair of electrons and at least one or more hydrogen atoms replaced by substituents such as alkyl or aryl groups [29] These compounds are classified into primary, secondary and tertiary amines based on the number of substituents present. A primary amine has one hydrogen atom replaced by a substituent; a secondary has two substituents, and tertiary has three substituents. The presence of substituents also impacts the availability of the base pair of electrons on the nitrogen atom for attack by an incoming reacting species. This is referred to as steric hindrance. Sterically hindered amines are less reactive and thus form weaker or less stable compounds when reacting with a chemical species.

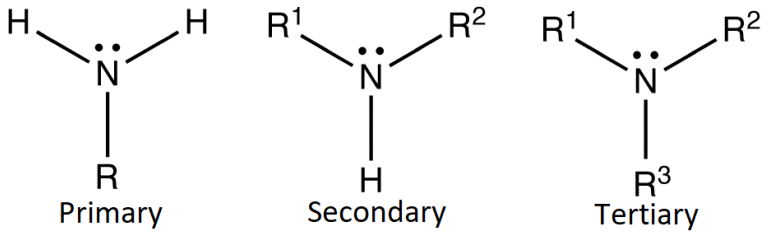

Figure 2.9: General structure of primary, secondary and tertiary amines

Amine-based carbon capture is currently the mature solution that dominates the industry's research. Primarily because it is the most cost-effective solution out there [30], amine scrubbing, as explained earlier, is a process with two major components: Absorption and Desorption column.
In a conventional design, the amine is made to flow from top to bottom, aided by gravity. The ambient air or flue gas containing the carbon dioxide is forced to flow upwards. This counter-current flow helps to enhance the mass transfer between the two phases [20]. The CO_2 present in the gas phase reacts with the amine and gets absorbed. The amine with a higher CO_2 loading is called the rich amine, which is forwarded to the desorption column wherein with the aid of the heat from the reboiler, a reversible reaction occurs, forcing the CO_2 out from the amine. The lean amine is then sent back to the absorber, and the cycle continues.
The difference between the rich and lean loading is called the *cyclic capacity*.

2.3.1 Amines: Physics of Absorption

Absorption of carbon dioxide is an exothermic process, and thus the reaction favours lower ambient temperatures. To model and understand the absorption process better, the two-film theory is utilised [23]. It is used in cases to analyse the mass transfer across fluid interfaces, according to the theory the maximum resistance to mass transfer is limited to a very thin region at the interface, which is called the film. This is a steady-state model, i.e. the concentration profiles are established almost immediately and assumes there is no accumulation of mass at the gas-liquid interface [20]. Another major assumption while using the two-film theory is that the liquid is non-volatile, and thus the reaction takes place only in the liquid film or bulk. In the case of amine-based carbon capture, the physical process of absorption is initiated with the diffusion of carbon dioxide into the amine-air interface. This is followed by the dissolution of CO_2 in the amine, dissolution doesn't imply a chemical reaction, the gas maintains its chemical identity, but it is surrounded by the less mobile molecules of the liquid sorbent. After dissolving, the carbon dioxide reacts with the amine forming the relevant product species. A concentration gradient is established between the film and the bulk of the liquid amine sorbent, which gives impetus to the diffusion of the product species from the interface into the bulk of the liquid.

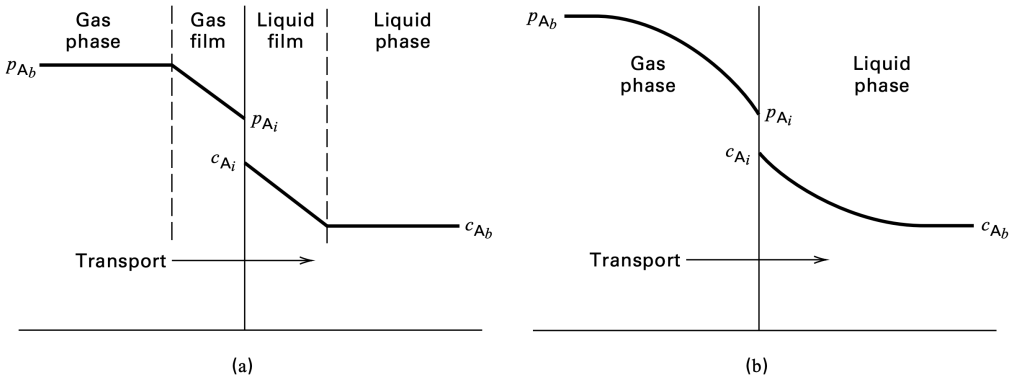

Figure 2.10: Schematic of the two film theory

The diffusion of carbon dioxide into the air-amine interface occurs due to the concentration gradient that exists across the bulk air-amine interface. The flux or mass transfer across this can be understood through Fick's law of diffusion.

$$J = -D\frac{dc_a}{dz} \tag{2.1}$$

The dissolution of the CO_2 into the amine is evaluated using Henry's law with the appropriate partial pressure of CO_2 and Henry's constant.

$$p_i = H_i \cdot c_i \tag{2.2}$$

Diffusion of the carbamate or bicarbonate species formed as a result of the reactions can be explained by the Stokes-Einstein equation, which is used to model the diffusion of solute species into electrolytic liquids.

$$D = \frac{k_B T}{6\pi\eta r} \tag{2.3}$$

2.3.2 Amines: Chemistry of Absorption

The type of products formed by the reaction between amines and CO_2 depends on the nature of amines. Primary and secondary amines undergo a series of reactions with CO_2 to form carbamates. Tertiary amines, on the other hand, cannot form carbamates and go through a simpler route to form bicarbonates. The reaction mechanisms can be explained as follows: Primary or secondary amines on reacting with CO_2 form a zwitterion, anionic species with both negative and positive charges on the same species.

$$R_1R_2NH + CO_2 \longleftrightarrow R_1R_2NH^+COO^-$$

The zwitterion then reacts with another amine molecule and undergoes deprotonation, by transferring the proton to the incoming amine molecule resulting in the formation of carbamate [31].

$$R_1R_2NH + R_1R_2NH^+COO^- \longleftrightarrow R_1R_2NH_2{}^+ + R_1R_2NCOO^-$$

It is possible that the carbamate is further hydrolysed to form bicarbonate along with the regeneration of an amine molecule.

$$R_1R_2NCOO^- + H_2O \longleftrightarrow R_1R_2NH_2 + HCO_3{}^-$$

It can be seen that to absorb a single molecule of CO_2, two amine molecules are required; thus the theoretical maximum loading possible with primary and secondary amine species is 0.5 mol CO_2 per mole of amine.

Tertiary amines, on the other hand, do not have the proton necessary to undergo the zwitterion route. Instead, they react with the CO_2 to directly form bicarbonates.

$$R_1R_2R_3N + CO_2 + H_2O \longleftrightarrow R_1R_2R_3NH^+ + HCO_3^-$$

Naturally, the maximum theoretical loading with tertiary amines is 1 mol of CO_2 per mole of amine; the reactions with tertiary amines are slower than the reactions with primary and secondary amines [32]. Compensating for the reaction rates is the lower heat of regeneration for tertiary amines as compared to primary and secondary amines; this is due to the stability of the carbamate species formed.

2.3.3 Amine Desorption

Desorption is endothermic, and thus, additional heat energy needs to be added into the system to reverse the carbamate formation reaction. The regeneration energy is composed of sensible heating, the heat of absorption, latent heat of vaporisation and also the energy demand from the reflux if it exists.
The two-film theory [20] discussed earlier can sufficiently explain the reversed mass transfer occurring during desorption. With the first step being, the conversion of carbamates (in case of unhindered primary or secondary amines) back into carbon dioxide and regeneration of the amine molecules. This is followed by the diffusion of H_2O and CO_2 molecules from the bulk into the thin gas-liquid interface. This happens due to the concentration gradient that exists. Once the water molecules have sufficient energy (latent heat), a phase transition occurs, and the water moves into the vapour phase along with the CO_2.

2.3.4 Amine Performance Characteristics

The performance of the amine is evaluated on the basis of several criteria, for ideal performance, an amine should possess the following characteristics:

- Large CO_2 capture capacity at ambient temperature.
- Low heat of regeneration.
- Fast reaction kinetics
- Low viscosity of amine
- Relatively high boiling point, to prevent evaporation of amines.

A higher loading capacity is desirable since a certain cycling loading can be achieved with a lesser amount of sorbent and thus a compact design. As explained earlier, **unhindered primary and secondary amines have a maximum theoretical loading limit of 0.5 moles of CO_2 per mole of amine. Tertiary amines, on the other hand, have a higher limit of 1 mole of CO_2 per mole of amine.** One way to increase the nominal loading capacity is to increase the number of reaction sites available for carbon capture by making use of polyamines.

Some other factors that influence the selection criteria are:

- Density and viscosity of the amine. The mass transfer characteristics are often heavily dependent on these fluid properties.
- Boiling point or vapour pressure. To prevent loss of amine through evaporation, it is desirable that the amine has a high boiling point or low vapour pressure under ambient conditions. Amine evaporation can pose a serious threat to the environment and personnel.

- Thermal and oxidative degradation: amines undergo degradation in the presence of oxygen and at high temperatures. It reduces the carbon carrying capacity and increases the corrosive nature of the amine.
- Cost and availability of the sorbent.

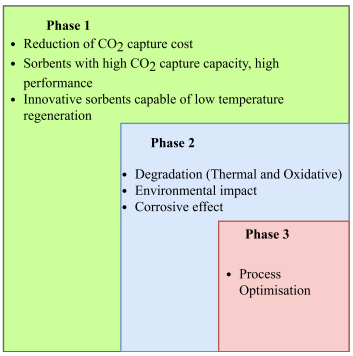

Figure 2.11: Schematic representing the phases involved in sorbent selection

A single amine cannot ideally fulfil all the criteria listed above, but it is possible to use a blend of amines to improve on certain characteristics. A mixture of primary, secondary and tertiary amines depending upon the composition will have lower heat of regeneration as compared to pure primary secondary amines and a faster reaction rate as compared to pure tertiary amines. In some cases, sterically hindered amines are also beneficial in lowering the regeneration energy since carbamates of low stability are formed, due to the hindrance offered to the incoming carbon dioxide group by the large alkyl and aryl groups present on the amine molecule. Moreover, with sterically hindered amines, the bicarbonate route is preferred; thus, leading to a higher carbon carrying capacity as compared to unhindered primary and secondary amines.

2.3.5 Polyamines

Polyamines are organic compounds, with two or more amine groups present. The presence of multiple lone pairs in one large molecule surrounded by alkyl or aryl groups gives rise to the possibility of multiple reaction sites and thus added carbon capture capacity and faster reaction rates.
The reactions between polyamines and CO_2 are complicated, since in addition to simple mono carbamates they also produce dicarbamates, bicarbonates, secondary carbamates etc. depending on the exact chain configuration of the polyamine. Thus, the species formed also impacts the heat of regeneration. From existing research carried out on monoethanolamine (MEA), Diethylenetriamine (DETA), Tetraethylenetetramine(TETA) and Tetraethylenepentamine (TEPA), it was seen that as the number of amine groups in the chain increases the carbon capture capacity (per amine) and the absorption rate also increases [28].

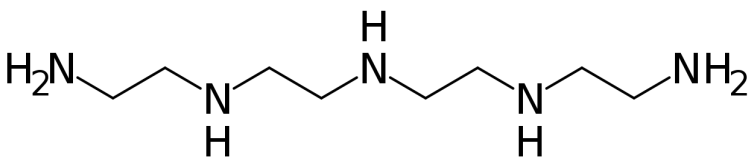

Figure 2.12: Chemical structure of Tetra-ethylenepentamine

Table 2.1: Thermophysical properties of TEPA

Parameter	**Value**
Molecular weight (grams/mole)	189.31
Density (g/cm^3)	0.99
Boiling Point (C)	375

MEA has a CO_2 capture capacity of 0.55 mole/ mole amine as compared to 2.12 mole/mole amine of CO_2 for TEPA, albeit these loadings were established in experiments with an enriched stream with 15% concentration of CO_2, thus orders of magnitude higher partial pressure than what we experience in the case of direct air capture. [28]. Moreover in the same set of results ([28]), it was observed that for higher-order polyamines, dicarbamates and secondary carbamates are more common products of the reaction with CO_2, and thus the energy required to break these bonds is lesser than the amount needed for primary carbamates. There exists a possibility that TEPA can exhibit better loading performance than MEA, for direct air applications, this is one of the reasons that TEPA was chosen as a sorbent by ZEF.

2.3.6 TEPA: Critical Issues

Tetraethylenepentamine (TEPA) due to its high equilibrium loading has been selected as the amine sorbent for the work at ZEF. TEPA is promising, but absorption and desorption experiments carried out by ZEF Team 6 showed that it is far from the ideal sorbent.

The main problem with TEPA have been highlighted below:

- **The viscosity of TEPA changes dramatically with the CO_2 loading.** The increase in viscosity at very high CO_2 loadings severely hinders the flowing abilities and thus inhibits mass transfer at lower temperatures [25].

Considering that the major issue revolves around the exponential increase in viscosity of TEPA at higher CO_2 loadings, which inhibits mass transfer, it makes sense that diluents are added to TEPA to improve its performance. The diluents should have the following characteristics, as identified by the sorbent selection team:

- Miscible with TEPA, in a wide range of proportions.
- Ability to lower the viscosity of the sorbent.
- The solubility of carbon dioxide.
- Low heat of regeneration.
- Low vapour pressure, to prevent evaporation of diluent.
- High resistance to thermal degradation.
- Relatively low cost.
- High availability

There are various candidates suggested by the sorbent selection team that meet these criteria, the experiments conducted in this work are limited to polyethylene glycol (PEG).

2.3.7 TEPA-PEG Sorbent

PEG: A Diluent

Polyethylene glycol is a common synthetic polyether compound. It is amphiphilic due to the presence of polar -OH and alkyl groups. It is non-toxic & biodegradable [33], miscible with water and TEPA and has the ability to absorb CO_2 via physical interactions between the strong polar groups present in either molecule [34] . These physical interactions are weaker than their chemical counterparts, and thus, PEG has lower values for the heat of regeneration.

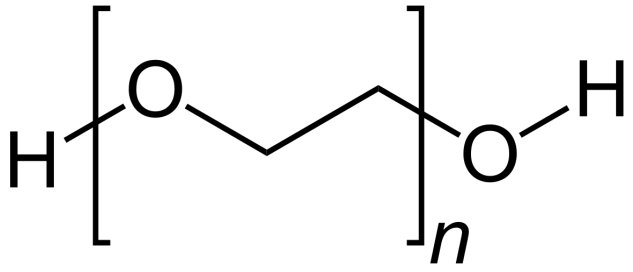

Figure 2.13: Chemical structure of polyethyleneglycol

Since it is a long-chain polymer, depending on the number of repeating monomer groups present the average molecular weight of the polymer varies. It should be noted that the viscosity scales proportionally with the molecular weight and the vapour pressure scales inversely. Earlier research shows that PEG-200, PEG-300 and PEG-600 are thermally stable and have better carbon capture capacities than PEI (polyethyleneimine) [34]. PEG-600 being a larger molecule than PEG-200 or 300 has a higher viscosity and lower availability of -OH groups to have polar interactions with incoming CO_2 molecules. PEG-200 and 300 have similar carbon-absorbing abilities, but due to lower viscosities, it was decided to go ahead with PEG-200 as a diluent for the system.

2.4 Micro-plant: Energy Demand

Based on the ZEF design specifications for a 3x system, three sets of PV panels of 300W each are to be used to power the entire micro-plant. The chart depicts the energy distribution between the subsystems.

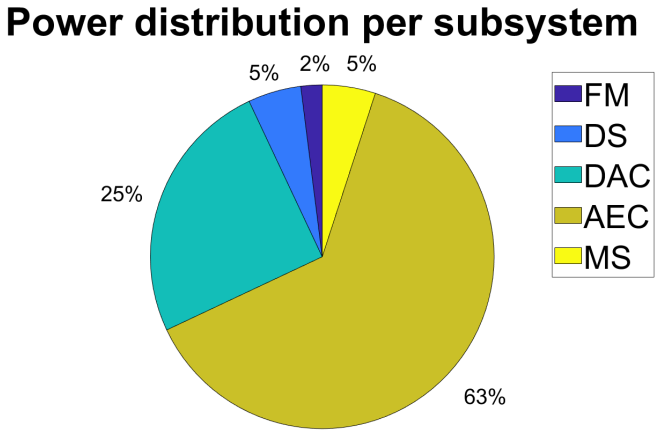

Figure 2.14: Energy demand distribution across subsystems in ZEF

2.5 Stripping

Stripping or desorption is used for the separation of dilute mixtures. A liquid mixture is brought into contact with a gaseous stream, to selectively remove desired components from the liquid into the gas phase. In our case, the liquid mixture is the quaternary sorbent mixture of TEPA-PEG-H_2O-CO_2, and the stripping gas is the hot steam generated in the reboiler. Strippers are not perfect, i.e. the separation isn't 100%, the lean sorbent that leaves the desorption column will have some amount of the desired absorbate still present in it. Before we get into details of the desorption column used at ZEF, it is important to understand the fundamentals of stripping which are highlighted in the following section.

2.5.1 Fundamentals of Stripping

A stripper column can have various designs the most common ones being: a trayed column, spray column and a bubble column [20]. Usually, the rich liquid sorbent enters the column from the top, it flows downwards over a series of trays or weirs and comes into contact with the stripping gas that is flowing upwards or counter-current to the liquid sorbent. The energy needed to generate the stripping gas is supplied by a reboiler.
The hot stripping gas that rises comes into contact with the incoming relatively cooler feed stream. Depending on the flow rates of the two streams and the size of the column, a temperature gradient is established across the height of the column. The lower portion of the column closest to the reboiler is the hottest region, while the top of the column where the top product leaves and the condensed reflux enters is the coolest part of the column. Normally, it can be approximated that the liquid and vapour phases leaving at each stage are in equilibrium with each other [20].
At the top, there is a partial or total condenser that cools the top product. A part of the this is taken out as the distillate; the remainder is fed back into the top of the column as reflux. Similarly, in the reboiler, a part of the lean sorbent is taken out as the bottoms product while the remainder is fed back into the column for further separation.
The ratio between the amount of reflux going back into the stripper column and the amount of distillate taken out as top product is called as the reflux ratio.

$$R = \frac{L}{D} \tag{2.4}$$

Similarly, the ratio between the amount of lean sorbent sent back into the column from the reboiler into the column and the heavy key taken out as the bottoms product is called the boil-off ratio.

$$V_B = \frac{V}{B} \tag{2.5}$$

These two ratios can be changed to control the composition of the top and bottoms product. Increasing the reflux ratio improves the purity of the top product, but also increases the energy demand from the reboiler and vice versa.
The number of equilibrium stages scales inversely with the reflux ratio. For a column with total reflux or R_∞, corresponds to the minimum number of stages, on the other hand, R_{min} corresponds to an infinite number of equilibrium stages. [20].

2.5.2 Stripper: Energy Requirements

As discussed earlier, the energy needed to reverse the absorption reactions is called the heat of regeneration. The heat of regeneration is made up of three components: sensible heat, latent heat of vaporisation and the heat of absorption or desorption. Another fundamental aspect that affects the heat energy demand in the stripper is the reflux sent back to the column from the condenser. Each principle is highlighted below:

Sensible Heat

The amount of thermal energy needed to raise the temperature of the incoming feed to the desorption temperature.

$$Q_{sensible} = \dot{m} \cdot C_p \cdot (T_{desorption} - T_{absorption}) \tag{2.6}$$

It depends on the mass flow rate, specific heat capacity and the temperature difference between the incoming and desired temperatures. [35]. The overall specific heat capacity also depends on the composition of the quaternary mixture, for the purpose of analysis, it can be taken as a weighted average of all the component-specific heats.

Heat of Desorption

The energy released during absorption due to the formation of chemical bonds. Desorption, involves breaking these chemical bonds, which requires energy. In order to reverse the carbamate and bicarbonate formation reactions, thermal energy needs to be supplied to the amine. Research shows that based on the bond strength primary carbamates are the hardest to regenerate which translates to more heat of desorption followed by p-p or p-s or s-s carbamates, secondary carbamates and bicarbonate or carbonate in decreasing order of enthalpy of regeneration and bond strength [28].

Heat of Vaporisation

The thermal energy needed to convert water from the liquid to the vapour phase is referred to as the heat of vaporisation. Sinha et al. [27] have experimented with different loadings of TEPA-H_2O binary mixture to evaluate the heat of vaporisation; they discovered the heat of vaporisation for the binary mixture to be higher on average than that for pure water. This can be ascribed to the additional energy needed to break the hydrogen bonding between the amine and water.

2.5.3 Stripper: Additional Thermal Loads

Reflux

To control the composition of the top product, in this case, a 1:3 ratio of CO_2:H_2O, part of the exiting water is condensed and returned back to the column, this is called external reflux. Under normal operating conditions, it is possible that some of the stripping gas condenses within the column on losing heat to the cooler liquid, the resulting condensate/reflux is circulated internally to the stages underneath and thus called internal reflux. The latter does not add to the energy demand of the stripper, since it falls within the essential operating regime of the stripper. External reflux, on the contrary, is a product that has already exited the stripper, condensed and returned back to the column thus there is a need to provide it with sensible heat and heat of vaporisation thereby increasing the energy demand of the stripper [20].

Heat Losses

The heat losses to the surrounding can be considerable depending on the dimensions of the column and the way it has been insulated. Since a temperature gradient exists across the column, with the temperature progressively decreasing from the bottom to top, it is expected that the reboiler section will have the maximum heat losses, followed by the stages closest to it. The thermal load on the reboiler can be minimised by pre-heating the feed entering the desorption column using waste heat from other sources within the plant or the exiting bottoms product [20].

2.6 Dynamics

The dynamics of the column can be broadly classified depending on the origin and time scales.

- **External Disturbances:** Varying ambient conditions induce changes in the performance of the desorption column. These can fluctuate on different time scales.
- **Internal:** The transient behaviour of the column during start-up and shut-down, and the dynamics associated with the chemical desorption of CO_2 are internal to the column.

2.6.1 External Disturbances

The impact of external disturbances on the absorption and the desorption process is highlighted in the schematic. Before quantifying the effect, an understanding of the variations in the external disturbances is needed.

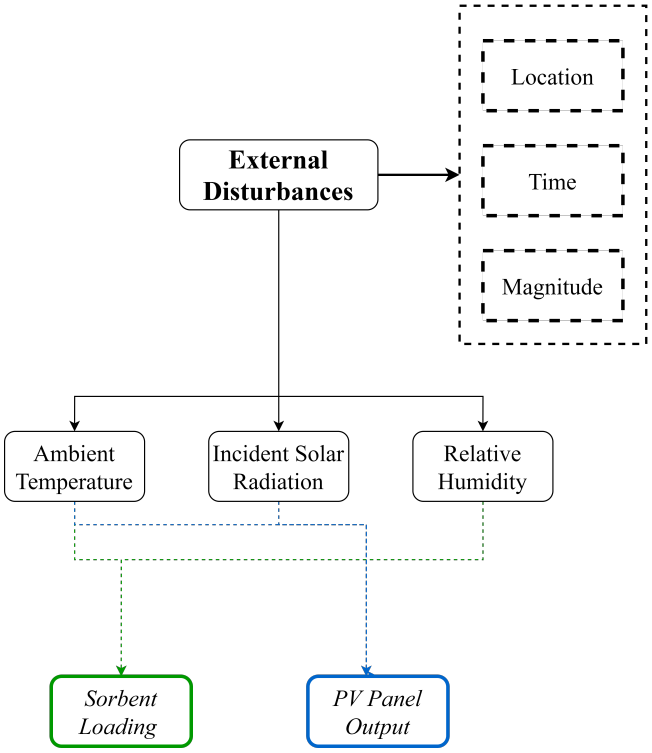

Figure 2.15: External disturbances and their first order effects

Firstly, the disturbances and their direct impact on the DAC process.

- Fluctuations in the ambient temperature and incident solar radiation impact the power output of the photovoltaic panel. The power output from the panel determines the operation window of the system, the operating temperatures and the production capacity. It also has a significant influence on deciding the sequence of operations during start-up and shut down.
- Fluctuations in the relative humidity and ambient temperature have an impact on the sorbent loading. Precisely, the amount of water vapour in the atmosphere determines the amount of water absorbed. The water loading of the sorbent affects the operating temperatures and pressures of the desorption column, which directly influences the cyclic capacity, energy efficiency, and thus the production of CO_2 and H_2O.

Secondly, the extent of the concerned variations is highlighted in the dashed rectangle.

- **Temporal domain:** The disturbances vary over different time scales. In the short term, fluctuations in the ambient temperature, relative humidity solar radiation vary over a few minutes to a couple of hours. Long term variations occur over a couple of months due to a change in seasons.

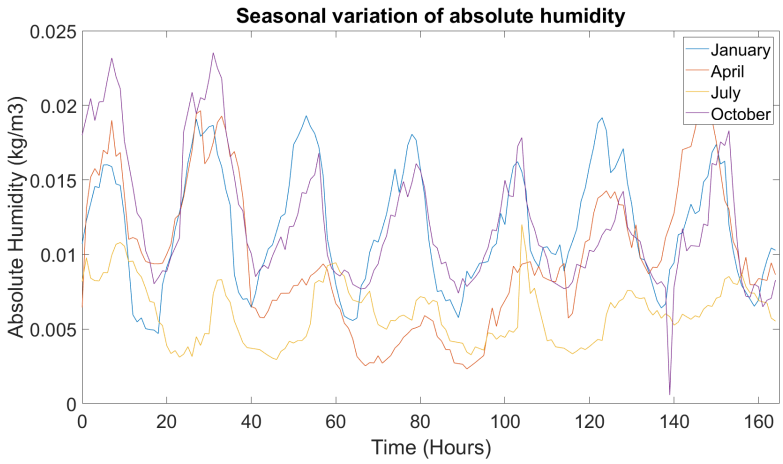

Figure 2.16: Seasonal variation in absolute humidity, in Bechar, Algeria (Sahara climate)

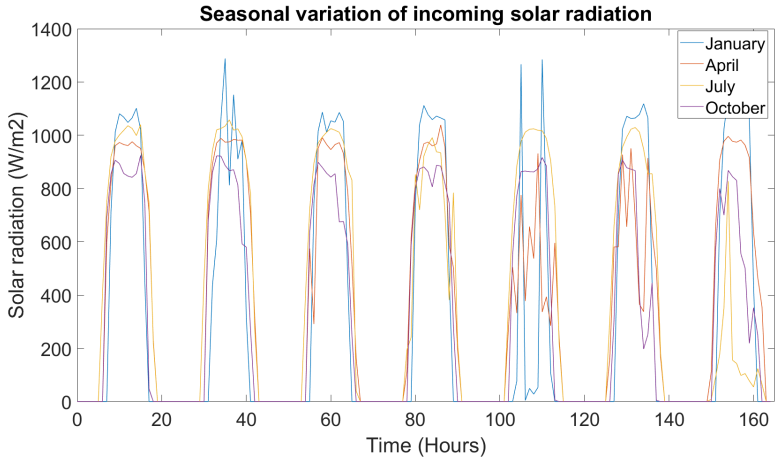

Figure 2.17: Seasonal variation in incident solar radiation, in Bechar, Algeria (Sahara climate)

- **Spatial domain:** Based on the geographic location, the climatic conditions can vary significantly. The earth has been divided into different climatic zones depending on the average temperatures and humidity conditions. Moreover, localised differences created due to the level of vegetation, type of soil also have an acute impact on the regional climate conditions of a place.

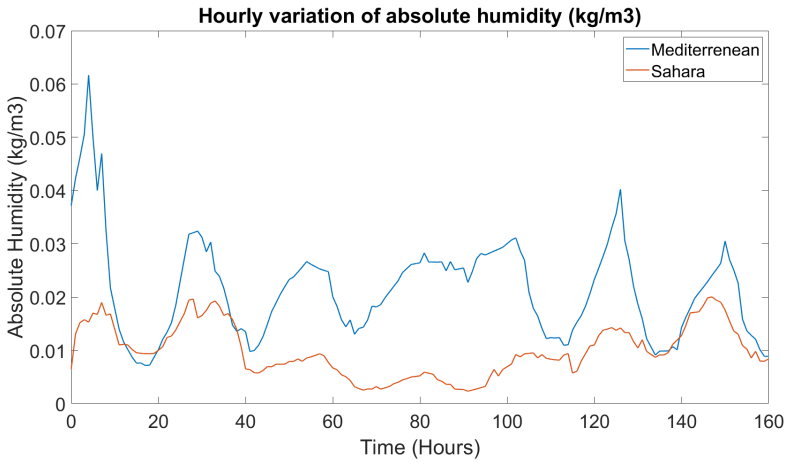

Figure 2.18: Spatial variation in incident solar radiation across two different locations Algeria & Portugal

2.6.2 Internal

Hold-Up Time

In chemical engineering, hold-up time is the time the substance spends in a reactor, depending on the nature of the reactor design; this can differ from residence time [36].

$$Hold-up\ Time = \frac{Volume\ of\ vessel\ (m^3)}{Net\ volume\ flow\ rate\ from\ vessel\ (m^3/s)} \tag{2.7}$$

Consider the rich sorbent has entered the reboiler vessel, as it desorbs, we are slowly approaching the desired lean sorbent concentration. Once the lean sorbent concentration has been achieved, it is seen that at a particular temperature and pressure, no further desorption is possible, i.e. VLE has been established [36].
Through repeated experiments under different conditions of temperature and pressure, it is possible to obtain a hold-up time curve, with sorbent loading on the y axis and time on the x-axis, with a distinct minimum theoretical hold-up time evident from the graph. This minimum hold-up time can then be used to resize the reboiler vessel for a given mass flow rate, such that the dynamics of the process are improved, the time to start up will decrease, and the energy consumption can also be optimised accordingly.

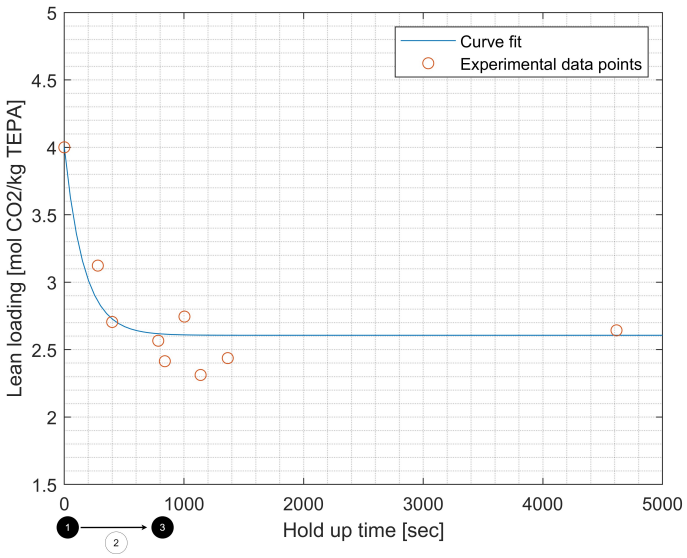

Figure 2.19: A typical hold-up curve for TEPA-H_2O-CO_2 [37]

Start-up and shut-down are extremely crucial components of the desorption process, quantifying these will help ZEF gain insights into the influence the stripper column has on the rest of the system.

Start-up & Shut-down

Start-up and shut-down of a desorption column are essential operations but do not add value to the final product; thus an effort should be made to quantify the time, analyse and optimise it to maximise the period during which the column is actually producing the final product. A study by AECOM investigated the possible improvements for start-up and shut down times of gas-fired carbon capture and utilisation facilities. Some of the main performance parameters they looked at were [38]:

- The time and associated energy costs related to start-up and shut-down. Their work reveals that the time associated with start-up and to a lesser extent shut down depends heavily on the nature and composition of the sorbent being used, which in their case was 35% MEA [38].
- CO_2 capture rates and residual emissions. The latter gives us insight into the processes occurring inside the desorption column after shut down. It is possible that some amount of CO_2 is generated even after the reboiler is shut down, due to the residual heat energy present in the column. Thus by quantifying the residual emissions, we can implement buffer tanks to store this CO_2 for future use during times of lower production.
- The thermal efficiency of the plant. The study took into account the heat losses and the heat of regeneration for the desorption of the amine. In addition to this, they realised that a good portion of the energy is used up in heating the thermal mass of the column itself. In literature, this accounts for 5% of the total energy usage [38]. Although this is not directly transferable to our system, it means that the thermal mass does play a role not just in the energy consumption, but adds inertia to the dynamic response of the system. The heat losses and energy consumption of the thermal mass depends on the design of the column and also the materials used.

2.7 Vapour-Liquid Equilibrium

2.7.1 VLE for TEPA-H_2O-CO_2

From the VLE data, it is possible to understand the compositions of the various components given the temperature and pressure. Research at ZEF by Dowling et al [25]. developed experimental VLE curves for the ternary mixture containing, TEPA, water and carbon dioxide, for certain values of temperature. These isotherms were then plotted to depict the CO_2 loading/mole of TEPA against different ranges of partial pressure. To expand on the experiments, a model was developed that could be used to extrapolate and gain data for wider temperature and pressure ranges.
The model takes into account the deviation of the ternary mixture from ideal behaviour by using activity coefficients. The activity coefficients are derived using the Specific Ion Interaction Theory (SIT) an improvement on the existing Extended Debye Huckle theory.

$$\log \gamma_i = -\frac{z_i^2 \cdot A\sqrt{I}}{1 + 1.5\rho^{-0.5}\sqrt{I}} + \sum c_j \varepsilon_{ij} \tag{2.8}$$

This theory is selected because of its computational simplicity and ability to predict VLE behaviour better than more complex models such as e-NRTL or UNIQUAC [25]. The model works as follows:

1. Using the chemical reactions that occur in the ternary mixture, chemical equilibrium equations are established. A relationship between the equilibrium constants, activity coefficients and temperature, is specified. Finally, a mass balance of all the species present is developed.
2. These species equations are solved to derive the concentrations of each component in the mixture at a particular temperature while taking inputs such as the weight percentage of TEPA, and partial pressure of CO2.
3. The concentration is then used to evaluate the partial equilibrium pressure of the carbon dioxide using modified Raoult's law. This value is then compared with the experimental value and iterated till a proper model fit is achieved.

It can be seen that the model adheres quite well to the experimental VLE curves obtained for temperatures between 313.15K and 393.15K and TEPA concentrations between 30-70% weight loading. Unfortunately, due to errors associated with the pressure sensors, there is a slight discrepancy in the model and experimental values for low loadings of CO_2.

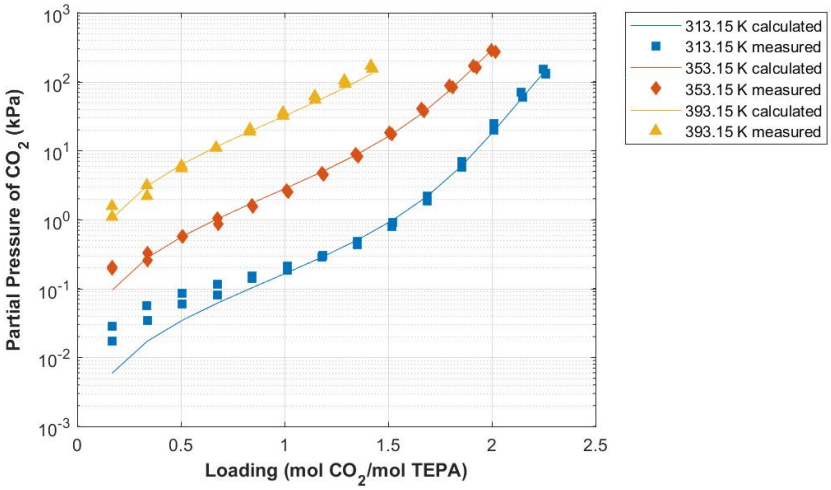

Figure 2.20: Model vs. Experimental VLE curves for 30%. TEPA [25]

The curves confirm our expectations, i.e. as the temperature increases, the amount of CO_2 held by the amine decreases, this is seen as an increase in the partial pressure of CO_2 in the vapour phase. Conversely, for the same value of partial pressure, higher CO_2 loadings are possible in the amine at lower temperatures. This is the principle behind absorption and desorption. Amine absorbs CO_2 at low temperature (ambient) and desorbs the CO_2 at a higher temperature. These graphs prove the effectiveness of VLE data as inputs for designing the DAC system at ZEF.

2.7.2 Vapour Curve

Similarly, a vapour curve for the binary mixture of TEPA-H_2O was obtained through experiments for different wt. Percentages of TEPA and temperatures. Using the experimental data, a model was developed to predict the partial pressure of H_2O [25]. The model works as follows:

1. The aim is to compare the total pressure predicted by the model to the experimental values obtained and develop a fit for the parameters accordingly.
2. Modified Raoult's Law is used to establish a relationship between the concentration of each component in the liquid phase and the corresponding partial pressure in the vapour phase. Modified Raoult's law was used to correct for liquid phase non-idealities, as explained in the previous section.
3. The saturated vapour pressure of the pure component is needed for Raoult's law. For H_2O, it is obtained from Antoine's equation, since sufficient data for the different coefficients exists in the case of water, but not for TEPA. Antoine's coefficient data was taken from the Dortmund Data Bank.
4. To evaluate the saturated vapour pressure of TEPA, the Clausius-Clapeyron equation was used. With the boiling point of TEPA as the reference temperature, implying Pref is the atmospheric pressure. Data for the boiling point and enthalpy of vaporisation was taken from the National Institute of Standards Technology.
5. Wilsons model was used to evaluate the activity coefficients for TEPA and water, due to its relative simplicity, since few parameters need to be tweaked to get a good parametric fit.
6. Then the model identifies the total pressure from the modified Raoult's law, compares it with experimental P-T-x data, and accordingly tweaks the lambda values in Wilsons activity coefficient model till an accurate fit is obtained (residuals are minimised)

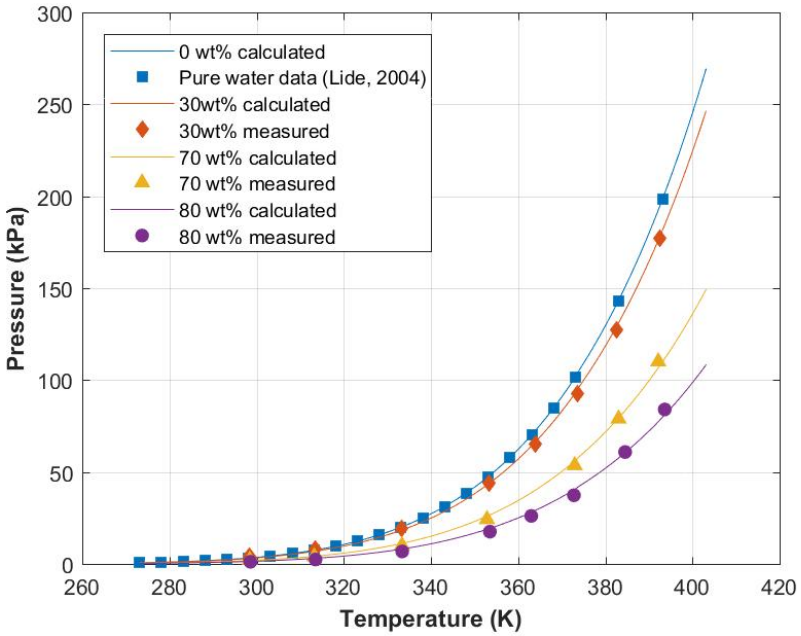

Figure 2.21: The equilibrium pressure of binary mixtures of TEPA and H2O with 30, 70 and 80 wt% TEPA and pure water as a function of temperature versus the binary model based on Wilson's activity coefficients

From the vapour curve, it is clear that for lower concentrations of TEPA in the binary mixture, the total pressure of the system is higher. With that for pure water is the highest. This is to be expected since, TEPA has a very high boiling point, very little of it moves into the vapour phase, as such a majority of the pressure is a contribution from the water vapour. One major assumption in this model and experiments is that the partial pressure of H_2O remains constant throughout, and is not influenced by the absorption of CO_2. This is not entirely true, as van der Poll's ([37]) work shows that there are some interactions initiated between the water and TEPA, as carbamates are formed.

2.7.3 Absorption-Desorption Cycle:

Figure 2.22 presents how VLE curves for the loaded sorbent are used to estimate the cyclic loading by deciding the absorption and desorption temperatures.

- The absorption temperature is the ambient temperature, varies between 20-40 °C depending on the location and time of day.
- The partial pressure of CO2 for absorption is fixed, that is 0.04 kPA (atmospheric concentration of CO2.
- Using the ambient temperature and partial pressure of CO2, from the VLE curves it is possible to figure the rich loading of the sorbent at equilibrium.
- Next we choose the desorption temperature of 120 °C and a system pressure of 100 kPa (atmospheric pressure). The corresponding partial pressure of H2O at this temperatures is obtained from the vapour curve, and is 75-80kPa.
- The deficit of 25-20 kPa is the partial pressure of CO2 at these conditions, the corresponding loading of the sorbent at this temperature and pressure is obtained from Figure 2.22.
- The difference between the loadings is the cyclic capacity possible at the chosen operating conditions.

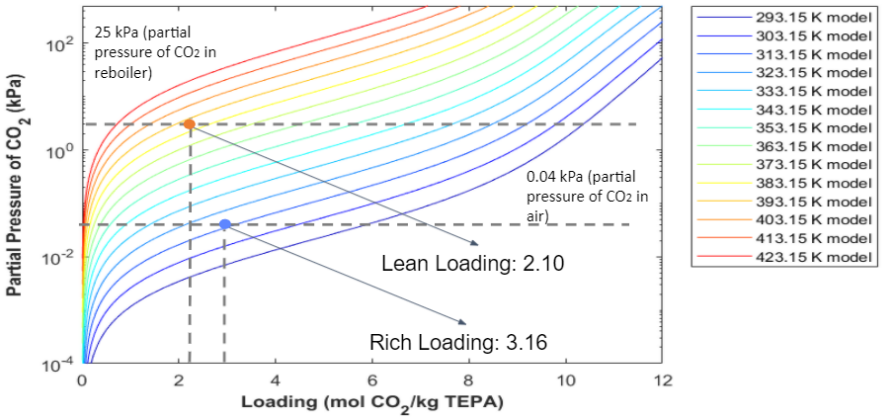

Figure 2.22: Representation of the absorption and desorption cycle occurring in DAC.[25]

2.8 Stripper: Modelling Approach

Binary distillation uses the graphical McCabe Thiel approach to determine the stage composition, optimum reflux ratio, number of equilibrium stages, bottoms and distillate flow rate while taking in a limited number of inputs. This approach is limited to simple two-component mixtures. For multi-component mixtures, design of the process requires rigorous determination of stream flow rates, stage temperatures, pressures, compositions, and stage-wise heat transfer. These quantities are linked to each other via mass balances, energy balances and equilibrium relations at each stage or the MESH equations. But these relations tend to be non-linear algebraic equations, which can be computationally expensive depending upon the approach taken to resolve these equations.
In ZEFs case, two processes are in the desorption column, reverse chemical reactions converting the carbamates and bicarbonates (depending on the amine species and loading) into CO_2 and water, followed by the mass transfer between the liquid and vapour phases. There are ways to model the mass transfer and chemical reactions, but the computational effort increases with increasing complexity and accuracy. In cases where chemical reactions are instantaneous, as is the case of amine desorption, an equilibrium-based approach for mass transfer and chemical kinetics is sufficient to model the behaviour accurately. But, to model the processes more accurately, a rate-based approach can be followed, albeit the latter is computationally expensive. Thus we must understand the chemical kinetics before deciding on a course.

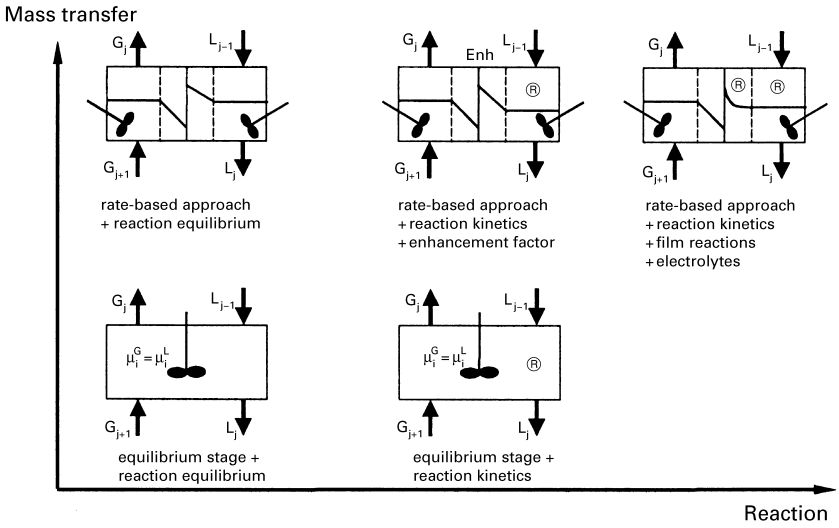

Figure 2.23: Schematic of different modelling approaches [39]

Equilibrium Modelling

The equilibrium approach is based on establishing relationships between different quantities at each stage using the *MESH* equations. It is based on the following assumptions:

- Phase equilibrium is achieved at each stage.
- No chemical reactions occur, or are instantaneous.
- Entrainment of liquid drops in vapour and occlusion of vapour bubbles in liquid are negligible.

A single equilibrium stage has multiple streams entering and leaving as shown in Figure 2.24, and some amount of heat transfer occurs. It is described as follows:

- The feed enters stage *j*, at a specific temperature and pressure, the composition of different components is expressed as $z_{i,j}$, and the overall molar enthalpy as $h_{F,j}$.
- An interstage liquid from the stage above *j-1* (if any), enters the stage *j* with a temperature T_{j-1},pressure P_{j-1}, enthalpy h_{j-1} and molar fraction $x_{i,j-1}$. Similarly a interstage vapour enters from a stage below, with a temperature T_{j+1}, pressure P_{j+1}, enthalpy h_{j+1} and molar fraction $y_{i,j+1}$.
- At every stage there are vapour and liquid streams that leave and are in equilibrium with each other. It is possible to split these into side-streams for different purposes.
- Heat transfer into the system is taken as positive, and vice versa.

Thus, associated with each general stage, we have the following equations:

- The **M**aterial balance for each component are expressed as:

$$M_{i,j} = L_{j-1}x_{i,j-1} + V_{j+1}y_{i,j+1} + F_j z_{i,j} - (L_j + U_j)x_{i,j} - (V_j + W_j)y_{i,j} = 0 \tag{2.9}$$

  where U_j and W_j represent the side stream flow rates.

- The phase **E**quilibrium relations for each component are written as:

$$E_{i,j} = y_{i,j} - K_{i,j}x_{i,j} = 0 \tag{2.10}$$

  Where $K_{i,j}$ represents the distribution coefficient.

- **S**ummation for the mole fractions are :

$$\begin{aligned}(S_y)_j &= \sum_{i=1}^{C} y_{i,j} - 1 = 0 \\ (S_x)_j &= \sum_{i=1}^{C} x_{i,j} - 1 = 0\end{aligned} \tag{2.11}$$

- And the ent**H**alpy relations for different components in the mixture:

$$H_j = L_{j-1}h_{L_{j-1}} + V_{j+1}h_{V_{j+1}} + F_j h_{F_j} - (L_j + U_j)h_{L_j} - (V_j + W_j)h_{V_j} - Q_j = 0 \tag{2.12}$$

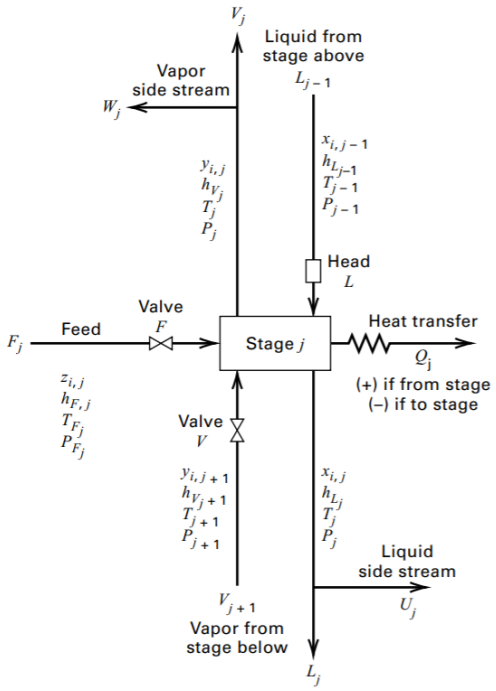

Figure 2.24: Schematic of a general equilibrium stage [20]

There are different mathematical approaches to solve the generalised MESH equations for each stage. Each varying in complexity [20]. A brief highlight of these methods is described below:

- **Stage by stage:** Developed by Lewis–Matheson in 1932 and Thiele–Geddes in 1933 based on equation tearing for solving simple fractionators with one feed and two products. These methods are more suitable for hand calculations and were found to produce unstable results when implemented on a computer [20]. A modification to the stage by stage method was carried out by Holland, called the *theta method* which can be implemented on computers without any issues.
- **Sum rates:** A study by Friday and Smith suggested that no single tearing of streams technique could solve all problem types. Thus they developed two methods:
  - Bubble point (BP) Approach: Is utilised when the feed contains components which have similar volatility.
  - Sum rates: For feeds containing components of widely different volatilities, the BP approach fails, in that case the sum rates approach is used.
- **Inside-Out method:** Boston and Sullivan came up with a stable solution for the MESH equations. They defined energy and volatility parameters, which are used as the primary successive-approximation variables. A third parameter, which is a combination of the phase flow rates and temperature at each stage, was employed to iterate on the primary variables—thus the name inside-out method.

2.8.1 ZEF:Design requirements

Zero Emission Fuels has an aim to develop a micro-plant that is capable of producing 600 grams of methanol per day. With each day amounting to 8 hour long shifts, on an average.

- For the required methanol production rate of 600 grams per day, 18.75 moles of CO_2 needs to be captured and processed by the system, which translates to a mass flow rate of 2.344 mol/hr

or 0.103 kg/hr.

- The reaction in section 1.2 needs water and carbon dioxide in a **3:1** molar ratio. Naturally, this puts the target for daily H_2O capture at 56.3 moles. The ideal mass flow rate for water is 7.031 mol/hr or 0.127 kg/hr.
- The economic goal is to capture CO_2 at cost of less than 100 Euros per Tonne, and produce methanol at a cost of less than 350 Euros per tonne. To make this business case viable, a large number of factors need to work side by side, but lowering the energy consumption from the stripper column is perhaps the most challenging aspect between now and the final goal.

2.9 Conclusion

2.9.1 Summary

- Research has highlighted the problems with pure TEPA based sorbents. The high viscosity and low mass transfer rates are a significant hurdle to achieve ZEF's desired rich and thus cyclic loading.
- Primary investigations with diluents have shown improvements in mass transfer. TEPA-PEG-based sorbents' influence on the performance of a stripper column needs to be investigated via experiments.
- Existing work has shown the impact of changing relative humidity on the water loading of the sorbent.However, the impact combined effect of external disturbances on the performance of the stripper needs to be analysed.
- Quantifying the start-up and shut-down dynamics of the column, will help develop an insight into the operation window of the DAC subsystem.
- Hold-up time, plays a crucial role in deciding the optimal design of the system. From Matteis's data [40], it can be seen the process is diffusion-limited. Experiments with TEPA-PEG sorbent under different temperatures and mass flow rate conditions will be performed to better understand the new sorbent's kinetics.

2.9.2 Research Gap

To regenerate the rich amine, ZEF relies on a stripping column. The issues with the previous system can be classified into two categories, as follows:

Engineering & Product Design Related

- Inability to control the mass flow rate of the sorbent entering the stripper column.
- Due to external heaters, it was not possible to evaluate the energy consumption accurately.
- The highly viscous nature of the loaded sorbent posed problems with sample collection at lower temperatures.
- No provision for reflux to control the outlet composition.

Science related

- The background research highlights the importance of start-up and shut-down operations. This work will focus on the transient behaviour of the column during start-up and shut-down.
- Preliminary analysis of chemical kinetics and hold-up time was carried out, but the influence of different parameters and behaviour of different sorbents wasn't investigated.

- Previous research focused on the design of the stripper column based on steady state conditions. External disturbances and their fluctuations were not included in the analysis, and thus need to be accounted for.

Chapter 3

Experimental Procedures and Equipment

This chapter provides insights into the equipment and methodology used to understand the dynamics of a desorption column with a **focus on the the start-up & shut-down behaviour of the column and the kinetics associated with desorption of CO_2** . Firstly, the experimental plan is laid out, followed by detailed description of the procedures used to conduct the experiments part of this work.

3.1 Experimental Plan

3.1.1 Start-up Shut-down

The main goal of the start-up and shut down experiments is to understand the energy and time consumption of a desorption column till it reaches a steady state. And to gain insights into which external parameters influence the KPIs identified. The set of experiments performed is listed below:

Table 3.1: List of start-up & shut-down experiments conducted to gain insights into transient behaviour of column

Experiment Number	Sorbent	Stages	Initial Temperature (C)	Final Temperature (C)	Initial Pressure (mbar)	Final Pressure (mbar)
1	Pure TEPA	3	20	118	700	1000
2	Pure TEPA	3	21	117	700	1000
3	TEPA-PEG200	3	20	118	700	1000
4	TEPA-PEG200	1	19	115	700	1000
5*	TEPA-PEG200	3	20	118	700	1000

3.1.2 Kinetics

A set of hold-up time experiments were performed, to understand the impact of temperature and liquid hold-up on the desorption process. The list of experiments is mentioned below:

Table 3.2: List of hold-up experiments conducted. Experiments 1-10 compare the impact of temperature on desorption kinetics. And Experiments 11-14 are used to understand the impact of liquid hold-up on the desorption kinetics.

Experiment Number	Temperature (Celsius)	Mass flow rate (g/s)	Liquid Hold up (ml)
1	110	0.02	188
2	110	0.04	188
3	110	0.09	188
4	110	0.06	188
5	110	0.13	188
6	120	0.02	188
7	120	0.09	188
8	120	0.03	188
9	120	0.08	188
10	120	0.26	188
11	120	0.07	150
12	120	0.08	150
13	120	0.04	150
14	120	0.03	150

3.2 Methodology

The experiment methodology is divided into three parts as can be seen in the schematic below :

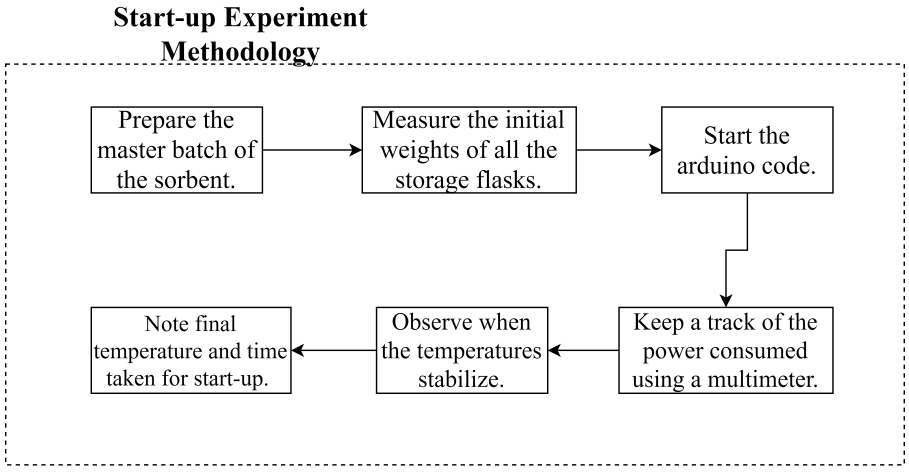

Figure 3.1: Flowchart representing the experimental methodology for the start-up experiments

Once the data for the start-up experiment has been obtained, one can proceed to the hold-up experiments, the methodology is elaborated in the schematic below:

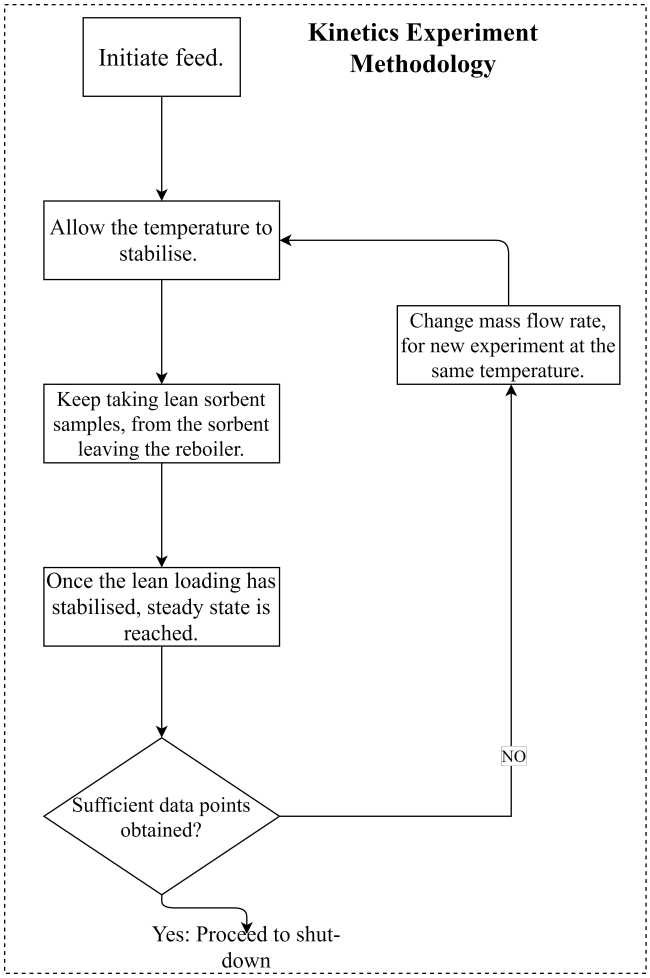

Figure 3.2: Flowchart representing the experimental methodology for the kinetics experiments

The final phase is the shut-down experiment, which directly follows the kinetics experiments.

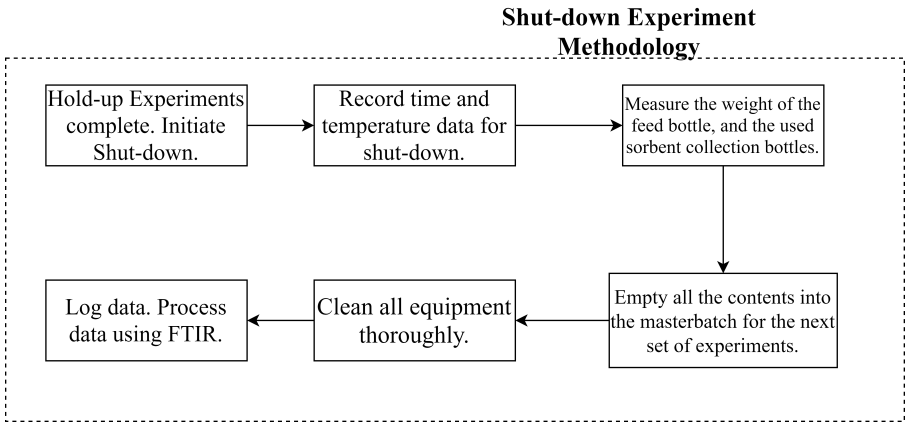

Figure 3.3: Flowchart representing the experimental methodology for the shut-down experiments

- The first step to an experiment is the preparation of the loaded sorbent, this is referred to as the master batch. The amount prepared depends on the length of the continuous experiment, and the mass flow rates that are to be tested. Preparation of the master batch is explained in section **??**.
- The second aspect of the experiment is to monitor the temperatures inside the column at every

stage. A track of the time and energy consumption needs to be maintained, till the temperatures inside the column stabilise, this represents the *start-up* phase of the column. Details about the start-up experiments are presented in subsection 3.3.1.

- Once the temperatures are stabilised, the kinetics experiments are conducted. A detailed procedure is outlined in subsection **??**.
- Finally, once a sufficient number of points have been collected for the kinetics experiments, the power input to the column is switched off. Temperature and pressure data is logged, to help in the analysis of the shut-down behaviour of the column.

3.3 Desorption Column Experiments

These experiments aim to gain insight into the dynamic behaviour of a stripping column i.e. start-up shutdown behaviour and an understanding of the kinetics of the desorption process. Firstly, the different desorption column setups are explained, followed by the assumptions and experimental procedures.

3.3.1 Desorption Column: Start-up & Shut-down

The core of the setup is a desorption column, with a provision to vary the number of stages. A reboiler sits at the bottom of the column with internal finned heaters. Each stage is provided with a sampling port, and the top stage has a provision for the incoming feed. A series of pumps are used to maintain the flow of the sorbent into and out of the system. The feed enters from the top, and leaves from the reboiler, after which it is collected in a lean sorbent tank. A condenser at the top of the column cools the vapours as they enter a flash tank. Here the condensed water is collected in a flask, while the CO_2 in the vapour phase is taken to the following storage tank.

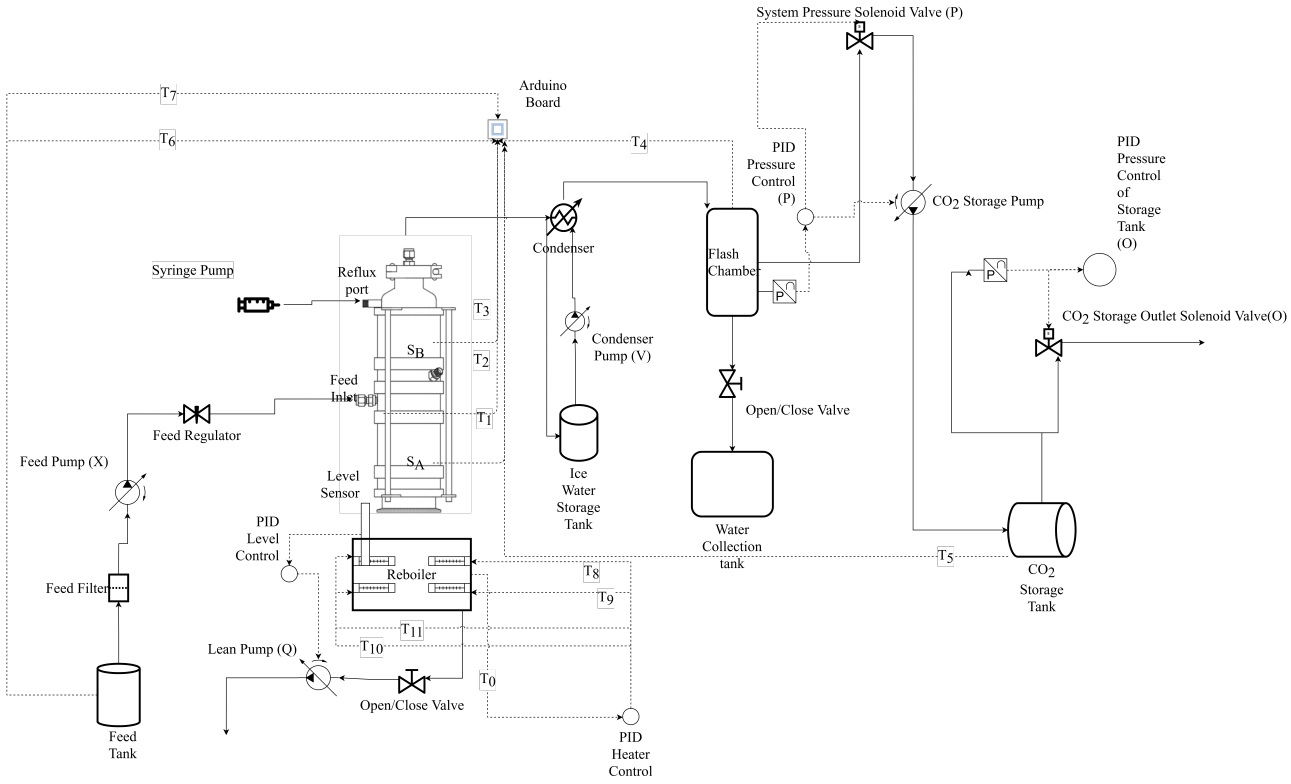

Figure 3.4: Schematic representation of the process flow occurring in the desorption column experimental setup

The process flow is described as follows:

- The loaded sorbent is pumped into the desorption column via a series of pipes using pump X. A filter in the inlet line is used to prevent solid impurities into the column. A needle valve is used to fine-tune the incoming feed flowrate.
- The sorbent enters at the top, descends through the stages and into the reboiler, where it is heated. A sensor maintains the level and prevents the flooding of the latter. Pump Q is activated by the level sensor and takes out excess lean sorbent from the system.
- The carbon dioxide and water vapour liberated rises up, heats the stages and eventually leaves the column from the top. An actively cooled shell and tube heat exchanger condenses the water vapour as it enters the flash tank.
- Inside the flash chamber, the condensed water collects at the bottom while the CO_2 remains in the gaseous phase. Over time, with the continuous release of vapour from the column, pressure builds up.
- Once the system pressure exceeds the specified set pressure, a solenoid valve opens, and a pump sucks out the excess CO_2 from the system into a downstream storage tank. The opening and closing of the valve and discharge of carbon dioxide from the column are used to maintain the system pressure.
- The CO_2 storage tank also has a specified set pressure. As the amount of CO_2 in the tank increases, pressure builds up; upon exceeding the pressure setpoint, valve Y opens to expel the gas into the surroundings. For safety, the outlet of the CO_2 storage tank is connected to flexible tubing that releases the gas into a fume hood.

Syringes are used to collect samples from the system at regular intervals. The lean sorbent collected is mixed at the end of the experiment, and its composition is analyzed.

Assumptions

- **Carbon dioxide desorbed and collected is assumed to be an ideal gas**. Based on this, it is possible to calculate the number of moles of CO_2 desorbed during the process.
- **There is no pressure drop across the stages in the column.**
- **The complete setup is assumed to be leakproof.** This is valid since the setup is repeatedly tested for leaks before every experiment.
- **The change in pressure inside the system is caused due to the accumulation of desorbed H_2O and CO_2.**

3.3.2 Desorption Column: Kinetics

The kinetics experiments were carried out on a prototype integrated direct air capture unit. It is a scaled-down version of the desorption unit used for start-up and shutdown experiments. It consists of a glass desorption column, with stages. A cylindrical reboiler with an immersion heater is used to supply energy to the system. A gear pump transports the rich sorbent from the feed tank to the inlet of the column at the top. An inline filter prevents solid impurities from entering the system. Finned heat exchangers cool the lean sorbent leaving the system before returning to the lean sorbent collection tank. The vapour generated leaves from the top of the column and is cooled passively by finned heat exchangers. The two-phase mixture of condensed water and CO_2 (gas) enters a flash chamber maintained at atmospheric pressure.

The process flow is described as follows:

- The loaded sorbent is pumped into the desorption column via a series of pipes using a gear pump. A filter in the inlet line is used to prevent the entry of solid impurities into the column. A needle valve is used to fine-tune the incoming feed flowrate.
- The sorbent enters at the top, descends through the stages and into the reboiler, where it is heated. The setup is operated at atmospheric pressure and a simple U-tube pipe mechanism is used to maintain a constant level of sorbent in the reboiler.
- The carbon dioxide and water vapour liberated rises up, heats up the stages and eventually leaves the column from the top. An air-cooled finned heat exchanger condenses the water vapour as it enters the flash tank.
- Inside the flash chamber, the condensed water collects at the bottom while the CO_2 remains in the gaseous phase. Carbon dioxide leaves the flash chamber through an outlet at the top and is allowed to proceed to the fume hood for safe expulsion.

Note: The purpose of the kinetics experiments is to monitor the variation of the lean loading depending on the hold-up times, and not monitor the amount of CO_2 and H_2O produced that has been accomplished in the start-up and shut down experiments.

Assumptions

- **The pressure and temperature inside the column are constant.** The temperature fluctuations are minimal, within $\pm$ 1°C.
- **A constant mass flow rate of the sorbent in and out of the desorption column is assumed.** Since the mass flow rate is controlled by a sensitive gear pump, and there are no pressure fluctuations, this assumption holds good.
- **There is no pressure drop across the stages in the desorption column.**

Chapter 4

Modelling Approach

This chapter provides insights into the modelling architecture used to answer the research objectives identified in chapter 1. Firstly, the model to evaluate the start-up and shut down dynamics of a desorption unit is explained, followed by an explanation into the integrated DAC model and its subsystems.

4.1 Modelling: Start-up Shut-down

Modelling the transient behaviour of the column during start-up and shut down has been done by solving the unsteady energy equation. Based on the inputs, the model gives insights into the final temperature and time taken by the stripper column at a steady state.

Table 4.1: Input & output parameters used in the transient start-up and shut-down model

Inputs	**Units**
Power	Watts
Mass flow rate	gram/s
Ambient temperature	Celsius
Thermal mass of the system	kilograms
Outputs	
Temperature at steady state	Celsius
Time to steady state	Seconds
Start-up energy consumption	kJ or kWh

The simplification of the model is based on a set of assumptions that are highlighted below:

4.1.1 Assumptions

- The model deals with the transient behaviour of the reboiler of the desorption column. It is assumed that the rest of the stages closely follow the temperature-time response of the reboiler, and thus there are no significant delays involved in the time required to heat the reboiler compared to the stages.
- The reboiler and its contents are assumed to be a lumped system. This assumption holds good for smaller liquid hold-ups with uniform mixing, allowing for high convective heat transfer coefficients.
- The pressure inside the system remains constant. The effects of fluctuating pressure due to the desorption of water vapour and carbon dioxide from the sorbent are assumed to have a negligible

impact on the energy requirements of the column.

- The specific heat capacity remains constant. The specific heat is taken as the weighted average of the different components of the sorbent.
- The heat of absorption remains constant, and this value depends on the temperature, pressure and CO_2 loading.

The unsteady energy equation is solved using explicit numerical integration methods. Explicit methods evaluate successive values of the variables based on the current time step values. Implicit methods evaluate successive values based on the current and future values of the variables. The latter is more challenging to implement but inherently stable irrespective of the size of the time step. The model aims to understand phenomenon over a time scale of minutes. An explicit method is selected for creating the model due to faster computation times and ease of implementation.

4.1.2 Equations

The unsteady energy equation is resolved using a MATLAB script

$$\rho V C_p \frac{dT}{dt} = \dot{Q} + \dot{Q}_v \tag{4.1}$$

. The unsteady term represents the rate of change of temperature. The thermal mass of the system adds thermal inertia to the response time of the system. The increase in temperature is achieved by the energy generation term on the right-hand side of the equation. Naturally, some amount of the heat generated is being lost to the surroundings. The rate of increase in temperature reaches equilibrium once the energy addition and loss terms are balanced.

Figure 4.1 represents a black-box approach to modelling the reboiler of the desorption column.

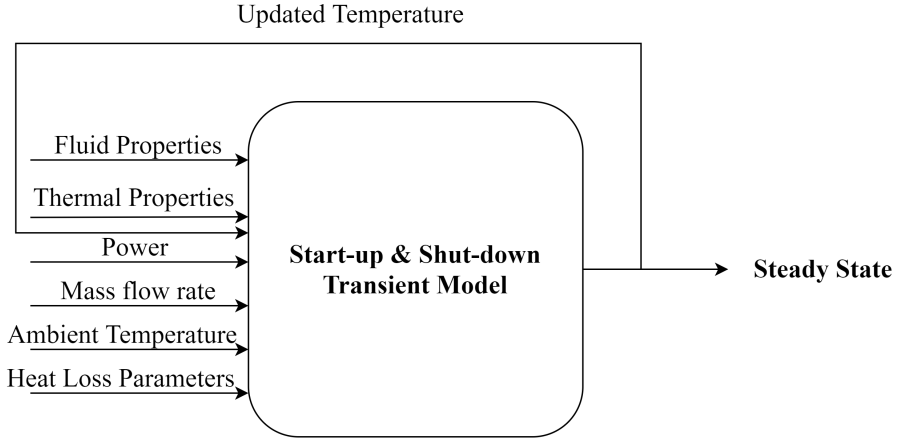

Figure 4.1: Schematic representing black box approach of the start-up & shut-down model.

Table 4.2: Input boundary conditions for the start-up model. The parameters are based on the approximate values obtained from the experimental setup.

Boundary Conditions	**Values**
Ambient temperature	20 C
Final temperature*	120 C
Mass flow rate	0.1 g/s
Power input	166 W
Column specific heat capacity	530 J/kgC
Sorbent specific heat capacity	2790 J/kgC
Desorption column thermal mass	2.54 kg
Sorbent thermal mass	0.45 kg

***Note:** The final temperature mentioned, is the desired desorption temperature. Which heavily depends on the power input and the mass flow rate, it is possible that in some cases of lower power input and higher mass flow rates, this temperature is not achieved. The same set of equations is used to determine the final temperature and time to steady-state during shut down. Except for the energy generation term, the desorption column is not consuming energy during this phase of operation and is only losing heat to the surroundings.

4.1.3 Algorithm

The external inputs such as power and ambient temperature are user inputs. Fluid and thermodynamic properties such as density and specific heat capacity are based on a weighted average calculation of the individual components of the loaded sorbent. The heat loss term in the energy equation is crucial. For this reason, the heat transfer coefficient has been obtained through the experimental data of this thesis. Specific parameters such as heat transfer and the system's thermal mass are system-specific and thus can be changed depending on the size and materials being used in the column. Figure 4.2 describes the flow of the MATLAB script to determine the final temperature and time taken by the system to reach a steady state.

4.1.4 Start-up Scenarios

Based on the design requirements for ZEF, different scenarios and conditions for start-up and shut down were developed. The scenarios are highlighted in Figure 4.3:

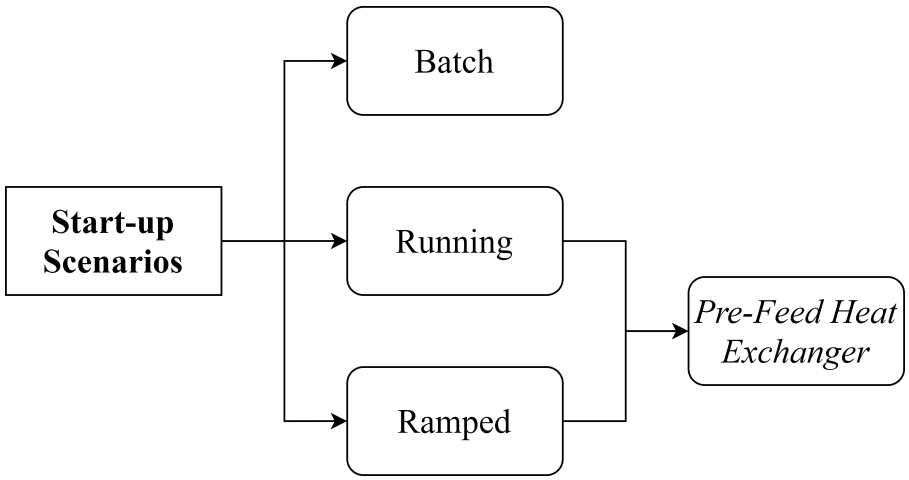

Figure 4.3: Different start-up scenarios identified.

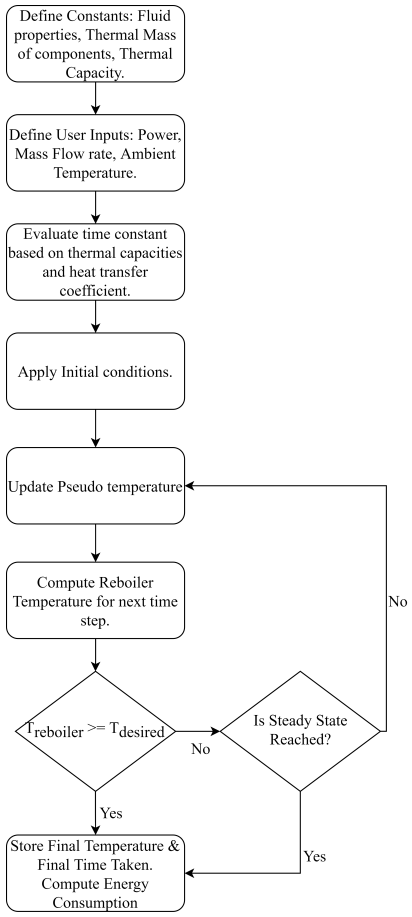

Figure 4.2: Flowchart representing the process flow of the start-up & shut-down model

4.2 Modelling: Integrated DAC Model

Based on experimental work in this thesis and previous work done at ZEF, an integrated model of the DAC subsystem was developed with a primary focus on understanding the dynamic behaviour of the desorption column in response to upstream fluctuations and external disturbances. **The desired outcomes of the model were to capture the variations in production capacity of DAC, the energy efficiency of the desorption process and the possibilities of developing an appropriate control philosophy for the DAC subsystem to maintain the top ratio of H_2O: CO_2 production to design spec levels.** The model was developed in MATLAB Simulink. Figure 4.4 depicts the different components of the model.

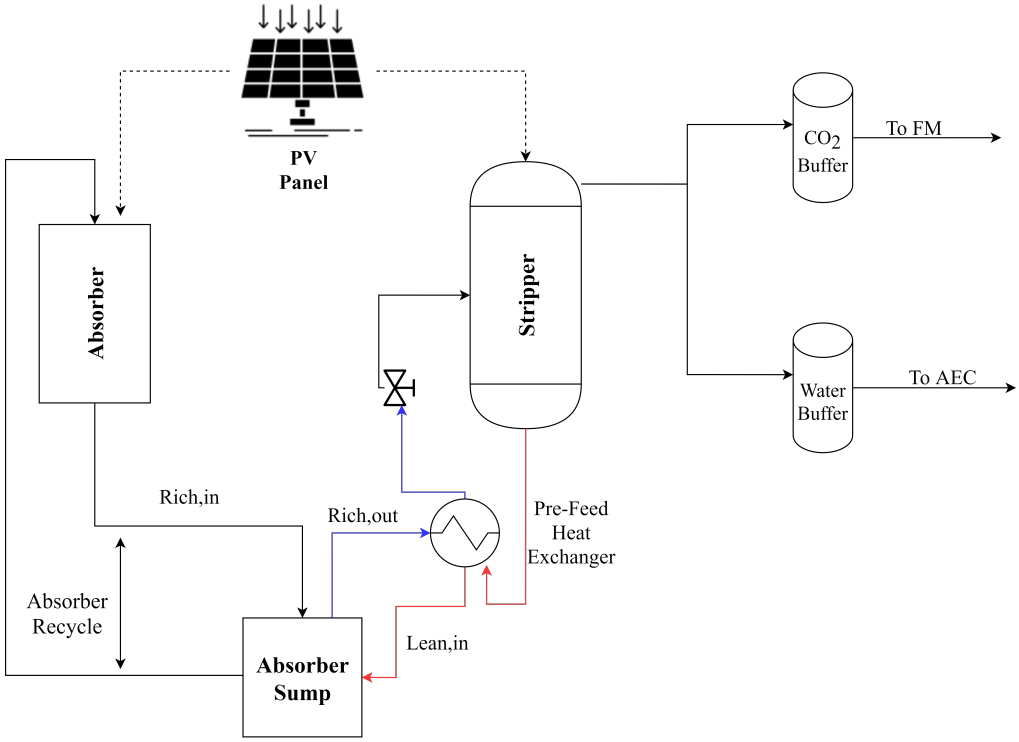

Figure 4.4: Schematic of the integrated DAC model

The model is divided into segments or 'micro models' for understanding. As depicted by Figure 4.5

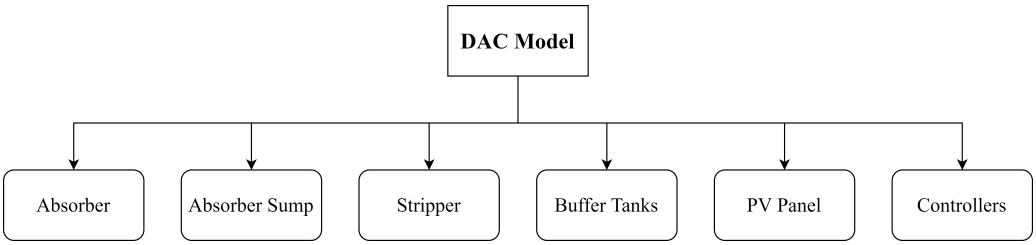

Figure 4.5: Components of the integrated DAC model

4.2.1 Micro-Model: Absorber

The absorber model has been designed based on experimental data from Mulder [41] for the suitable sorbent. The model doesn't dive deep into the mass transfer characteristics of the CO_2 and Water but instead focuses on the variations in sorbent loading based on the space-time yield curves.
Unlike earlier research, one cannot consider an absolute STY for the design of the absorber since that assumption holds during steady-state operation.Thus, the absorber model operates along a varying space-time yield curve for each of the absorbed species that depends on the factors depicted in Figure 4.6:

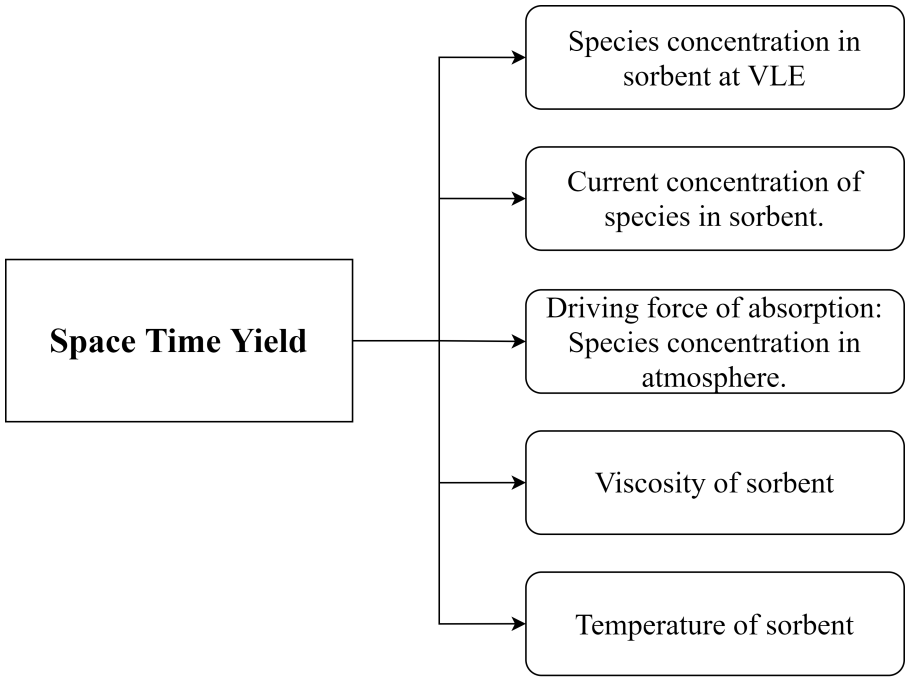

Figure 4.6: Factors determining the space time yield of a species during absorption

Absorber Model: Black Box

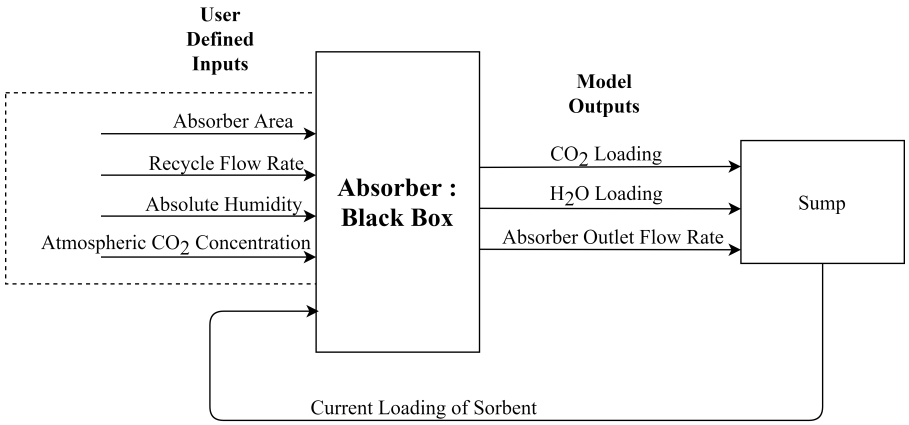

Figure 4.7: Schematic representing the black box approach for the absorber micro-model

The model works based on user-defined inputs specified externally, and internal inputs that are received from other parts of the integrated DAC model as shown in Figure 4.7. The absorber micro model converts these inputs into the new loadings of the sorbent based on the space-time yield curves. A detailed overview of the input and output parameters is provided in Table 4.3:

Table 4.3: Input & output parameters being used by the absorber micro-model

Model Inputs	**Units**
Absorber area	Sq. m
Recycle flow rate	Mol/s
Absolute humidity	Kg/m3
Atmospheric CO_2 concentration	Ppm
Current loading of sorbent*	Mol fraction
Model Outputs	
CO_2 Loading	Mol CO_2/kg TEPA
H_2O loading	Mol H_2O/kg TEPA
Absorber outlet flow rate	Mol/s

Assumptions

- **The effect of viscosity on the space-time yield of each absorbed species has been neglected due to the absence of relevant experimental data.** This is an important parameter considering that varying loadings significantly impact the sorbent's viscosity and thus the space-time yield.
- The **effect of ambient temperature on the absorption of CO_2 and H_2O has been neglected**.Although existing research suggests absorption favours lower temperatures, but the impact of temperature on the space time yield is yet unexplored. In the range of ambient temperatures that the system operates in, the partial pressure of CO_2 & H_2O in the vapour phase are very small, thus this assumption holds.
- **The absorption of CO_2 is assumed to be completely independent of the water loading of the sorbent.** This assumption needs to be experimentally verified, considering the addition of water affects the viscosity of the sorbent and is expected to affect the mass transfer rates.
- **The repumping rate is assumed to be a constant,** and thus we have a constant residence time over the absorber. Realistically, there will be small changes in the residence time due to the absorption of water into the sorbent, which in turn changes the volume and viscosity.

Absorber Model: Algorithm

A detailed flowchart of how the model converts the specified inputs into the desired outputs is given in Figure 4.8:

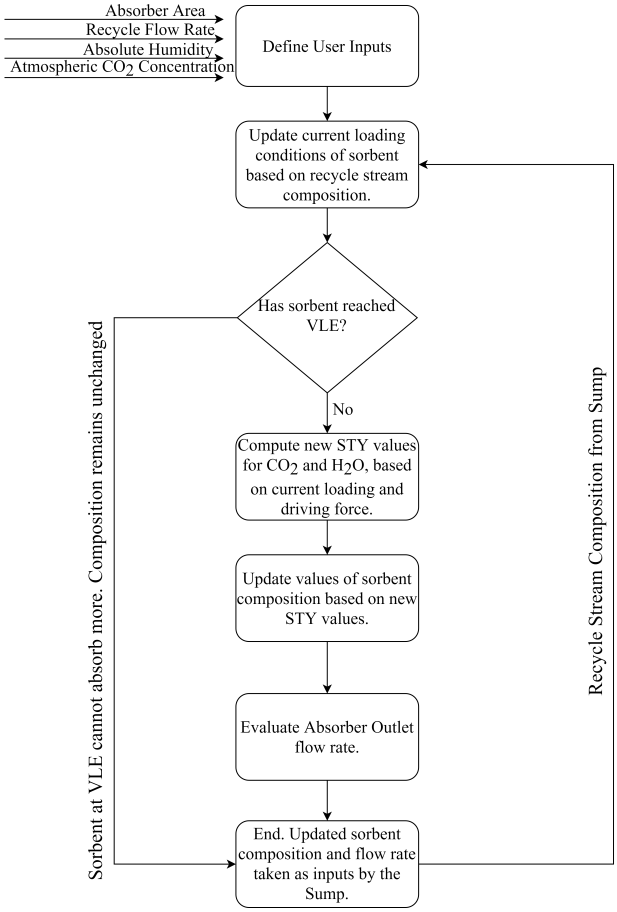

Figure 4.8: Flowchart representing the process flow of the absorber micro-model

Based on experimental data, space-time yield curves were developed for CO_2 and H_2O, relevant information is available in the appendix.

4.2.2 Micro-model: Absorber Sump

The purpose of the absorber sump is to dampen the effect of the fluctuating sorbent loading on the desorption column's production and thus ensure smoother operations for subsystems downstream. The sump is modelled as a constantly stirred mix tank, devoid of chemical reactions.

$$\frac{dN}{dt} = (F_{absorber} z_{absorber} + F_{lean} z_{lean} - F_{recycle} z_{recycle} - F_{stripper,in} z_{stripper,in}) \quad (mol/s) \tag{4.2}$$

Based on the model equation, the size of the sump influences the dampening effect. Thus, the model aims to predict an appropriate size of the sump, capable of handling the daily and seasonal fluctuations in sorbent loading.

Absorber Sump: Black Box

Figure 4.9 depicts the sump model. It converts the compositions and flow rates of the input streams from the absorber and desorption column into an averaged output composition based on the CSTR equation. The sump volume is the only user-defined input that is used repeatedly in the model, while the rest are sourced internally from the absorber and stripper micro models. The inputs and outputs to the model are highlighted in Table 4.4:

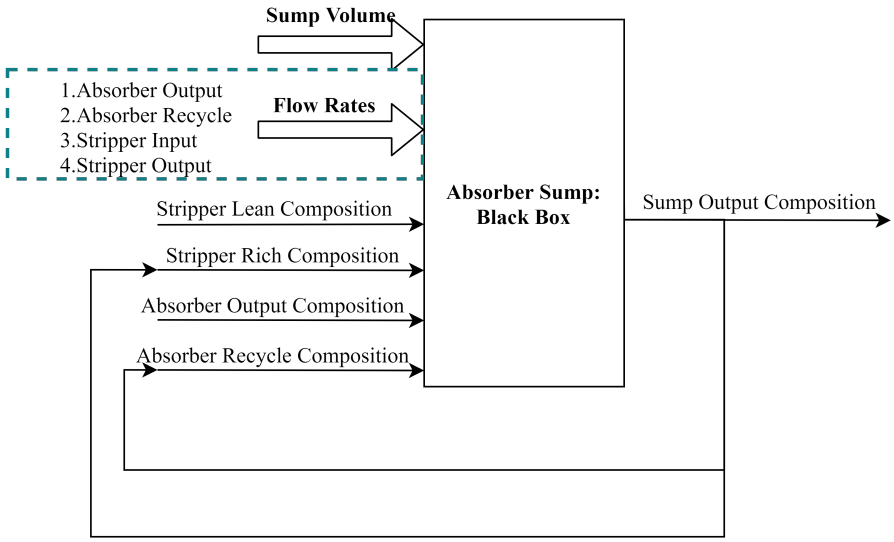

Figure 4.9: Schematic representing the black box approach for the absorber sump micro-model

Table 4.4: Model inputs and outputs for the absorber sump micro-model

Model Inputs	**Units**
Sump volume	Cubic meter
Absorber outlet flow rate	Mol/s
Absorber recycle flow rate	Mol/s
Stripper input flow rate	Mol/s
Stripper output flow rate	Mol/s
Absorber output composition	Mol fraction
Stripper output composition	Mol fraction
Stripper input composition	Mol fraction
Absorber recycle composition	Mol fraction
Model Outputs	
Sump output composition	Mol fraction

Assumptions

- **The composition inside the sump is assumed to be uniform**.
- **No chemical reactions take place inside the sump**.This assumption is valid considering no absorption of CO_2 and H_2O take place in the sump provided it is closed from the atmosphere.
- **The effect of heat transfer due to the mixing of incoming streams at different temperatures has been neglected**. This assumption is valid considering the flow rates of the high-temperature streams from the stripper column are an order of magnitude lower than the absorber flow rates. Thus, the sump temperature remains more or less at the ambient levels.

Absorber Sump: Algorithm

A detailed flowchart of how the model converts the specified inputs into the desired outputs is given in Figure 4.10:

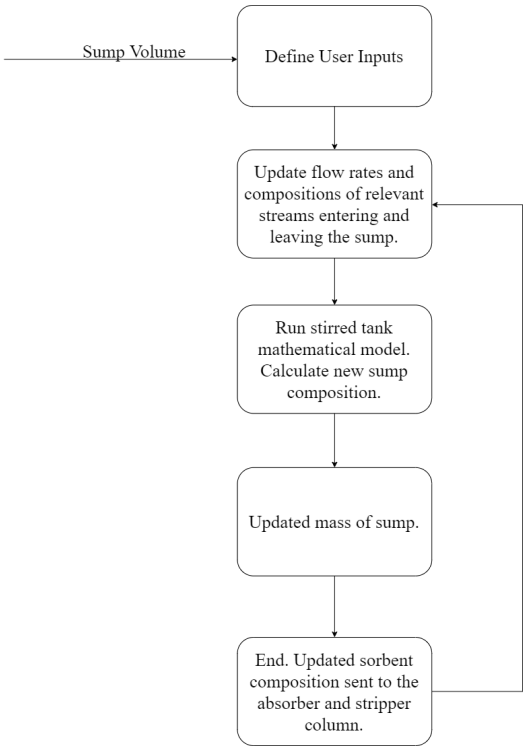

Figure 4.10: Flowchart representing the process flow of the absorber sump micro-model

4.2.3 Micro-model: Desorption column

The model of the desorption column is the core of the integrated DAC model. The desorption column comprises multiple stages. After taking in specific user-defined inputs and initial guesses, the model uses the Rashford-rice methodology to solve each stage's mass balance equations and energy balance equations. The outputs are then compared to their initial values or guesses. Depending on the error tolerance, the model moves on to the next iteration by updating the value of the initial guess with the computed output. If the error value is small enough and satisfies the criteria, the model converges and delivers the final results. The flow of information and calculations in the model is highlighted in the following sections:

Partial Pressure: CO_2 & H_2O

To compute the outputs from each stage of the column, partial pressure data for CO_2 and H_2O is required corresponding to different temperatures. It is not practically feasible to obtain vapour curves and VLE data through experiments for all ranges of operating temperatures and compositions. Thus, the experimental data for the TEPA-PEG quaternary system is accurately fit, following which the Clausius-Clapeyron equation is used to evaluate the partial pressures at different temperatures while using a known value as the reference or starting point. In this fashion, an entire field of VLE isotherms is obtained.

$$\ln\left(\frac{P_2}{P_1}\right) = \frac{\Delta \mathrm{H}_{absorption}}{R}\left(\frac{1}{T_2} - \frac{1}{T_1}\right) \tag{4.3}$$

Once the vapour curve and VLE data for the sorbent are accurately fitted and isotherms plotted, the partial pressures of CO_2 and H_2O are obtained from these data sets to function the desorption column model. The two functions are highlighted below :

$$P_{CO_2} = f(T, L, w) \tag{4.4}$$

$$P_{H_2O} = f(T, x) \tag{4.5}$$

The partial pressure of water is evaluated from modified Raoult's law, as it takes into account the liquid phase non-idealities.

$$y_i \phi_i P_{tot} = x_i \gamma_i P_i^{sat} \tag{4.6}$$

The saturation pressure of pure water is evaluated using Antoine's equation. Sufficient data for Antoine's coefficients is available for water.

$$\log_{10} P_{H_2O}^{sat}(T) = A - \frac{B}{C + T} \tag{4.7}$$

The activity coefficient for water used in Raoult's law is evaluated using Wilson's theory for binary system. The Wilson's parameters are tweaked till the resulting output of partial pressure of water matches the experimental data from vapour curves.

$$\ln(\gamma_1) = -\ln(x_1 + \Lambda_{12} x_2) + x_2 \left[\frac{\Lambda_{12}}{x_1 + \Lambda_{12} x_2} - \frac{\Lambda_{21}}{x_2 + \Lambda_{21} x_1} \right] \tag{4.8}$$

Finally, the partial pressure of water is calculated by using Raoult's law while neglecting the vapour phase non ideality.

$$p_{H_2O} = \gamma_1 x_1 P_{H_2O}^{sat}(T) \tag{4.9}$$

Single-stage model

Solving the mass and energy balances for each stage individually is the crux of the desorption model. For our understanding, a single stage of the column can be simplified to a flash tank.

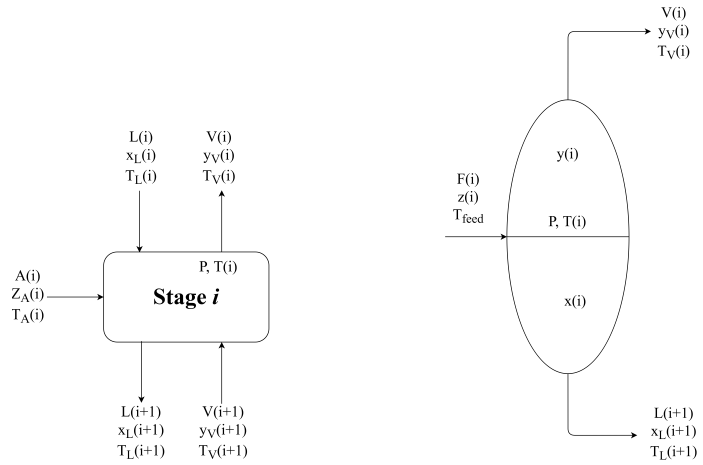

Figure 4.11: Simplification of a single stage i to a flash tank i at P and T(i) including the relevant mass flows, compositions and temperatures with (a) single stage i and (b) flash tank i.

The incoming mass flows into the stage are combined into a single mass flow F_i which has a composition z_i.

$$F_i = A_i + L_i + V_{i+1} \tag{4.10}$$

$$z_{i,j} = \frac{A_i z_{A_{i,j}} + L_i x_{i,j} + V_{i+1} y_{i+1,j}}{F_i} \tag{4.11}$$

Mass Balance

The mass balance at each stage or flash takes into account the overall and component-specific mass flow of incoming and outgoing streams.

$$F_i - L_{i+1} - V_i = 0 \tag{4.12}$$

$$F_i z_{i,j} - L_{i+1} x_{i+1,j} - V_i y_{i,j} = 0 \tag{4.13}$$

To solve the mass balance equations, an iterative method is required based on initial guesses. The rashford -rice equation is used to find the iterative solution.

$$x_{i,j} = \frac{z_{i,j}}{1 + \beta(K_j - 1)} \tag{4.14}$$

Although this method is time-intensive, the benefit is that it always converges.

Energy Balance

The energy balance in each stage has to take the sensible heating of the sorbent, the heat of absorption or desorption associated with each stream entering and leaving the stage. The losses for the stripper are accounted for in the power being supplied to the column, an explanation for this is given in later sections. The following equation gives the overall energy balance:

$$Q_{tot_i} = Q_{L_i} + Q_{V_i} + Q_{A_i} + Q_{abs_i} \tag{4.15}$$

The equations for the individual components for the energy balance are highlighted below:

$$Q_{L_i} = \sum_{j=1}^{C} L_i x_{i,j} c_{p,liq} (T_{L_i} - T_i) \tag{4.16}$$

$$Q_{V_i} = \sum_{j=1}^{C} V_{i+1} y_{i+1,j} c_{p,vap} (T_{V_{i+1}} - T_i) \tag{4.17}$$

$$Q_{A_i} = \sum_{j=1}^{C} A_i z_{A_{i,j}} c_{p,liq} (T_{A,i} - T_i) \tag{4.18}$$

$$Q_{abs_i} = \sum_{j=1}^{C} (V_{i+1} y_{i+1,j} - V_i y_{i,j}) H_{abs} \tag{4.19}$$

Note: When the amount of vapour leaving the stage is greater than the amount entering, the effect of desorption is dominant and thus the process consumes energy. The total energy consumed by each stage is used to compute the temperature at each stage. Firstly, the average specific heat capacity of the streams entering the stage is calculated and multiplied with the overall mass flow rate of the input streams. This represents the enthalpy entering the stage. Since heat losses have been accounted, and energy is conserved, the incoming enthalpy should be equal to the enthalpy leaving the stage. Which is a product of the average thermal capacity of each stream and the respective mass flow rate of the vapour and liquid phases.

$$F_i c_p = \sum_{j=1}^{C} L_{i+1} x_{i+1,j} c_{p_{liq}} + \sum_{j=1}^{C} V_i y_{i,j} c_{p_{vap}} \tag{4.20}$$

The differential change in temperature is calculated using the total energy consumed.

$$dT_i = \frac{Q_{tot_i}}{F_i c_p} \tag{4.21}$$

Which is then used to update the initial temperature.

$$T_{new,i} = T_i + \frac{dT_i}{500} \tag{4.22}$$

The flowchart of the energy balance and the updating of temperature is highlighted below:

Multi-stage model

The multi-stage model is an extension of the single-stage version. For a 'N' staged column, the top stage is labelled as 1, while the reboiler is stage N.

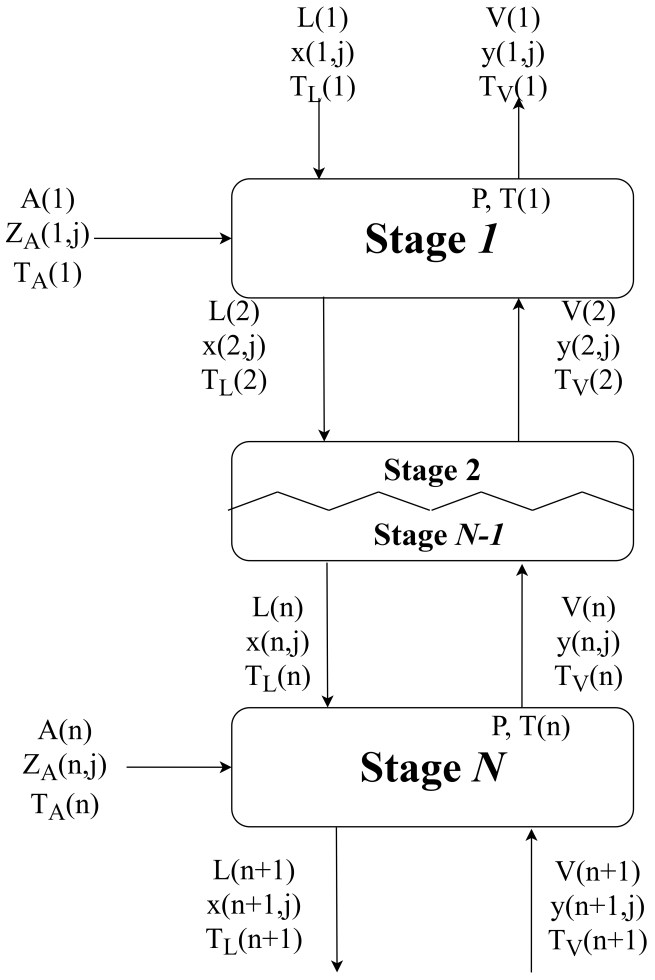

Figure 4.12: Schematic representation of a multi stage model in a desorption column

Note: No vapour stream enters the reboiler, thus V_{n+1}=0. Similarly, the liquid stream entering the top stage is the reflux. The reflux is a function of the vapour stream leaving the top stage and is assumed to be pure H_2O.

$$L_1 = V_1 y_{1,2} \frac{R}{1+R} \tag{4.23}$$

Assumptions

- **Heat losses in the stripper column are assumed to be constant and accounted for in the power input to the column.** During operation a Δ T exists between the system and surroundings, which is used to evaluate the heat losses. For a well insulated column, the temperature fluctuations inside the column are minimal and thus a constant average temperature difference can be used to approximate the heat losses during steady state operation subsection D.0.3 .
- At every time step, the column is assumed to be at equilibrium. In other words, the outputs we observe are derived from the VLE and vapour curve at equilibrium conditions.
- The TEPA+PEG mixture is assumed to be a non-volatile component. Thus the vapour phase contains only water and CO_2.
- The thermodynamic properties such as the specific heat and the heat of desorption of the different components are assumed to be constant.
- The vapour curves for water, reflect the partial pressure of H_2O alone. It is assumed the presence of CO_2 in the vapour phase has a negligible effect on the vapour curve of H_2O. Essentially, the desorption of H_2O is independent of the CO_2 present.[25]
- A pre-feed heat exchanger is assumed to heat the rich stream to a temperature 10 °C below the reboiler temperature while taking energy from the hot lean stream leaving the stripper column.

4.2.4 Micro-model: Buffer tank

Philosophy

The need for a CO_2 and water buffer arises due to the varying throughput of the desorption column. The production of carbon dioxide and water vapour depends on the following factors:

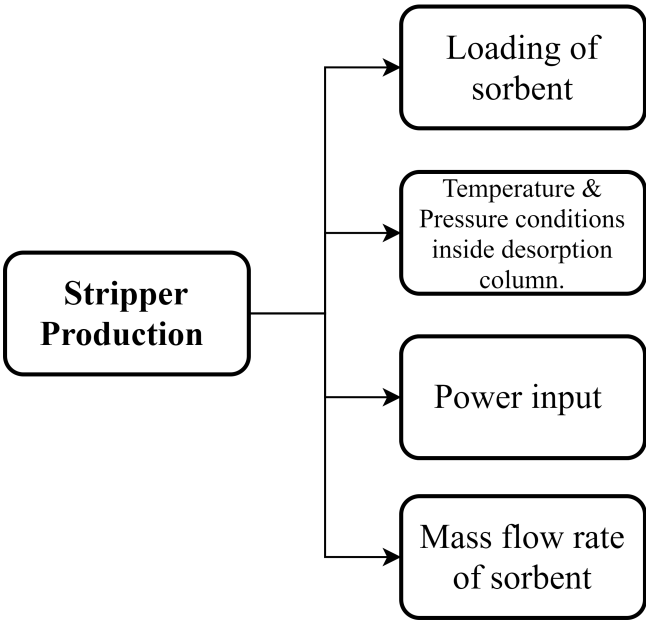

Figure 4.13: Factors affecting the production of CO_2 and H_2O

ZEF aims to run the DAC using energy from a PV panel. Naturally, the varying output of the panel influences the internal stripper conditions, thus the throughput. In periods of sufficient power input, it is possible to have a production surplus, but we can expect a production deficit during periods of insufficient power.

Buffer Tank: Black Box

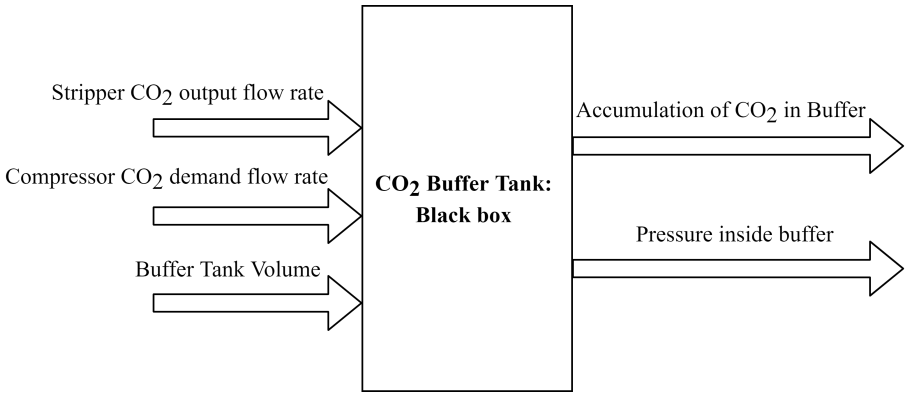

Figure 4.14: Schematic representing the black box approach for the CO_2 buffer tank micro-model

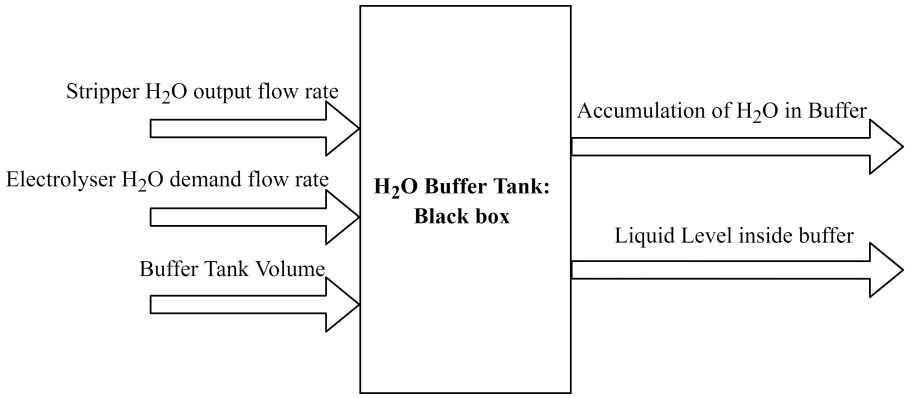

Figure 4.15: Schematic representing the black box approach for the H_2O buffer tank micro-model

The buffer tank model for CO_2 (Figure 4.14) and H_2O (Figure 4.15) performs a mass balance based on the species' incoming and outgoing flow rates, respectively. The output is a reflection of the amount of CO_2 and H_2O accumulated in the tanks.

Table 4.5: Model inputs and output parameters for the Carbon dioxide buffer tank micro-model

Model Input (CO_2 Buffer)	**Units**
Stripper CO_2 output flow rate	Mol/s
Compressor CO_2 demand flow rate	Mol/s
Volume of buffer	Cubic meter or litres
Model Output	
Accumulation of CO_2 in buffer	Moles, kg
Pressure inside buffer	bar

The sizing of the buffer tanks is a design input and has been dealt with later.

Assumptions

- Pure components are assumed to accumulate in the respective buffer tanks. This assumption is valid considering a complete separation of the product species is achievable on proper flashing and condensation of the vapour liberated after desorption.
- The pumping power to transfer the products into the buffer tanks has been neglected.

Table 4.6: Input and output parameters for the water buffer tank micro-model

Model Input (H_2O Buffer)	**Units**
Stripper H_2O output flow rate	Mol/s
Electrolyser H_2O demand flow rate	Mol/s
Volume of buffer	Cubic meter or litres
Model Output	
Accumulation of H_2O in buffer	Moles, kg
Liquid volume inside buffer	litres

Buffer Tank: Algorithm

A detailed flowchart of how the model converts the specified inputs into the desired outputs is given in Figure 4.18:

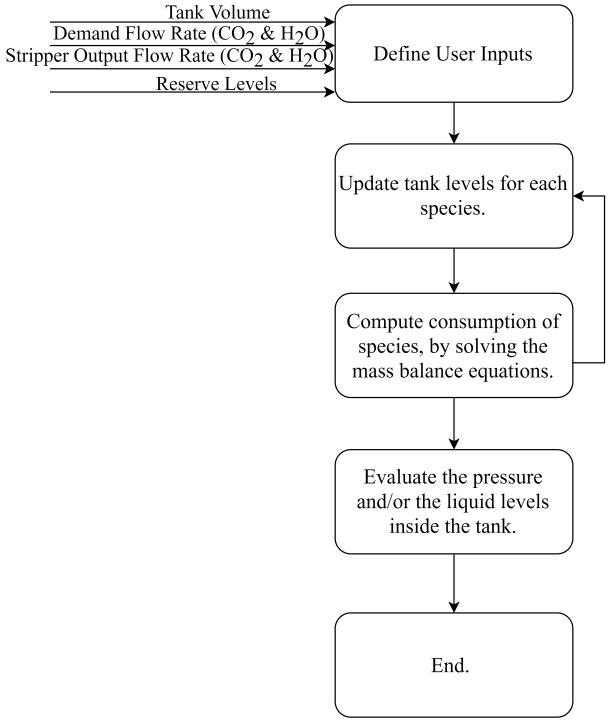

Figure 4.16: Flowchart representing the process flow of the buffer tank micro-models

4.2.5 Micro-model: PV Panel

The model delivers the electrical power output based on the incident solar radiation and ambient temperature. The model comprises two layers as shown in Figure 4.17:

- **Thermal Layer:** This part of the model is designed to calculate the panel's temperature by solving the energy balance equations. It takes into account the incoming solar radiation, convective and radiative heat losses to the surroundings.

$$T_{sky} = 0.0552 \times T_{ambient}^{3/2} \tag{4.24}$$

$$G \cdot A - h_{conv} \cdot A \cdot (T_{panel} - T_{ambient}) - h_{rad} \cdot A \cdot (T_{panel} - T_{sky}) = 0 \tag{4.25}$$

- **Electrical Layer:** This part of the model is designed to predict the power output from the panel based on the panel temperature obtained from the 'Thermal Layer' and the incident solar

radiation. *The electrical layer is grossly simplified since the accurate modelling of a PV panel is not the primary scope of this thesis.*

$$I_{load} = \left(\frac{G_{incident}}{G_{ref}}\right) \cdot (I_{isc} + K_{isc} \cdot (T_{panel} - T_{ref})) \tag{4.26}$$

$$P = I_{load} \cdot V \tag{4.27}$$

PV Panel: Black box

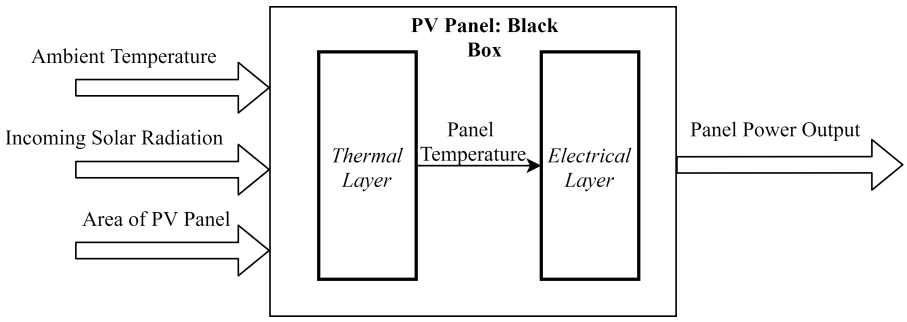

Figure 4.17: Schematic representing the black box approach for the PV panel micro-model

Table 4.7: Input and output parameters for the PV panel micro-model

Model Inputs	**Units**
Ambient temperature	Celsius
Incoming solar radiation	W/m2
Area of PV panel	Sq. m
Model Output	
Panel Power Output	Watts

Assumptions

- Heat transfer in the thermal layer is assumed to be one dimensional and quasi-steady state. This assumption is valid since the panel's thickness is minimal compared to the rest of the dimensions.
- The thermal capacities of the PV panel are assumed to be negligible. Thus the effect of thermal storage is neglected. Any changes in the ambient temperature and incoming solar radiation are reflected immediately in the panel temperature.
- The thermal conductivity of the panel is assumed to be a constant, and the average temperature of the panel is uniform.
- The photocurrent developed by the panel is assumed to be the final output from the panel since the shunt resistance in the electrical circuit has infinite resistance, and the line resistance is negligible. Realistically the photocurrent will differ slightly from the load current.
- The operating voltage of the panel is constant. The effect of temperature and solar radiation on the operating voltage is neglected. It is possible to achieve this using complex electrical structures, the modelling of which remains outside the scope of this thesis.

PV Panel: Algorithm

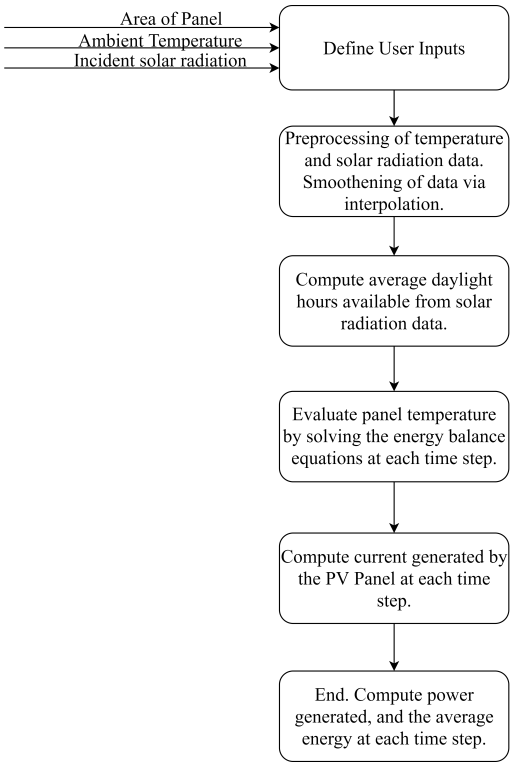

Figure 4.18: Flowchart representing the process flow of the PV panel micro-model

4.2.6 Micro model: Control Scheme

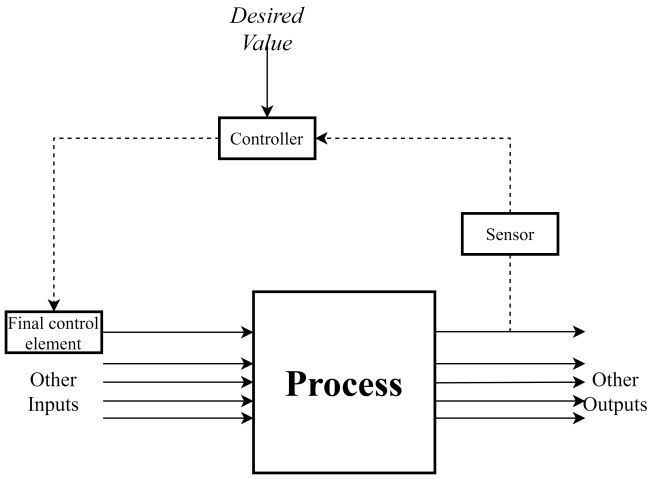

Figure 4.19: Schematic representing a typical feedback control loop

Control is necessary to deal with external disturbances or a change in the desired value of the output. *The variable whose value is to be maintained at the desired level is called the* **control variable.** *The selected process variables to be adjusted are termed as* **manipulated variables**, *and external inputs that are beyond the scope of control but have an influence on the process are termed* **external disturbances** [36].
The process variables for the desorption column in DAC have been depicted in the Figure 4.20:

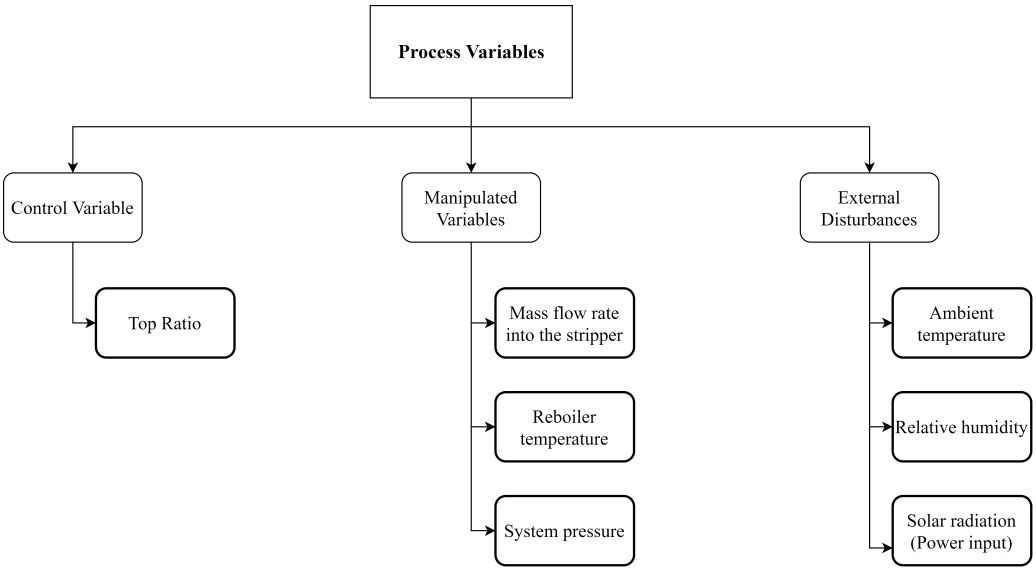

Figure 4.20: Process variables of the DAC subsystem

Control Loops

From the schematic, it was clear that the manipulated variables available for adjustment were limited. The design started off with a basic single-loop control and then evolved into the final control scheme.

- **Mass flow control:** Starting with single loop control, the design focuses on reboiler temperature control. The setpoint is decided based on median values of water loading for different months in the year. Thus to maintain a constant temperature and respond to the fluctuations in power, the controller adjusts the mass flow rate accordingly. Figure 4.21 depicts the mass flow control scheme.

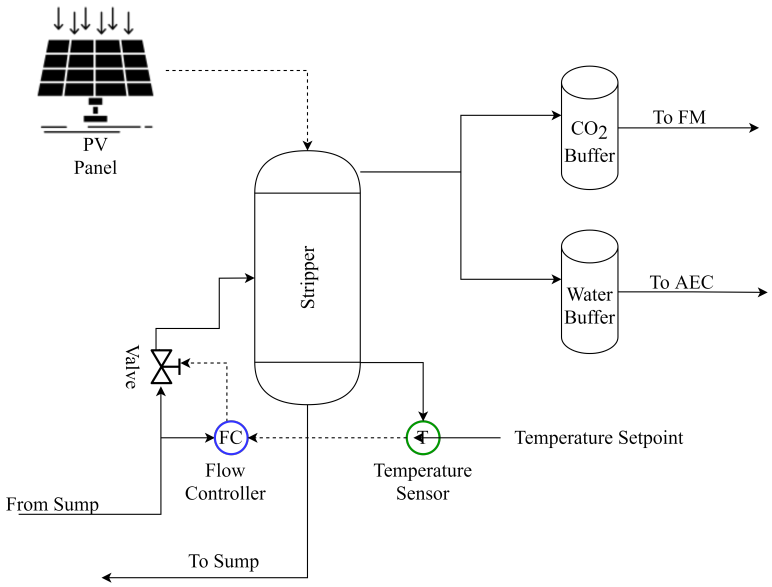

Figure 4.21: Schematic representation of the mass-flow control loop

- **Mass flow-temperature cascade control:** The setpoint for the top-ratio is user-defined, which manipulates the temperature setpoint for the secondary control loop. The latter adjusts

the mass flow rate accordingly to maintain the reboiler temperature. The scheme is represented in Figure 4.22

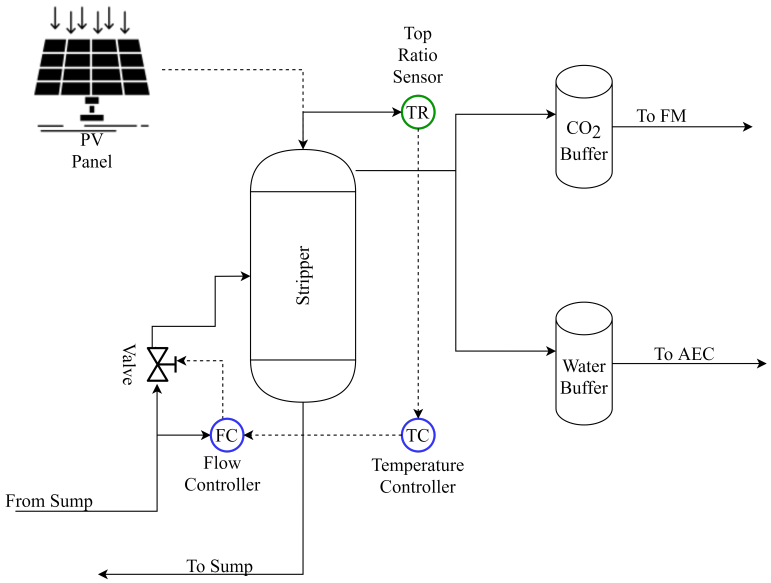

Figure 4.22: Schematic representation of the mass-temperature cascade control loop

- **Pressure control:** The top ratio is the control variable, and the column pressure is the manipulated variable. The setpoint is user-defined, and according to changes in the top ratio, the pressure is adjusted accordingly. In this case, the temperature of the reboiler remains constant (Figure 4.23).

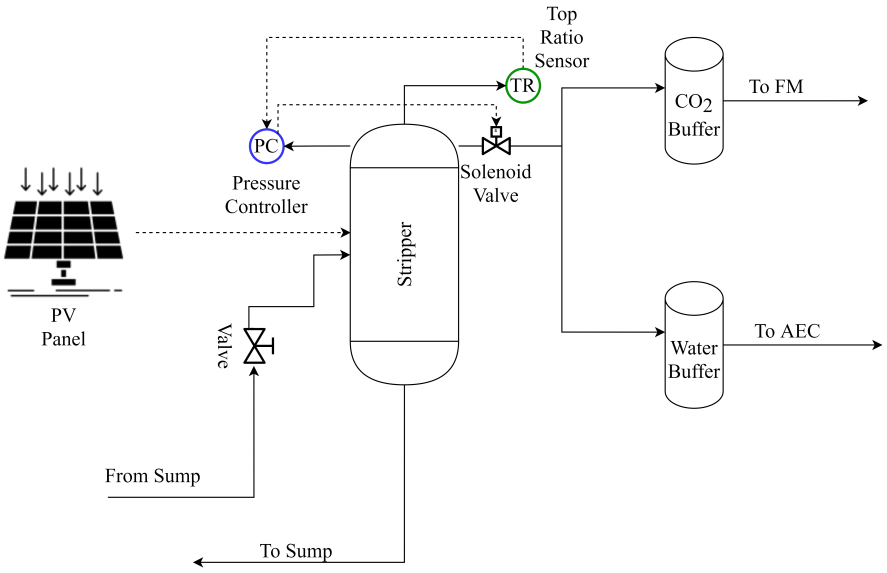

Figure 4.23: Schematic representation of the pressure control loop

Final Control Scheme

The final design involves a parallel action of cascade and single-loop control, acting on different process variables as shown in Figure 6.4.

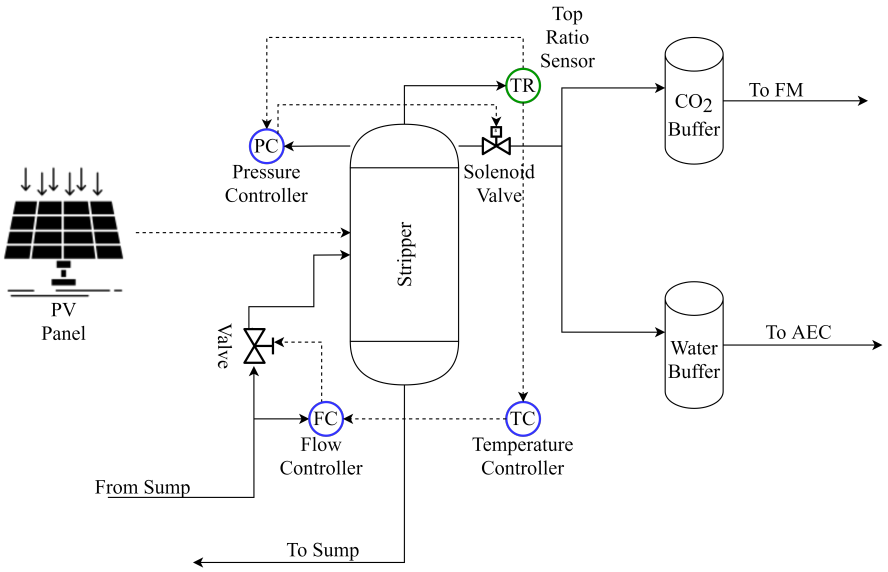

Figure 4.24: Schematic representation of the final control scheme

The action of each controller depends on how the top ratio responds to changes in temperature and pressure. It is observed that when the top ratio is above the setpoint, it is required to lower the operating temperature and increase the system pressure. Similarly, when the reboiler temperature is above the setpoint, it is required to increase the mass flow rate of the sorbent into the column [36]. Thus, the control action for the controllers is listed in Table 4.8:

Table 4.8: Controller action

Controller	**Control Action**
Mass flow controller	Direct acting
Temperature controller	Reverse acting
Pressure controller	Direct acting

Controller Limits

To counter the disturbances and maintain the control variable's value, ideally, the manipulated variables can attain any values dictated by the controllers. Practically, these significant adjustments are usually not feasible due to process constraints. Thus, each controller has a specified output saturation that ensures the process constraints are not violated while dealing with the disturbances [36]. The limits are listed in Table 4.9.

Table 4.9: Controller saturation limits

Controller	**Lower Limit**	**Upper Limit**	**Reason**
Mass flow	1e-3 mol/s	0.05 mol/s	The lower limit corresponds to the minimum load conditions of the pump, and the upper limit has been identified on the basis of historical performance data.
Temperature	102 Celsius	120 Celsius	The lower limit corresponds to the single phase limit within the desorption column, while higher temperatures are possible for the upper limit, 120 is the cap set by ZEF to minimize sorbent thermal degradation.
Pressure	1 Bar	1.5 Bar	The lower limit is set as a cap by DAC, ideally it would be possible to operate at higher upper limits, but the possibility of implementing higher pressure limits needs to be investigated.

Chapter 5

Results & Discussions

This chapter provides answers to the research objectives identified in Chapter 1. Each research objective is highlighted, followed by a detailed description of the results obtained via experiments and simulations.

> ***Research Objective 1:*** *What is the impact of varying environmental conditions (disturbances: relative humidity, temperature and solar radiation)* ***on the inputs to the desorption column****?*

- The **direct impact of the external disturbances on the inputs to the desorption column (sorbent composition and PV Panel output) are termed *first-order effects***
- The **effect of disturbances on the performance of the desorption column are termed as *second-order effects*** as indicated in Figure 5.1.

5.1 First Order Effects : Absorption

The impact of external variations in the ambient conditions on the rich loading of the sorbent has been investigated in the past at zero-emission fuels via Mulder[41].

5.1.1 Absorption: H_2O

The changes in relative humidity are observed to impact the amount of water absorbed by the sorbent significantly. This was obtained from the airfarm experiments conducted by Mulder [41] to simulate the performance of different sorbents under different climatic conditions.

- As the relative humidity changed from 25% (Sahara climate) to 60% (Mediterranean climate), it increased the water loading from 5-10% to 23-26% [41]. The equilibrium loading for water is reached within 24 hours of testing, much faster than the rate of CO_2 absorption. The increase in the water absorption reduces the viscosity of the sorbent. Reduced viscosity is beneficial in terms of lower frictional losses while pumping the sorbent, and it also promotes better mass transfer. Figure 5.2 depicts the variation of water loading of sorbent with the change in absolute humidity.

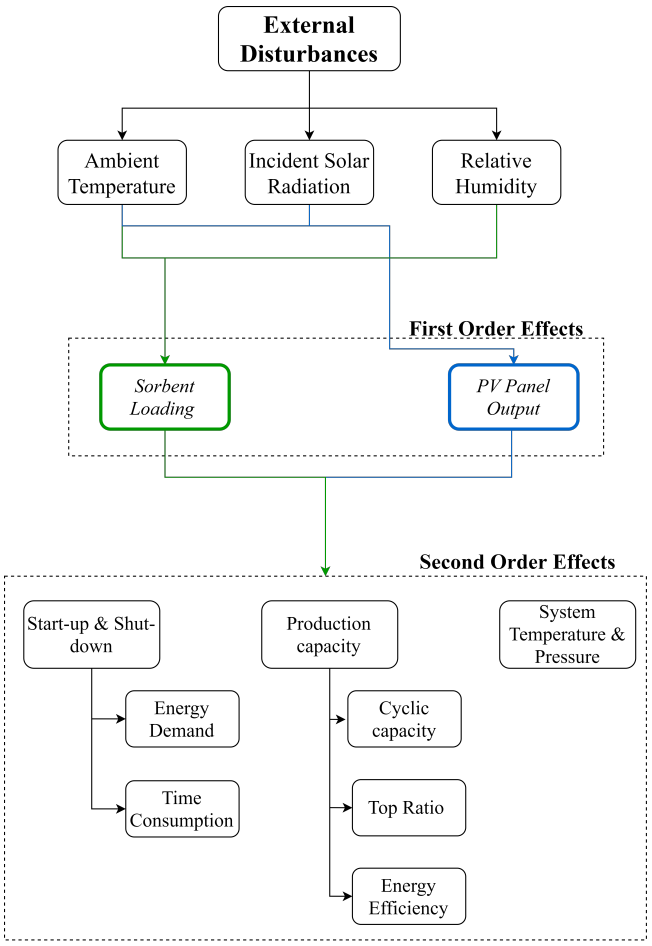

Figure 5.1: Resultant first order and second order effects of the external disturbances onto the DAC process

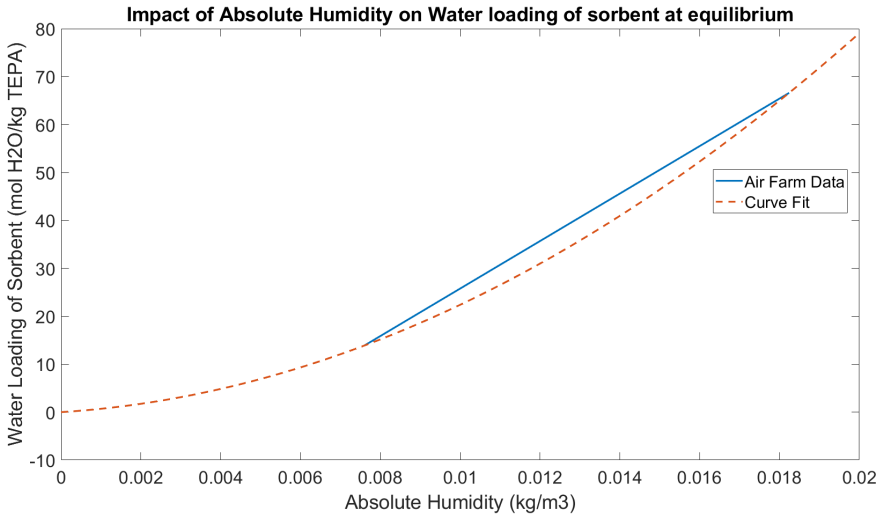

Figure 5.2: Impact of increasing absolute humidity on the equilibrium water loading of the sorbent.

5.1.2 Absorption: CO_2

- The driving force, i.e. the partial pressure of CO_2 in the atmosphere, remains constant over the time scales concerned. The relative humidity conditions indirectly impact the CO_2 loading.

Increasing relative humidity results in a higher H_2O loading, decreasing the viscosity of the sorbent. Lower viscosity, enhances mass transfer , therefore higher CO_2 loadings are possible.

5.1.3 Absorption: Conclusion

It is clear from existing research at ZEF that CO_2 and H_2O are absorbed via different mechanisms, while the process for absorption is diffusion-limited.**The space-time yields for H_2O are an order of magnitude higher than CO_2. Naturally, the equilibrium loading of H_2O is achieved much faster than the equilibrium loading of CO_2. Therefore, the design of the absorber is decided by the rate of absorption of carbon dioxide, not water.** Moreover, it is evident from the air farm data, that the sorbent composition, especially **the water loading is significantly affected by the absolute humidity. Thus, it is expected the sorbent composition will vary on short time scales and will have an impact on the production of components from the desorption column.**

5.2 First Order Effects: PV Panel Output

- **Short term variation:** Over a day, the incident solar radiation increases gradually from sunrise, reaches a peak at midday and then declines slowly till the sunsets. **Under clear skies and sunny conditions, the output from the panel will follow the trend of the incident solar radiation for a couple of hours. The periodic dip in the panel's production at midday corresponds to the decrease in panel efficiency due to increased panel temperature as shown in Figure 5.3.**

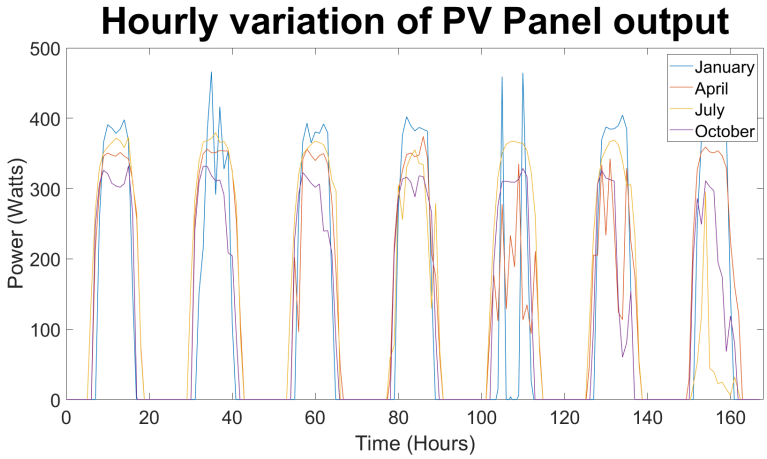

Figure 5.3: Hourly variation in PV panel output over seasons in Bechar,Algeria (Sahara climate), based on historical weather data for the year 2016 [42]

Sudden changes in the panel's output are possible depending on local weather phenomena, such as dust storms covering the panel surface, a stream of clouds covering the sun momentarily, or a thunderstorm. These events aren't periodic but are often statistically possible.

- **Long term variation:** In the long run, the general profile of the panel output remains the same. **But depending on the time of the year, the amount of daylight available also changes (Figure 5.4). Thus, the number of daylight hours available directly impacts the power output and, naturally the operating window of the system.** These variations are cyclical.

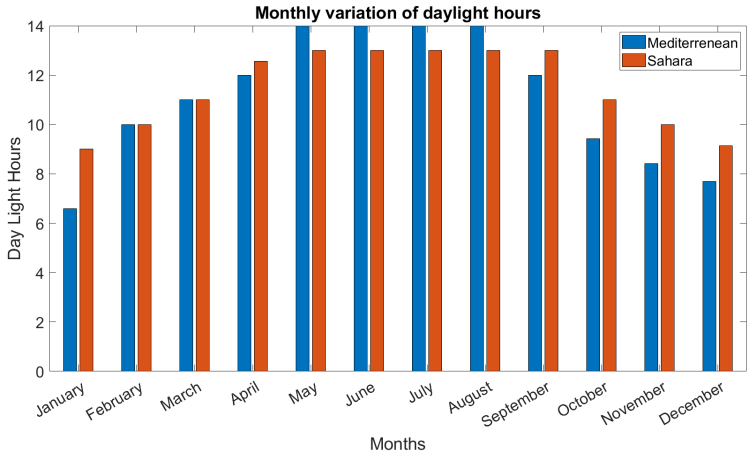

Figure 5.4: Monthly variation of daylight hours at two different locations. Bechar, Algeria (Sahara climate) and Oleiros, Portugal (Mediterranean climate). Based on average values from historical weather data for the year 2016 [42]

- **Location-based variation:** The incident solar radiation and the average number of daylight hours available also vary significantly across seasons depending on the site's location. **Seasonal variations are more pronounced as we move away from the equator, as seen in Figure 5.4 Portugal has a much higher variation in the number of daylight hours, as compared to Algeria. Since the latter is much closer to the equator**.

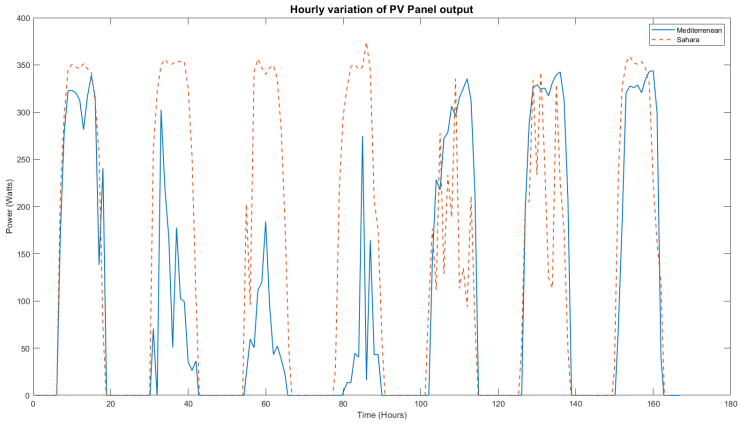

Figure 5.5: Hourly variation of PV Panel output at two different locations, for the month of April. Bechar, Algeria (Sahara climate) and Oleiros, Portugal (Mediterranean climate). Based on historical weather data for the year 2016 [42]

5.2.1 PV Panel Output : Conclusions

- **The output from the panel determines the operating window and the sequence of operations of the DAC subsystem.** The energy demand of each subsystem at ZEF and the functional window determine the power distribution philosophy of the process. Figure 5.6 depicts the variation in the energy production:

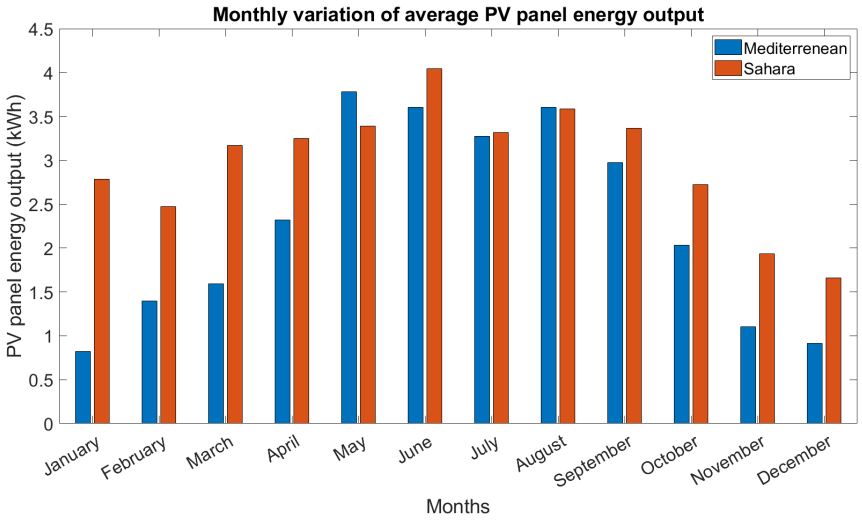

Figure 5.6: Daily average energy production from a PV Panel based on historical data for Bechar, Algeria (Sahara climate) and Oleiros, Portugal (Mediterranean climate). Based on historical weather data for the year 2016 [42]

- **The output from the PV panel remains consistent for the Sahara climate compared to the Mediterranean climate (Figure 5.5).** Therefore, it can be expected that short term variations in the PV panel output (Figure 5.3) in the **Mediterranean climate will have a greater impact on the production capacity of the *desorption column*, than the Sahara climate.**

  Q 2: *What is the impact of start-up and shut-down on the operation window of the desorption column? What are the factors influencing the start-up of the column ?*

5.3 Second Order Effects: Start-up & Shut-down

It is necessary to quantify the start-up's impact and shut down on the column's steady-state performance window. This section aims to give insights into the factors that affect start-up and shut down, the possibilities for starting up and finally, the criteria for starting up and shutting down the desorption operation and how the first-order effects influence it.

5.3.1 Experimental Observations

A set of experiments were performed to understand the transient response of a desorption column under conditions, such as constant sorbent loading and power input. The energy demand and the time consumed by the system during start-up were monitored. The start-up times observed are recorded in Table 5.1.

Table 5.1: Results of the start-up experiments.

Experiment Number	Start-up Time (seconds)
1	6144
2	5866
3	4435
4	3755
5	7392

The temperature curves for a typical experiment are depicted in Figure 5.7.

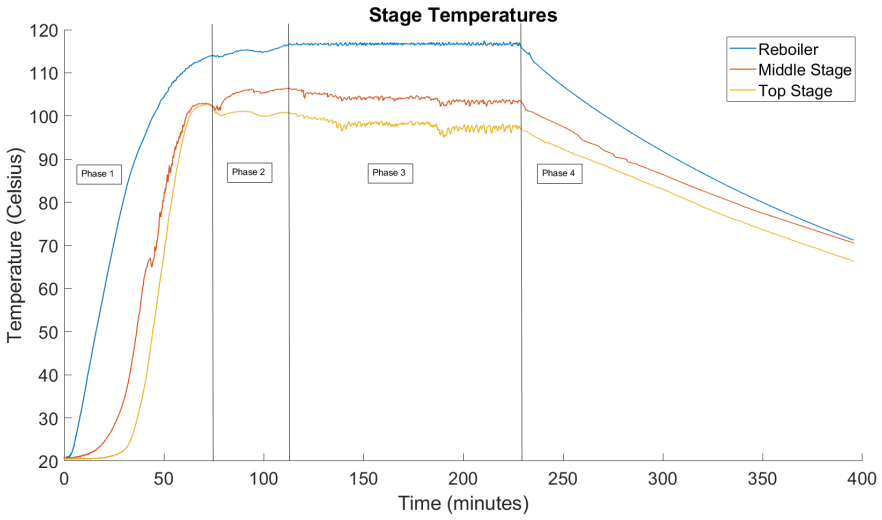

Figure 5.7: Temperature variation in the stages, across an entire experiment. Each line demarcates the start and end of a phase

Figure 5.7 highlights the four phases of the experiment as indicated in Figure 5.8, and each phase is explained in detail in the Appendix D.

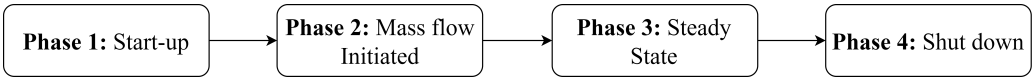

Figure 5.8: Schematic representation of the phases of the desorption column operation.

The experimental energy demand is calculated using the power demand details. The theoretical energy demand is estimated via simplistic heat transfer models while considering the experimental values of the column temperatures. The experimental and theoretical energy demand values are compared in Table 5.2.

Table 5.2: Comparison of experimental energy & theoretical energy demand

Experiment	Experimental Energy Demand (kJ)	Theoretical Energy Demand (kJ)	Error (%)
4	734	689	6.16
5	1229	1026	16.48

Observations

- The **difference between the theoretical demand and the experimental value is quite significant (Table 5.2)** in several cases. This can be **because of an underestimation of the heat losses to the surroundings**. Moreover, it is possible some of the water vapour condenses and remains trapped inside different segments of the setup, such as the flash chamber and bends in the pipe, leading to an underestimation of the heat of absorption.
- Out of the total energy consumed by the system (Table 5.3), based on the theoretical calculations, **the largest share of energy (apart from the losses) is the sensible heat requirements for the sorbent followed the heat of desorption.**
- The **energy required to heat up the system's thermal mass is the most significant component of the losses**, followed by the losses to the surroundings via convection.

- Losses to the surroundings are proportional to the temperature of the component. Therefore, these losses decrease progressively as we move higher up the column and away from the reboiler.

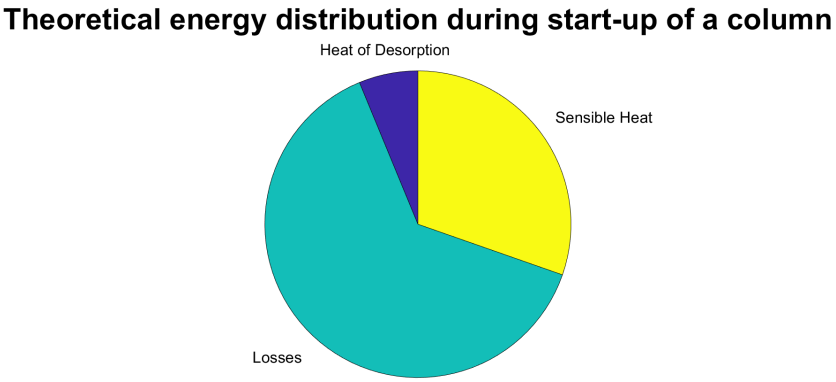

Figure 5.9: Energy distribution as predicted by the theoretical model, during a typical start-up process for the desorption column analysed.

Table 5.3: Theoretical energy distribution during start-up of a desorption column.

Experiment	Heat of Desorption (kJ)	Sensible Heat (kJ)	Heat Losses (kJ)
4	43	209.3	437.25
5	17.77	209.3	799.68

Based on the experimental insights, a MATLAB model of the reboiler of the desorption column was developed to simulate the start-up of the system under different operating scenarios.

5.3.2 Experiment Vs. Model

This section compares the transient response of the reboiler predicted by the model to the experimental values.

Table 5.4: Input parameters for the transient start-up model, based on the experimental column design.

Parameter	Value
Initial Temperature	22°C
Desorption column thermal mass	2.54 kg
Sorbent thermal mass	0.45 kg
Column material	Stainless steel
Column specific heat capacity	530 J/kg °C
Sorbent specific heat capacity	2790 J/kg °C
Power input	166 W

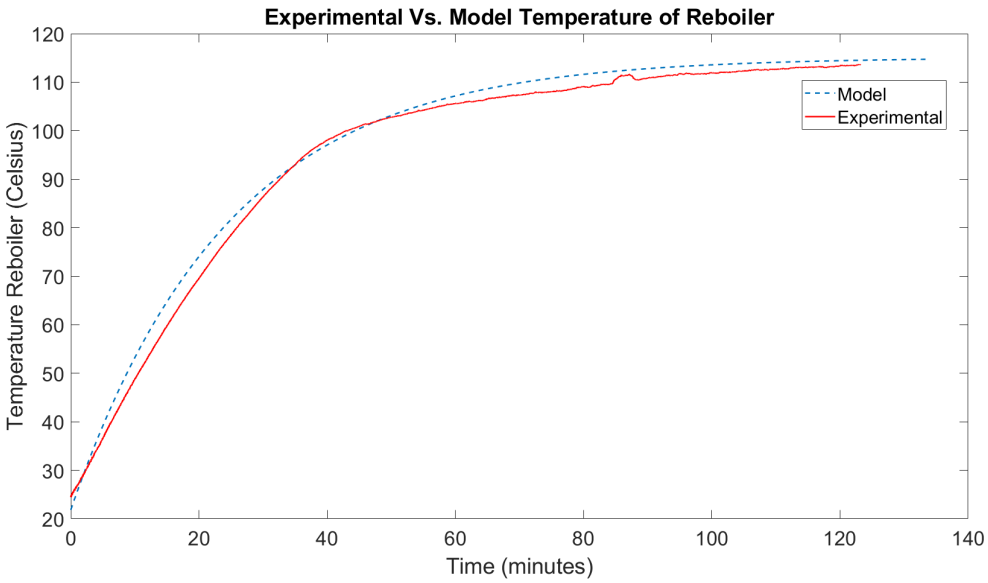

Figure 5.10: Comparison of the reboiler temperature predicted by the model against the experimental value observed.

Table 5.5: Validation of the model, with respect to experimental values.

R^2	0.9754
Mean Square Error	13.433

Since the model considers the reboiler to be a first-order system, the predicted increase in temperature does not initially delay as observed in the experimental values. This assumption is valid since the fraction of delay time vs the total start-up time is insignificant.
A sensitivity analysis is carried out using the model, to understand the factors influencing start-up time and energy demand.

5.3.3 Start-up: Sensitivity Analysis

The parameters that have an impact on the transient response are highlighted in Figure 5.11:

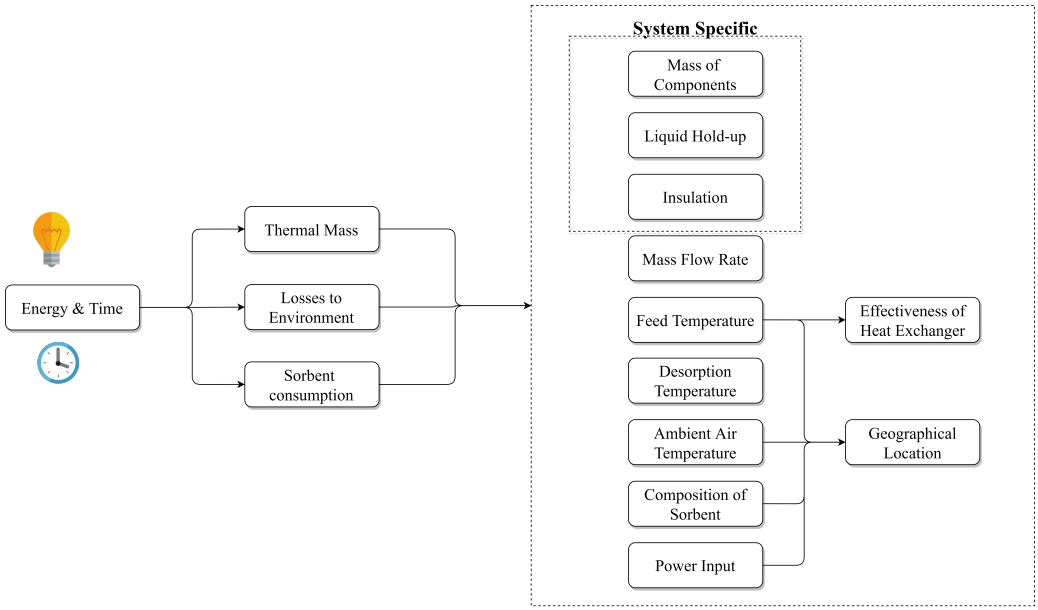

Figure 5.11: Schematic representation of factors affecting the start-up time and energy consumption.

The effect of the most important parameters is elaborated below:

- **Thermal mass:** As the components' mass increases, the start-up time and energy also increase as seen in Figure 5.12. **Adding thermal mass to the system increases the sensible heat demand and adds inertia to the transient response.**

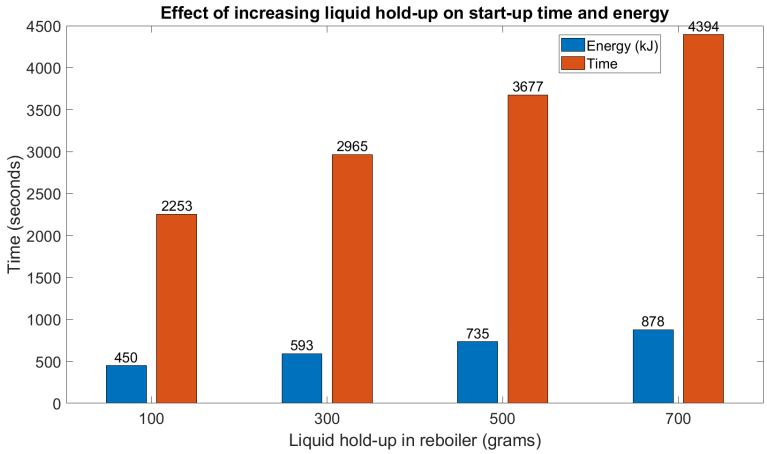

Figure 5.12: Variation of start-up time and energy consumption with increasing thermal mass of the system

- **Mass flow rate:** A **higher mass flow rate increases the sensible heating demand and lowers the reboiler temperature (if the power is constant).** Therefore, increasing the start-up time and energy consumption as seen in Figure 5.13

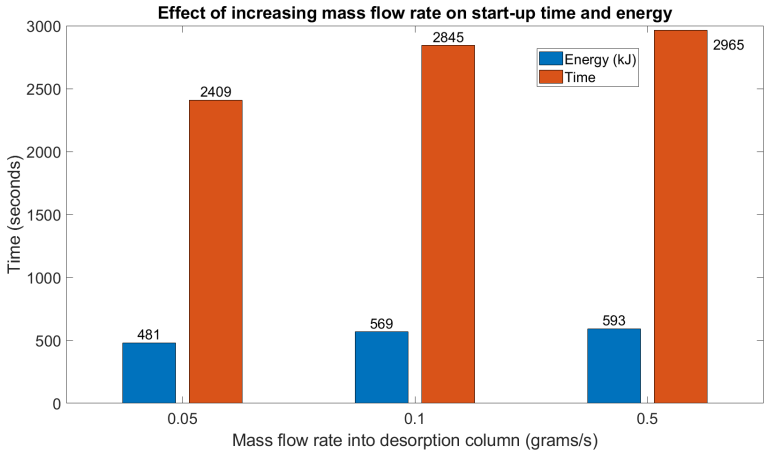

Figure 5.13: Variation of start-up time and energy consumption with increasing thermal mass of the system

- **Desorption temperature:** A higher desorption temperature increases the time and energy demand of the system, assuming that the PV panel can supply sufficient power to the system. **In cases of insufficient power, the reboiler might not reach desired temperatures.**
- **Power input:** It is seen that the **response time varies inversely with the power input. This is expected, since a higher amount of enthalpy being added to the system per unit time will heat the system faster.** *In cases of insufficient power input, the system takes a very long time to reach steady state, and does not reach the desired temperature as seen in the* ***first two data points*** *in Figure 5.14*

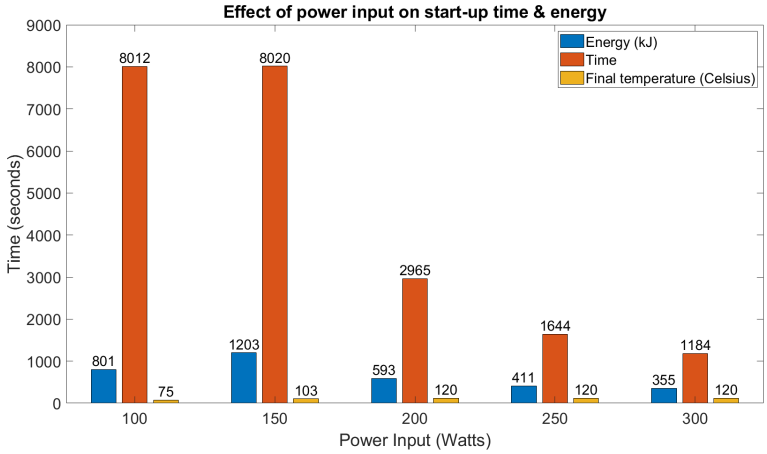

Figure 5.14: Variation of start-up time with increasing power input

5.3.4 Start-up: Scenarios

Following the sensitivity analysis, we need to identify the best possible way to start up the column. Different start-up scenarios were identified in **??**, the transient response of the system for each scenario is highlighted in Table 5.6.

- **Batch mode: The simplest and perhaps the most efficient method to start up a desorption column**. *Initially, there is no feed entering the column,* the power input is used

to warm up the thermal mass, and the liquid hold up inside the system. **Once the column is warm enough, the feed is initiated**.

- **Running:** In this case, **the mass flow is initiated from the very beginning (t=0).** Thus, in addition to the thermal mass and liquid hold up, the heaters have to heat a stream of cold sorbent entering the system continuously. As expected, **the running method requires the highest energy and time to reach steady state**.
- **Ramped:** Similar to the running method, the **incoming stream's mass flow rate is increased gradually until it reaches the desired limit**. *Faster than running, but still consumes more energy and time than the batched approach.*

  For the running and ramped methods, it is possible to use a pre-feed heat exchanger. This is used to heat the incoming feed stream via the hot outgoing lean stream from the reboiler.

Table 5.6: Comparing start-up scenarios in terms of energy and time consumption.

Scenario	Energy (kJ)	Time (seconds)	Power (Watts)	Mass flow rate (g/s)
Batch	437.21	1748.87	250	0.2
Running	796.76	3187.05	250	0.2

5.3.5 Start-up: Energy & Time fractions

Realistically that power input to the desorption column is not constant; **instead, during start-up, the power input increases gradually as the PV panel starts generating power** and thus effects the way the column is heated. The **temperature inside the column, follows the profile of the power input** as shown in Figure 5.15.

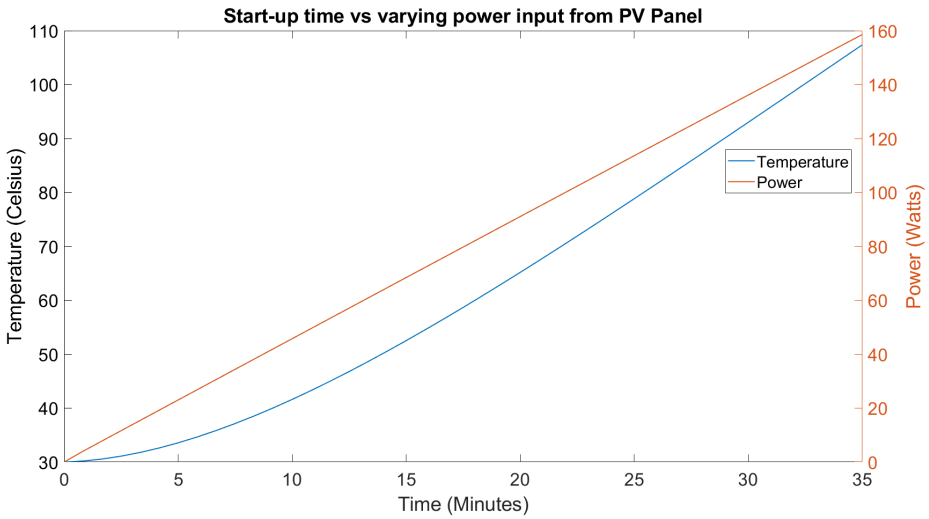

Figure 5.15: Start-up time of a desorption column with a average varying power input. Based on historical weather data for Bechar, Algeria (Sahara climate) for the year 2016 [42].

Since the amount and duration of energy available is **limited**, it is essential to quantify the impact that starting up has on the overall operation window.
The key performance indicators to quantify the effect of start-up on the total operation window are the **energy fraction and time fraction**, a brief explanation is provided in Appendix D.

Table 5.7: Base case values for start-up transient model used to evaluate the start-up time and energy fractions.

Base case	**Values**
Ambient temperature	20 °C
Final temperature	120 °C
Mass flow rate	0.1 g/s
Power input *	0 to 300 W
Column specific heat capacity	530 J/kg °C
Sorbent specific heat capacity	2790 J/kg °C
Desorption column thermal mass	1.54 kg
Sorbent thermal mass	0.3 kg

***Note:** The power input to the desorption column is obtained from the PV Panel model. Depending on the solar radiation the power output can vary between 0 to 300 Watts. *In cases of excess solar radiation, it is possible for the panel to exceed the rated power output.*

For the base case (Table 5.7) tested, **the model predicts a start-up time of 30-45 minutes (Figure 5.15)** depending on the power input available, which varies in the long term across seasons. **Moreover, the energy needed for a start-up is 1-6 % of the total energy that is available per day as shown in Figure 5.16**.

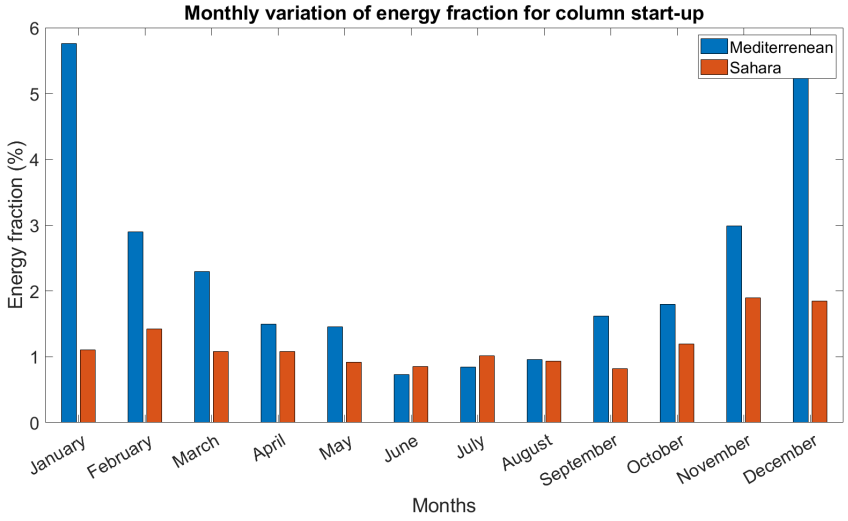

Figure 5.16: Monthly variation of start-up *energy fraction* at two different locations.

The *time fraction* for start-up varies between 1.5 to 6 % of the total day light hours available per day, as shown in Figure 5.17.

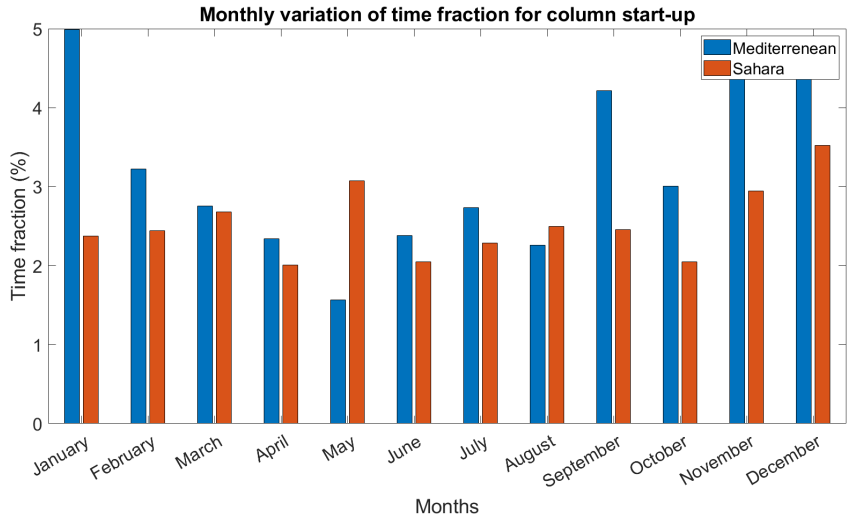

Figure 5.17: Monthly variation of start-up *time fraction*

5.3.6 Start-up: Conclusions

- Based on the sensitivity analysis, **the thermal mass of the components, power input, desorption temperature and mass flow rate of sorbent play a crucial role in determining the transient response time and energy** demand of the desorption column.
- The **most efficient way to start a column is via the batch method,** only initiating the feed once the column has warmed up sufficiently.
- Adding a pre-feed heat exchanger lowers the time and energy requirements of a start-up.
- The **energy and time fractions of a start-up are quite small, and thus the steady-state operation is >90% on most days.** A wide operation window means more value addition.
- **Power input to the system has to overcome the stripper heat losses**; thus, it is impossible to run the stripper column below a certain threshold.

5.3.7 Shut-down : Conclusions

The analysis of shut-down focuses on identifying the minimum threshold for operating the desorption column.

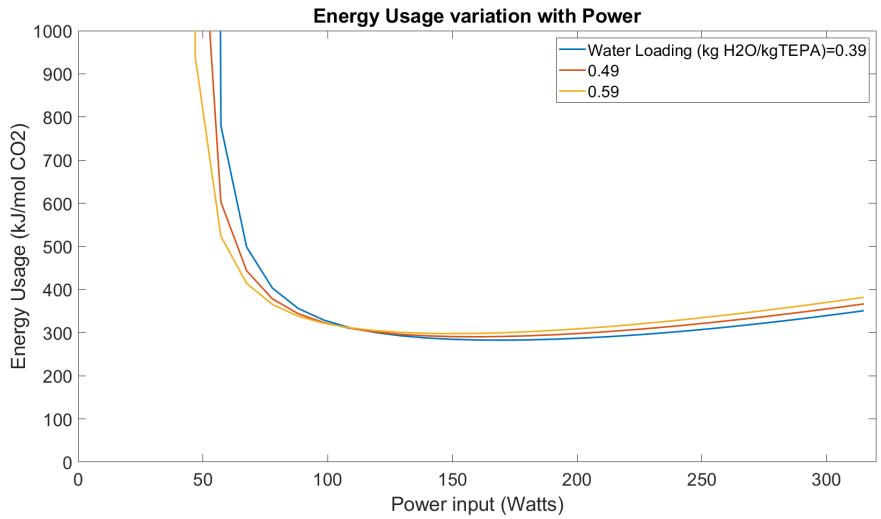

Figure 5.18: Variation of Energy efficiency of the desorption column as a function of power, & water loading in the sorbent

- Minimum **power required to overcome the pumping energy and the stripper heat losses is 20 Watts.**
- The desorption column consumes energy, **an upper limit of 450 kJ/mol of CO_2 is set as the operating threshold in terms of energy demand.** The energy consumed per mole of CO_2 produced **depends on the water loading of the sorbent and the power input as shown in Figure 5.18**.

- The desorption **column is shut down when the buffer tanks are completely filled.** The subsystems downstream of DAC continue to run, and deplete the buffer. Operation resumes as soon as the buffer reaches reserve levels.

5.4 Additional Loads

The desorption column is the primary energy consumer within the DAC subsystem. Moreover, there are additional power consumers such as the absorber and stripper pumps & the heat losses from the stripper column that need to be overcome in order to maintain the temperature inside the column.

Note: To simplify the operation of the integrated DAC model, **the power input for the desorption column adjusts for the pumping and heat losses calculated in this section**.

Pumping power

A simple analysis of the pumping energy is carried out while considering the **effects of viscosity and the mass flow rate** (Details:Appendix D). The design conditions for the pump are highlighted in Table 5.8.

Table 5.8: Relevant parameters for evaluating the pump losses, dimensions are based on experimental setup at ZEF.

Parameter	**Value**
Viscosity	0.93 Pa.s
Density	1.1 g/cm3
Mass flow rate	0.15 mol/s
Static head	1.5 meters
Pipe diameter	12 mm
Pump Power	5 Watts

Note: The pumping power evaluated in the current work is significantly smaller than the 80 Watts computed by Mulder [41], the difference can be explained by the values of the mass flow rate & viscosity, Mulder's work assumes the mass flow rate to be approximately **4 times** and viscosity **1.6 times** higher than the current work. Such a high recycle flow rate for the absorber is not necessary as will be highlighted in the following sections.

Heat Losses

The design parameters used for evaluating the stripper heat losses are indicated in Table D.1.

Table 5.9: Dimensions and related parameters of a typical desorption column based on the miniature plant at ZEF, for analysing the stripper heat losses.

Parameters	**Value**
Column height	0.4 m
Column diameter	0.05 m
Column temperature	120 Celsius
Ambient temperature	30 Celsius
Prandtl number (Air @ 30 °C)	0.72
Thermal conductivity	0.02 W/mk
Kinematic viscosity	1.749e-5 m2/s
Thermal conductivity (Rockwool)	0.035 W/mK
Heat Losses	15 Watts

Research Objective 3: *What is the impact of varying environmental conditions (disturbances: relative humidity, temperature and solar radiation)* ***on the performance (outputs) of the desorption column****?*

5.5 Second Order Effects: Performance of desorption column

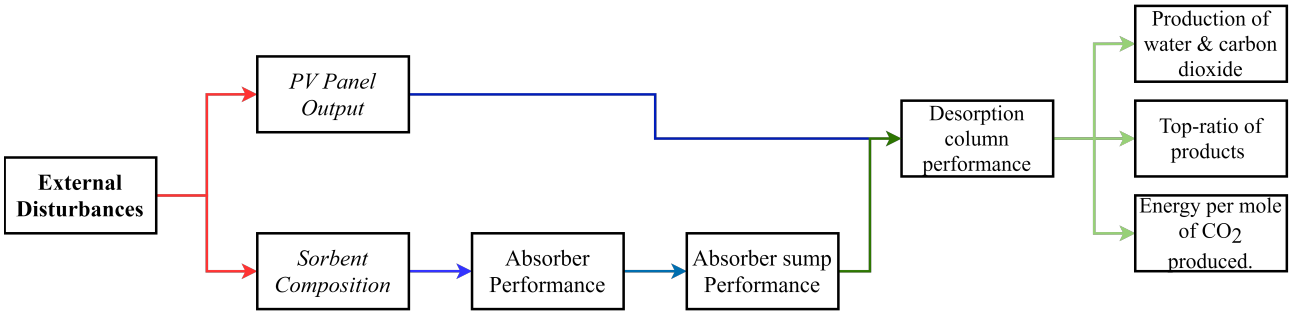

Figure 5.19: Schematic depicting the pathway of how the disturbances influence the performance of the column.

This work has described the *first-order effects* of the external disturbances on the **sorbent composition and the PV panel output.** Figure 5.19 depicts the pathway of the external disturbances and the link with the performance of the desorption column.
The PV panel output has a **direct impact on the desorption column**. In contrast, the varying sorbent composition is a **consequence of external disturbances interacting with the absorber and the absorber sump. Thus, the latter has an indirect impact on the performance of the desorption** column.
The indirect interaction between the *varying sorbent composition* & the desorption column, leaves room for tweaking the design parameters of the absorber and the absorber sump as shown in Figure 5.20. This was done using the integrated DAC model. In section 5.6 the results of the sensitivity analysis for the absorber and sump are provided first, followed by the impact on the desorption column.

5.6 Design Inputs

Based on the sensitivity analysis, a base case design for the desorption column is presented at the end of this section. **The choice of each parameter is based on the performance of the concerned component, as it is tested over a *single day of operation* using the integrated DAC model.**

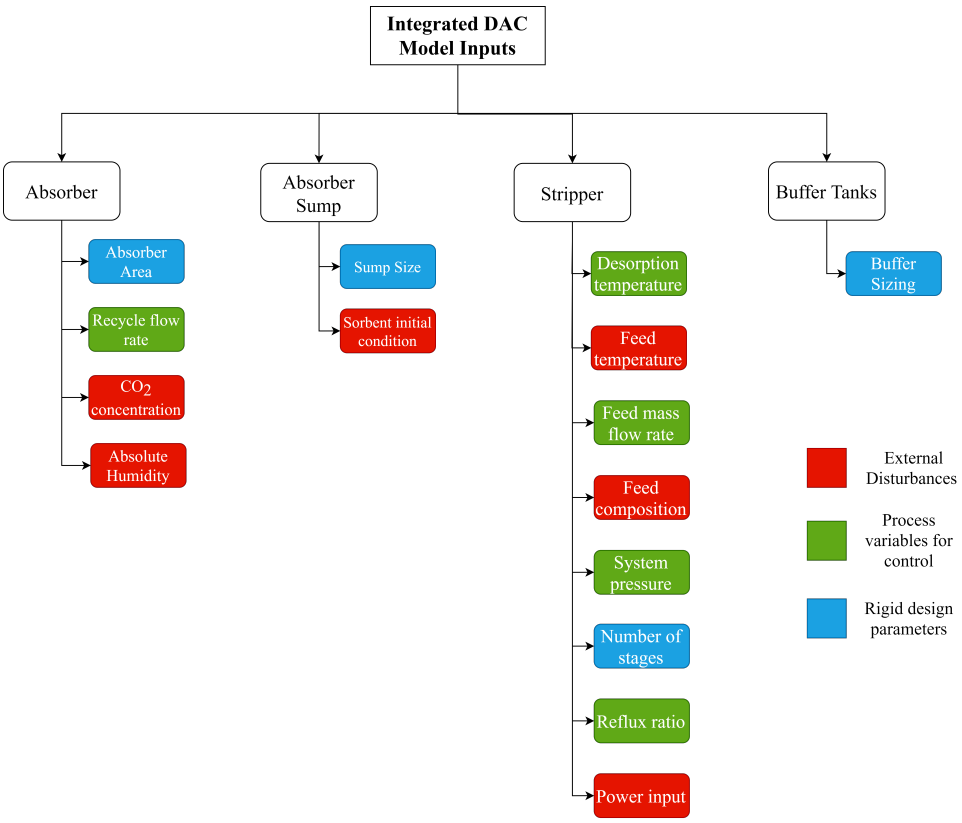

Figure 5.20: Schematic depicting the different inputs that have an impact on the performance of the DAC system

5.6.1 Design Inputs: Absorber Area

The absorber area is determined by the desired capture rate of the CO_2 and H_2O and the space-time yield. **Existing research suggests the CO_2 absorption is the rate-limiting step due to lower space-time yields than water** [41] (subsection 5.1.3). Thus, the sizing is done in accordance to the CO_2 absorption criteria. **Essentially higher the space-time yield of CO_2, the lesser contact area is required.** Figure 5.21 indicates the influence of the absorber area on the resulting CO_2 & H_2O loadings from the absorber.

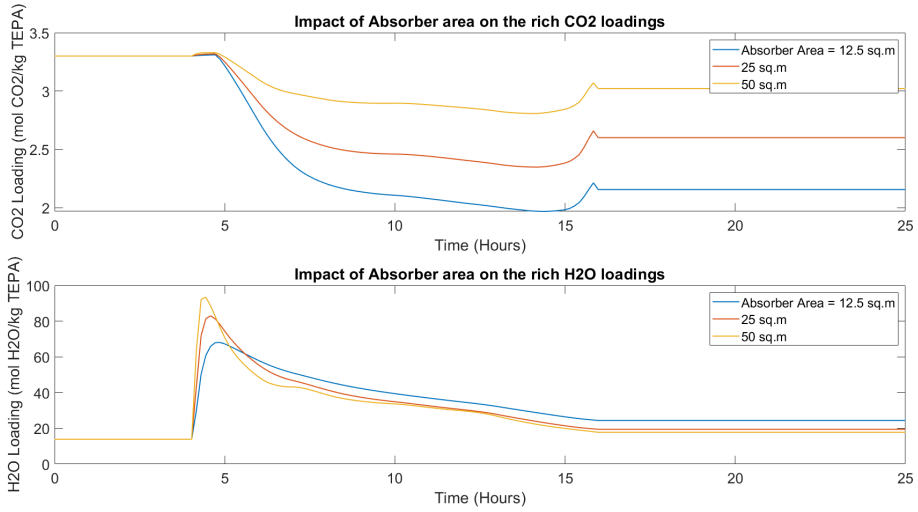

Figure 5.21: Impact of absorber area on the CO_2 and H_2O rich loadings. Results derived for a typical day in May, 2016 (historical weather data[42]) for Bechar,Algeria.

It is clear **with an increasing area, higher rich loadings are a possible. Moreover, a faster recovery of the sorbent composition once the stripper is shut down is possible**. The energy demand in the stripper column decreases for higher rich loadings [37]. Depending on which size meets the nominal demand of CO_2 and H_2O, appropriate size is selected.

5.6.2 Design Inputs: Absorber Sump Volume

The sump volume determines the rate at which the composition changes inside the sump. Larger the sump, the greater the dampening effect and slower the differences in composition as shown in Figure 5.22. Unfortunately, we cannot have an infinitely large sump for practical purposes. The sump size should be sufficient to allow the rich loading to remain high enough while the stripper is operating to ensure adequate CO_2 and H_2O are produced.

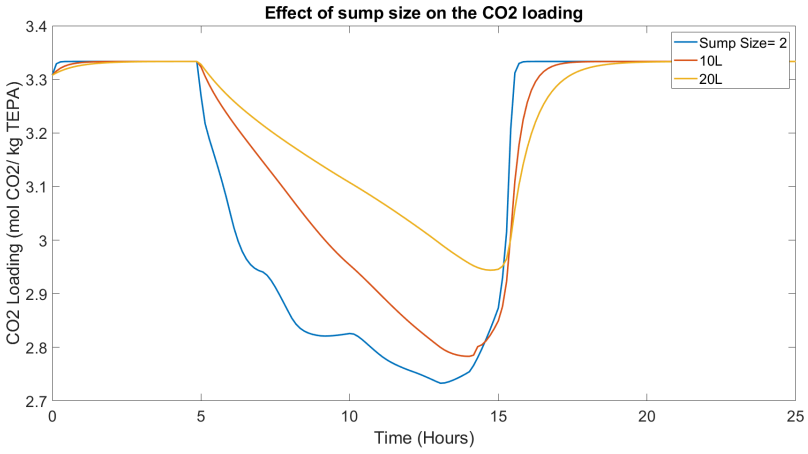

Figure 5.22: Impact of absorber sump size on the CO_2 rich loading and the stripper production capacity.Results derived for a typical day in May, 2016 (historical weather data[42]) for Bechar,Algeria.

Note: To understand the impact of sump size variation, the absorber was supplied with constant power. To get insights into how long does it take for the sump to return to it's original composition at the end of a day's operation.

5.6.3 Design Inputs: Desorption Column

- **System temperature & pressure:** The pressure and temperature affect the VLE conditions inside the column, and thus decide the cyclic capacity of the process. **While maintaining a constant system pressure, increasing the desorption temperature results in higher product ratios at the top of the column.** It is observed, the energy consumption also increases as the difference between the feed temperature and reboiler temperature increases. In contrast, while the desorption temperature is kept constant, **higher system operating pressures result in a decrease in the top ratio , and lower lean loadings** as shown in Figure 5.23 [37].

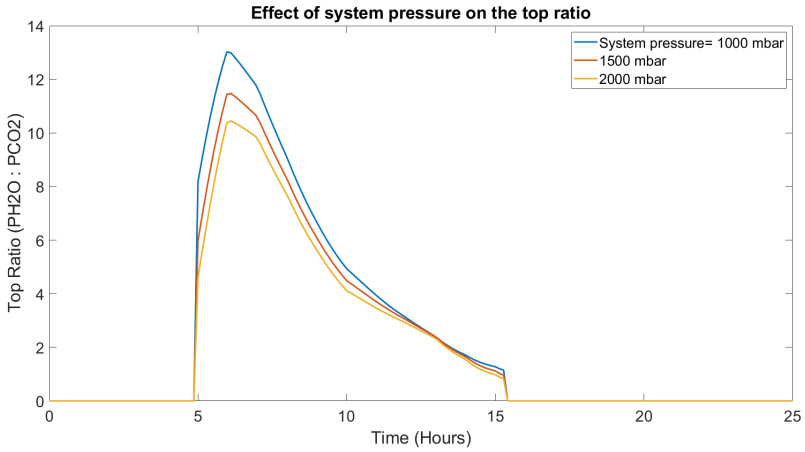

Figure 5.23: Impact of system pressure on the top ratio. Results derived for a typical day in May, 2016 (historical weather data[42]) for Bechar,Algeria.

- **Reflux ratio: Increasing the reflux ratio increases the energy demand of the desorption column**, but increases the weight fraction of H_2O in all the stages including the reboiler. Higher reflux ratio **results in a higher partial pressure of H_2O and therefore a larger top ratio.** as shown in Figure 5.24.

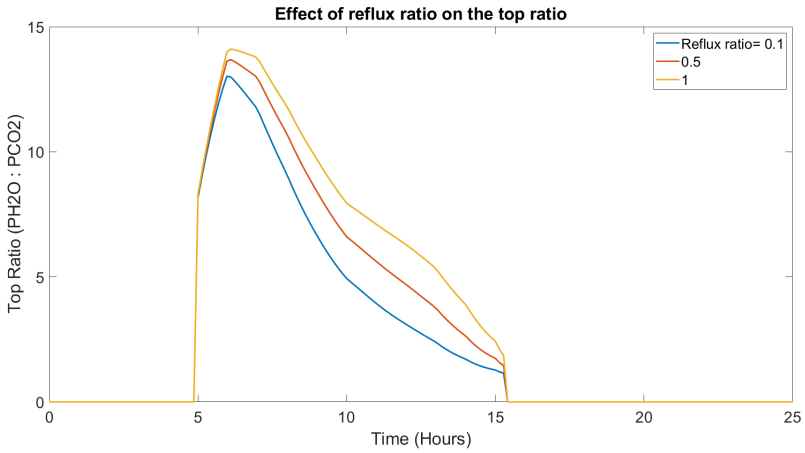

Figure 5.24: Impact of reflux ratio on the top ratio. Results derived for a typical day in May, 2016 (historical weather data[42]) for Bechar,Algeria.

- **Number of stages: Increasing the number of stages increases the cyclic capacity and results in lower top ratios.** Due to the temperature profile, the partial pressure of H_2O

in the reboiler is the highest as compared to the rest of the stages [37]. Resulting in a lower partial pressure of CO_2, allowing for more CO_2 desorb from the loaded sorbent and thus leaner loadings. *Depending on the operating climate and the resulting water loading, we can decide on the number of stages to ensure the desired top ratio is achieved.* **For a wetter climate, the stripper will need a higher number of stages.**

5.6.4 Base Case

Based on the inputs from the sensitivity analysis, a base case for the integrated DAC model was identified. The model inputs for the base case are listed below:

Table 5.10: Input parameters for the base case of the integrated DAC model

Model Inputs	**Value**
Absorber area	50 sq.m
Absorber recycle flow rate	0.15 mol/s
Stripper feed temperature	95
Stripper desorption temperature	112 Celsius
Stripper operating pressure	1000 mbar
Stripper mass flow rate	0.012 mol/s
Stripper reflux ratio	0.1
Number of stages in stripper	2
Sump initial conditions	3.3 mol CO_2/kg TEPA, 20 molH_2O/kg TEPA
Sump Size	10L
Absolute humidity*	0.009 to 0.02 kg/m3
Power Input*	0 to 300 W

***Note:**

- The absolute humidity and power input is based on historical weather data for a particular location, for the year 2016 [42]. The range mentioned inTable 5.10 represents the maximum and minimum limits of the absolute humidity values encountered in the data set.
- The range for power input is the nominal output of the panel. Although, the panel regularly exceeds the rated power, when the incident radiation is higher than the standard radiation for which the panel is rated.

The model was made to run with the base case for an equivalent time period of 4 days each for different months in the year. The input for external disturbances was based on historical weather data for Bechar, Algeria [42] for the year 2016. The key performance indicators identified earlier, are analysed in this section:

- **Top Ratio:** The ratio of the partial pressures of H_2O and CO_2 from the top stage, depends on water concentration in the sorbent. Thus, based on the sorbent concentration, and the power input, the partial pressure of H_2O in the column will fluctuate over a wide range as seen in Figure 5.25. **Short term variation in the top ratio of the products is more pronounced, since the water concentration follows the short term changes in absolute humidity in the atmosphere.** Ideally, ZEF wants to operate at a molar ratio of 3:1 (P_{H_2O}:P_{CO_2}).
- **Energy Consumption (per mole of CO_2): The energy consumption is determined by the water loading of the sorbent**. Van der poll [37] identified an optimum water loading that requires the minimum amount of energy per mole of CO_2. A similar observation can be made for the TEPA-PEG sorbent; within a certain range of water loading, the energy per mole of CO_2 remains within an acceptable range. Except for two cases:

- Excess amounts of water in the sorbent increases the sensible heating demand, resulting in a higher energy per mole of CO_2.
- Water loadings below 11 mole/kg TEPA, in such cases the partial pressure of water in the column is very low, as such higher lean loadings are observed. Since not a lot of CO_2 is desorbed, a higher energy per mole of CO_2 is required.

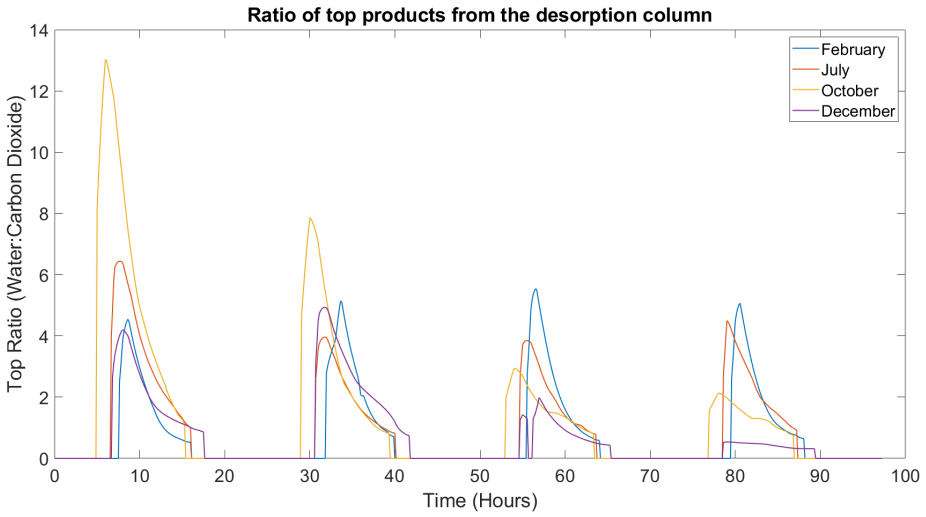

Figure 5.25: Seasonal variation of stripper top ratio and energy consumption per mole of CO_2 desorbed. Results are for Bechar, Algeria

- **Stripper CO_2 & H_2O Production:**
  - **The production of CO_2, as seen in Figure 5.26, follows the profile of the power input into the system.**
  - In case of **low water loading of the sorbent**, despite the availability of power to the system, **insufficient amounts of H_2O and thus CO_2 are produced**.
  - **In the dry months**, for a large portion of the operating window, **insufficient water is produced. This calls for increasing the desorption temperature in the column or stripping at lower pressures.**

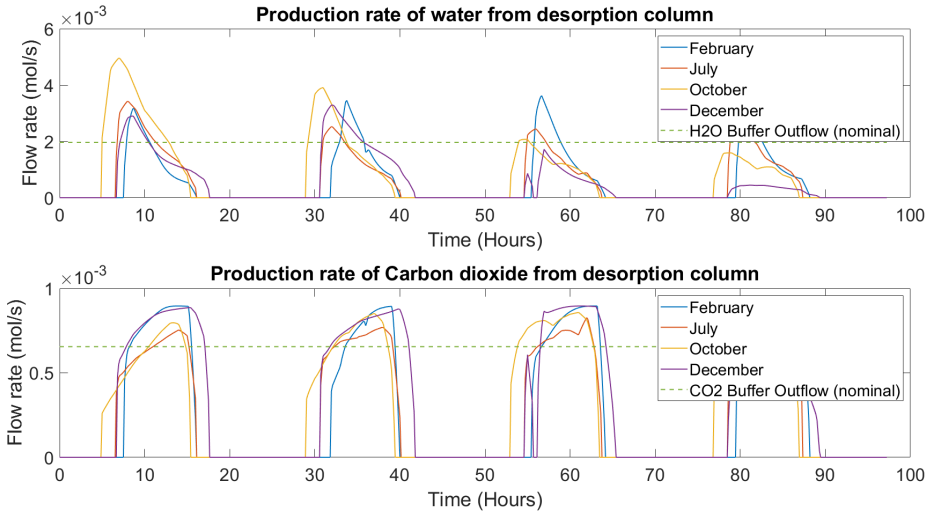

Figure 5.26: Seasonal variation of stripper CO_2 and H_2O production. Results for Bechar, Algeria (Sahara climate).

- **Buffer accumulation:**
  - Production of CO_2 & H_2O above the nominal demand rate, accumulates in the buffer. **The surplus is utilised in periods of lower production, therefore ensuring smoother operations of subsystem downstream**
  - Figure 5.27 indicates a negative balance for H_2O, this corresponds to drier months. **Negative balance is not realistic, but it proves that insufficient production of water results in a large buffer requirement.**
  - Employing larger buffers is not the most effective solution. **Controlling the top-ratio of products via adjustments in temperature and pressure of the system can yield more effective results.**

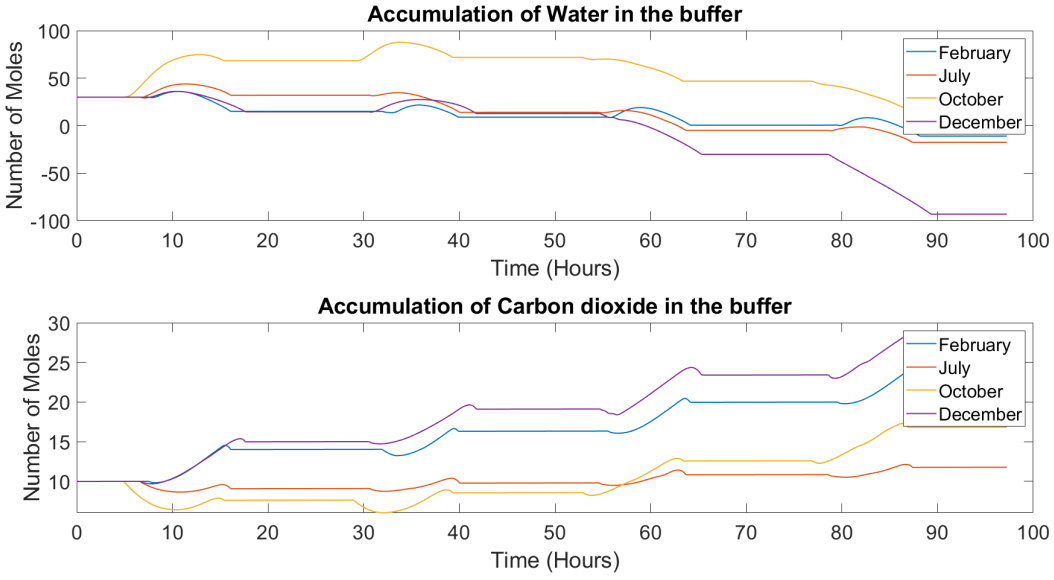

Figure 5.27: Seasonal variation of buffer levels. Results for Bechar, Algeria (Sahara Climate).

5.6.5 Design Inputs: Conclusion

It is evident from the functioning of the open model; the KPIs are deviating significantly from ZEF specifications.

- The production of Carbon dioxide and water from the desorption column, follows the profile of the power input. Thus, **short term variations in the power input from the panel, have a direct impact on the production capacity of the system.**
- **Short term variations in the absolute humidity, cause the The top ratio of products to fluctuate between 12-1**, ideally, this should be 3:1 (molar ratio). Controlling the top ratio requires adjusting the temperature and the pressure of the system.
- **Short term variation in the absolute humidity have a greater impact on the energy consumption per mole of CO_2 produced than the the power input.** ZEF aims to operate at a threshold of 450 kJ/mole of CO_2. The operating limit needs to be incorporated in the start-up and shut-down functions of the desorption column via a feedback control loop.
- The temperature inside the column is a function of the mass flow rate, sorbent composition and the power input. **The sorbent composition varies on longer time scales than the power input.** Thus to maintain the top ratio of the products, we need to maintain the temperature inside the system in accordance to the power input, this calls for an adjustable mass flow rate.

The conclusions of the open model provides clear motivation to **incorporate adjustable parameters in the final design**. Thus a control scheme was developed for the final model, as explained in subsection 4.2.6. The results of each scheme will be presented in chapter 6

Research Objective 4: *What is the limiting step for desorption of CO_2 from the TEPA-PEG sorbent mixture?*

5.7 Kinetics

To understand the rate-limiting step in the desorption process while using the TEPA-PEG 200 sorbent, hold-up time experiments were performed on the mini-DAC setup (subsection 3.3.2). Existing research at ZEF by Matteis [40] and van der poll [37] quantified the diffusion coefficient of CO_2-TEPA binary system and the Hatta number for the same species pair. Their conclusions aligned with literature which indicated the absorption and desorption of CO_2 is diffusion-limited.
The kinetics vs diffusion debate is resolved through a qualitative analysis of the hold-up experiments based on the following expectation:

- If the process is **diffusion-limited, the steady-state composition of the sorbent will vary depending on the hold-up times**. With sorbent loading approaching VLE as the hold up time increases.

5.7.1 Kinetics: Effect of Temperature

In Figure D.13, the lean loadings for the 110°C are much higher as compared to the 120°C for the same values of the hold-up time, which implies that the process is **diffusion-limited**. **Since the boiling is more vigorous at higher temperatures (depending on the pressure),the effective diffusion length decreases, improving mass transfer and thus lower lean loadings are possible.**

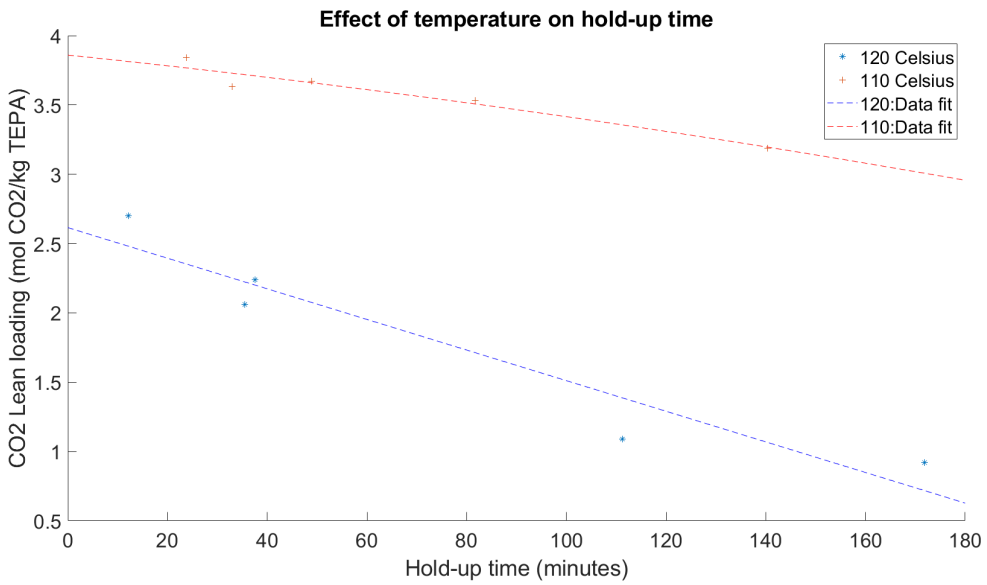

Figure 5.28: Effect of reboiler temperature on hold-up times and the lean loading of the sorbent.

5.7.2 Kinetics: Conclusions

- At **higher temperatures, lower lean loadings are possible** for the same hold-up times due to the **vigorous boiling observed at higher temperatures. Lowering the effective diffusion length**, and thus, improved mass transfer. Thus the process of desorption is diffusion limited.
- It is clear that, during the experiments, one has not reached VLE . Extrapolating the curves suggests massive hold-up times to get VLE. This is not ideal, and begets the question is it necessary to operate the desorption column at VLE ? **It is possible to reduce hold up times , by using higher mass flow rates and smaller liquid hold-up volumes.**
- Decreasing the liquid hold-up, improves the mass transfer and thus lower lean loadings for the same temperature and pressure. Thus, smaller liquid hold-ups are preferred.

Chapter 6

DAC System Engineering

This chapter deals with the final research question and aims to present a complete design of the desorption column, and auxiliaries based on the insights obtained from the integrated DAC model developed in section 4.2 and the sensitivity analysis carried out in section 5.6.

> **Research Objective 5:** *What are the optimal design conditions for a continuous desorption process that meets ZEF's requirements?*

Based on the conclusions presented in subsection 5.6.5 it is clear that some form of control action is required to fine tune the performance of the desorption column to meet ZEF's requirements. The following sections deal with the different control schemes developed.

6.1 Mass Flow Control

The control scheme is highlighted in Figure 4.21. In this mode, **it is desired to maintain the reboiler at a pre-set temperature** that is decided based on historical absolute humidity data for a given location and thus the expected water loading. The **temperature is controlled by adjusting the mass flow rate into the desorption column, depending on the power input.** The results for the mass flow control are presented in Figure 6.1.

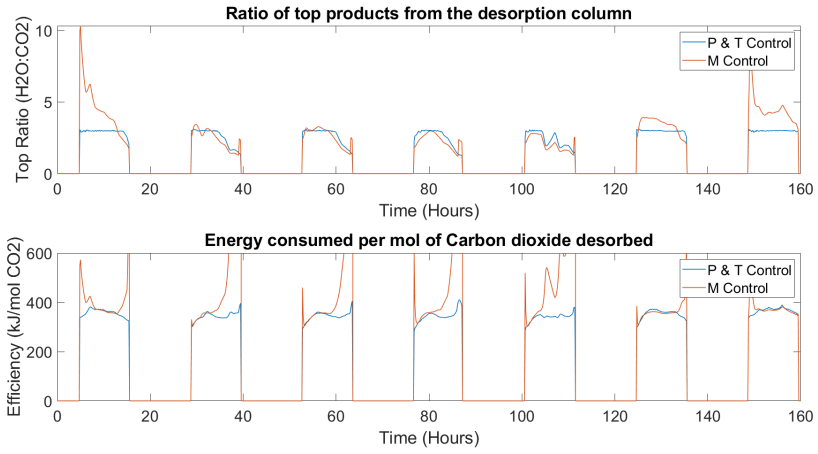

Figure 6.1: Caption

6.1.1 Conclusion

- The control scheme adjusts the mass flow rate according to the power input, and maintains a constant temperature. But, **the control action fails to meet the top ratio design specifications**. Since, the latter depends on the sorbent composition, that varies significantly due to the absolute humidity fluctuations.
- Thus, **a constant temperature set-point that does not take into account the varying water loading in the sorbent, is not a viable solution** to achieve good control over the top ratio of the products.
- Therefore, **an additional layer of control is desired, that adjusts the temperature set-point according to sorbent composition and the top-ratio produced.** This leads to a cascade control loop as shown in Figure 4.22.

6.2 Temperature-Mass Flow control

The cascade control loop has been explained in section 4.2.6. The *primary control loop* senses the top-ratio and adjusts the temperature set-point for the secondary control loop. The latter, responds to the changes in the temperature set-point by varying the mass flow rate.

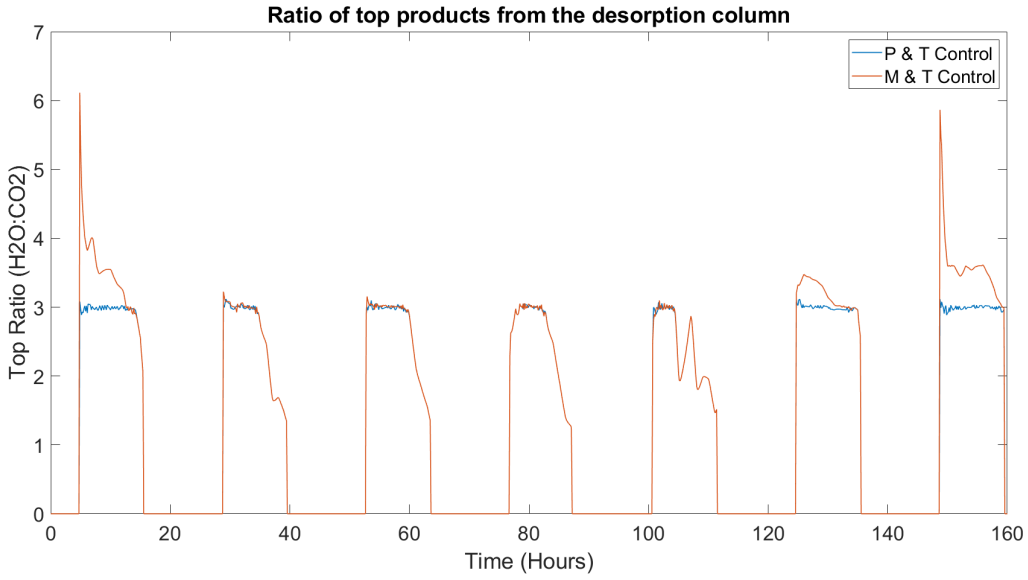

Figure 6.2: Comparing the effect of cascade control against parallel control on the top ratio of the stripper column. Simulation carried out for the month of March, 2016 in Bechar, Algeria (Sahara Climate).

6.2.1 Conclusion

- The cascade control loop performs better in terms of control action, to maintain the top-ratio of products within desired levels, as compared to single loop mass flow control.
- For wetter climatic conditions, **higher water loadings in the sorbent call for a lower desorption temperature**. Unfortunately, the control action of the cascade controller has a lower saturation limit of 100 °C. Therefore, **in cases of excessive water loadings (>45 mol H_2O/ kg TEPA), the cascade loop fails to maintain the top ratio at desired levels as shown in Figure 6.2**.

- In case of excess water loadings, reduction of top ratio can be accomplished by operating at higher system pressures.

6.3 Pressure Control

Single loop pressure control is tested, the control action is compared with the final design . A simple feedback of the top ratio is used to adjust the system's pressure accordingly. The results are presented in this section.

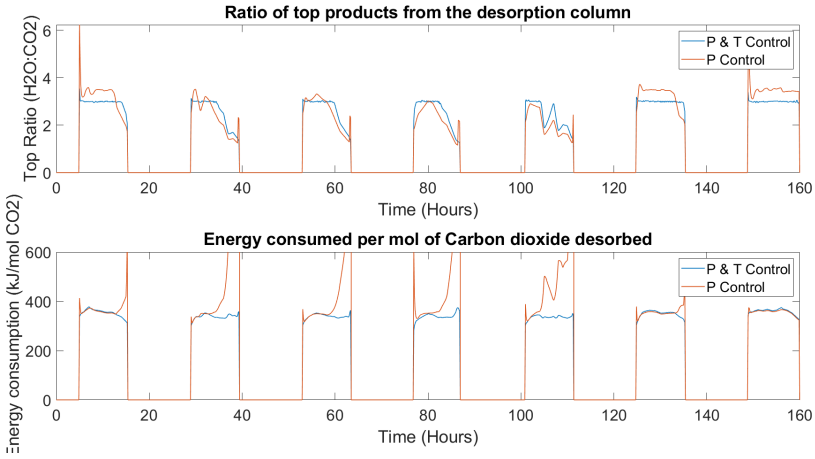

Figure 6.3: Comparing the effect of single loop pressure control and the final control scheme, on the top ratio & energy consumed per mol of CO_2 desorbed

Conclusion

- Single loop pressure control is not capable of maintaining the top ratio at the desired levels at all water loadings. **This might indicate that the temperature of desorption has a greater impact in adjusting the partial pressures of the species desorbed as compared to adjustments in system pressure.**
- **Single loop pressure control results in ineffective desorption of CO_2 from the sorbent**, when the latter starts running dry. Due to which, **energy consumption per mole of CO_2 desorbed exceeds the threshold value** decided for the system as shown in Figure 6.3.
- But in cases of moderate to high water loadings, **adjusting the system pressure can be viewed as an auxiliary solution to reigning in the top-ratio while working in parallel with the mass flow-temperature control loop**.

6.4 Final Control Scheme

Based on the results of the base case and single loop control schemes, it was concluded that the former is not sufficient to achieve the desired specification of ZEF. Therefore, the final design operates based on a parallel control scheme combining the Temperature-Mass cascade controller and the single loop pressure control.
The design parameters for the DAC subsystem are highlighted in subsection 6.4.1 followed by the operation critera and finally the performance of the final design are presented. Figure 6.4 depicts the final control scheme for the desorption column:

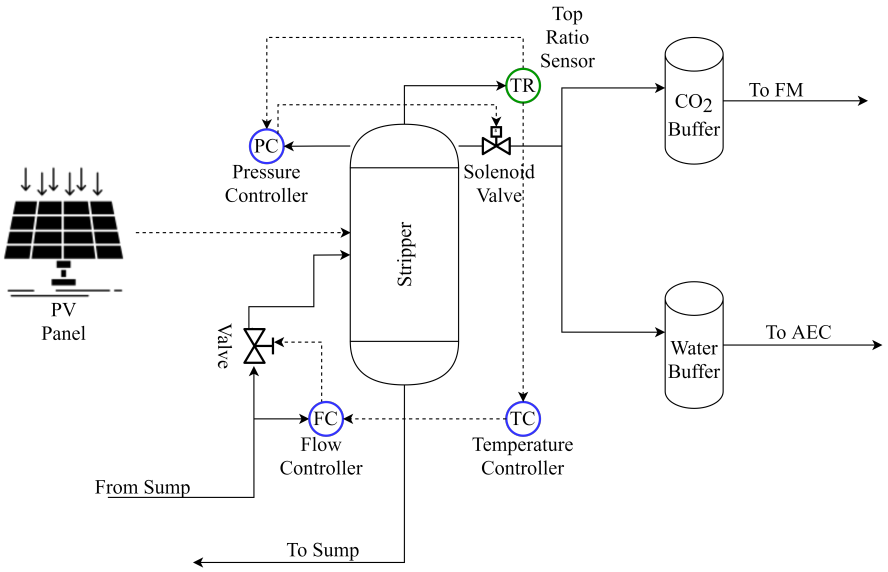

Figure 6.4: Schematic representation of the final control scheme for the desorption column.

6.4.1 Design Considerations

- **Absorber Area:** High rich loadings are favourable, thus during continuous operation, the absorber should be capable of maintaining high enough rich loadings while the stripper continues to return lean sorbent. **An area of 50sq.m was found to be sufficient to ensure the rich CO_2 loadings remained within the 2.9-3.5 mol of CO_2/kg TEPA envelope.**
- **Absorber Sump size:** The sump size is crucial in cushioning the effects of varying sorbent composition. The lean loading of CO_2 depends on the partial pressures of H_2O in the desorption column, thus the sump is meant to dampen the effects of varying relative humidity. **From the sensitivity analysis, a sump size of 10L is found to be appropriate for the system, it sufficiently filters the ripples and maintains rich loadings of CO_2 within the desired 2.9-3.5 mol of CO_2/kg TEPA envelope.**
- **Stripper Pressure: The pressure inside the column is adjustable depending on the top ratio. The control action varies the pressure between 1000-1600 mbar. The lower limit of pressure is set by ZEF, the upper limit is a user input.** It is possible to operate at higher pressures, but it would require more robust construction of the column, since repeated pressure cycles will subject the column and it's joints to fatigue loads.
- **Stripper Temperature:** The temperature and the pressure determine the VLE conditions of the sorbent. **The upper limit of operation is 120°C, which is limited by the thermal degradation properties of the sorbent. The lower limit is 100°C, is determined by the partial pressure of water at that temperature. Below this, the P_{H_2O} is too low, to produce any CO_2 efficiently.**
- **Buffer sizing:** The production of CO_2 and H_2O varies throughout the day, an adequate buffer ensures consistent availability of raw material to the subsystems downstream.
  - *Reserve level:* **The lower limit, is set as 4 hours' worth of production demand.** The CO_2 buffer has a reserve capacity of 10 moles, while the H_2O buffer has a reserve of 30 moles.
  - *Maximum level:* **The upper limit is set as 8 hours' worth of production demand excluding the reserve capacity.** Therefore, the CO_2 buffer has a maximum capacity of 30 moles while the H_2O buffer has a maximum capacity of 90 moles.

6.4.2 Operation Criteria

The sequence of operations is depicted in Figure 6.5:

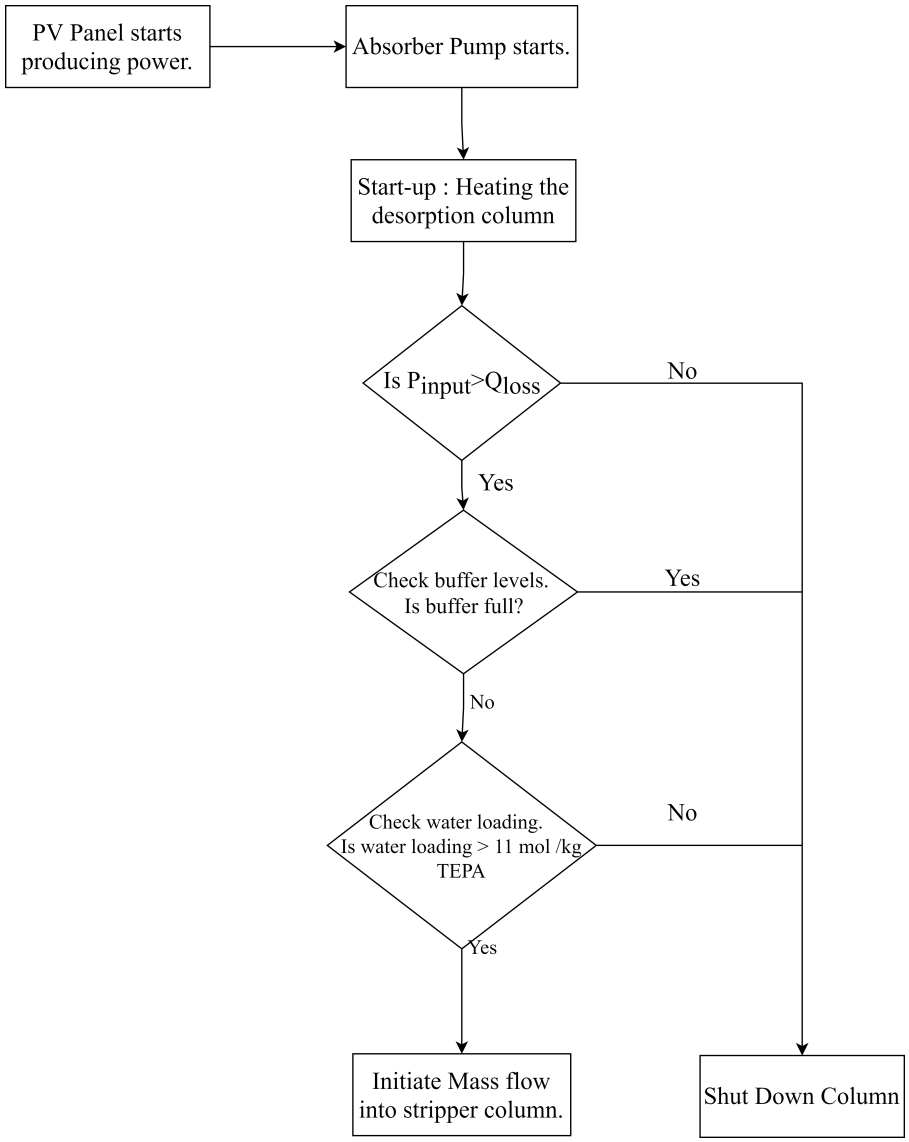

Figure 6.5: Flowchart depicting the sequence of operations in DAC.

1. As soon as the PV panel starts producing power, the system supplies energy to **drive the absorber pump and to heat up the column.**
2. If the **power input is sufficient** to **overcome the stripper heat losses, and achieve the minimum operating temperature of the column**, the algorithm proceeds to the next step.
3. **The buffer tank levels are checked**, provided the tanks are not filled to capacity, the system proceeds to the next operation.
4. The water loading of the sorbent should be sufficiently high (>10 mole H_2O /kg TEPA). **The humidity conditions are checked to ensure sufficient water loading is available in the sorbent.**
5. If all the aforementioned **conditions are met, the mass flow of the sorbent is initiated** into the desorption column.

However

6. If any of these conditions are **not met at every time step, the desorption column is shut down**.

6.4.3 Final Design: Performance

The results from the final design of the system, are presented in this section. Each set of graphs compares the performance of the system in the Sahara and Mediterranean climate.

Table 6.1: Locations selected for the purpose of comparing the operation of the system in two different climatic regions. Historical weather data has been gathered for each site from Wunderground [42], for the year 2016.

Climate	Location
Sahara	Bechar, Algeria
Mediterranean	Oleiros, Portugal

- **Top-ratio:** Figure 6.6 indicates the final control scheme maintains the top ratio of the products within the design specifications.
  - From Figure 6.6 it is evident, the control action for the Mediterranean operation is far superior as compared to the Sahara operation.
  - This is not a limitation of the control scheme itself, but an issue with the amount of water present in the sorbent. Below a certain threshold, it is not possible for the system to maintain higher partial pressures of H_2O due to the temperature limits imposed on the controller action based on the thermal degradation properties of the sorbent.

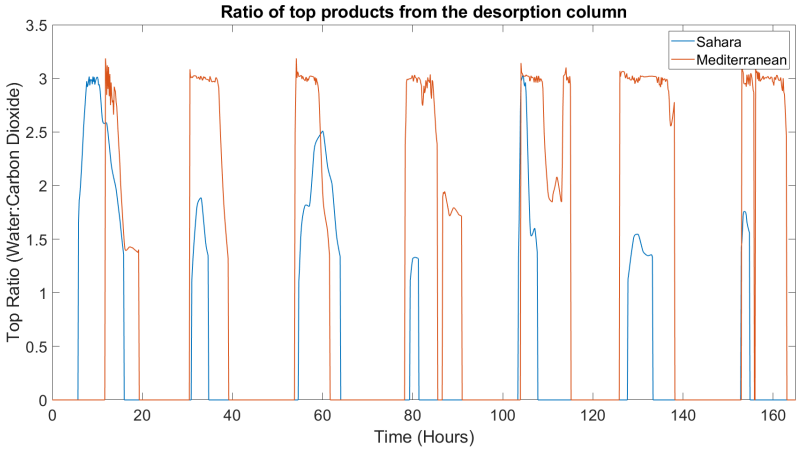

Figure 6.6: Comparison of top-ratio of products in the column across two different climates - Sahara and Mediterranean for the month of July,2016

- **H_2O & CO_2 Production:** Figure 6.7 indicates the production follows the profile of the power input. **For Sahara climate, the production of water remains below the nominal demand** for a greater proportion of the operating window as compared to the Mediterranean. The lower production of water in the **Sahara climate is due to lower water loadings** in the sorbent (due to low absolute humidity) as compared to the Mediterranean location. In contrast the **decreased production in the Mediterranean is due to short term fluctuations in the power input**.

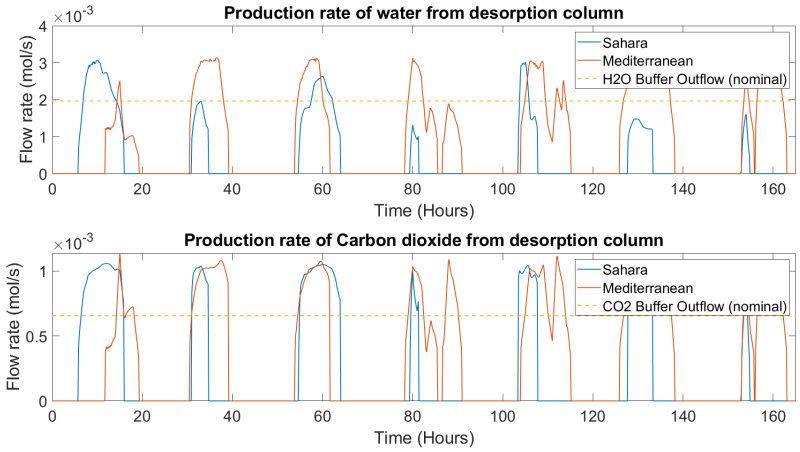

Figure 6.7: Comparison of production rate of water & carbon dioxide in the stripper across two different climates - Sahara and Mediterranean for the month of July, 2016

- **H_2O & CO_2 Accumulation:** Figure 6.8 indicates a surplus of CO_2 being accumulated while for both the climatic regions.
  - For the Mediterranean a surplus of H_2O and CO_2 is observed in periods of sufficient power input.
  - In contrast, a surplus of CO_2 is observed for the Sahara climate due to the system operating at higher desorption temperatures.
  - The controllers sense the lower top ratio of products being generated in the Sahara climate, and prompt the system to operate at higher desorption temperatures to increase the amount of water being desorbed from the already dry (low water loading) sorbent.

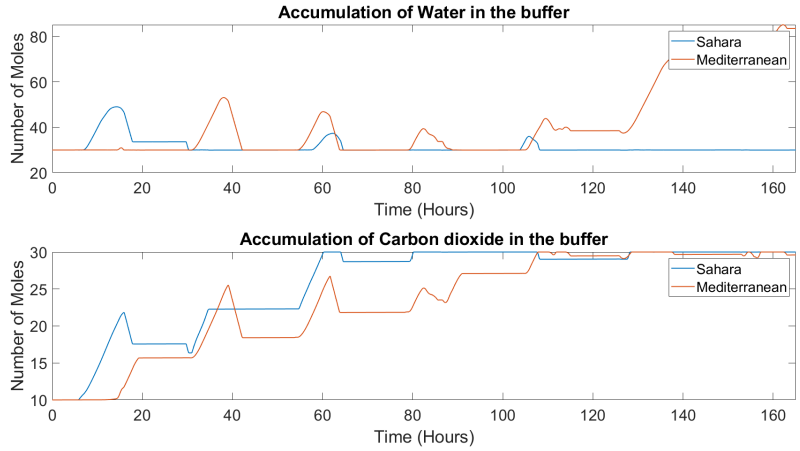

Figure 6.8: Comparison of accumulation of water & carbon dioxide in the buffer across two different climates - Sahara and Mediterranean for the month of July, 2016

Conclusion

- The final control scheme employs parallel control action, that adjusts the temperature and pressure of the system according to the power input and the top ratio.
- The parallel control scheme is capable of maintaining the top ratio of the desorption column at the desired levels for most operating conditions.

- The production in the Sahara climate is limited by the dryness of the atmosphere, in contrast the production in the Mediterranean climate is limited by the availability of consistent power.
- Fluctuations of power input have a greater impact on the performance of the system as compared to the fluctuations in absolute humidity.

Chapter 7

Conclusions & Recommendations

7.1 Conclusions

7.1.1 First Order Effects

- Changing ambient conditions have a significant impact on the sorbent composition. **The water loading of the sorbent is affected the most due to changes in absolute humidity.** The latter can occur over shorter time scales, i.e. a few hours, and thus affect the performance of the desorption column. The equilibrium loading also varies depending on the location-based climatic conditions.
- **Changing solar radiation affects the output of the PV panel.** The output is a function of the incident solar radiation, panel temperature, and for longer time scales, the daylight hours available. Naturally, higher incident solar radiation, coupled with cool panel temperatures, is optimum for max production. **Summer months usually see an increase in the average energy output from the panel due to increased daylight hours.** However, in hotter climates, this effect can be nullified by the decrease in panel efficiency.

7.1.2 Second Order Effects

Start-up Shut-down

- Primary factors affecting the start-up of a desorption column are the **thermal mass, heat losses and the power input to the system.** A **significant portion of the energy consumed during start-up is for heating the thermal mass of the column, while the second-largest component is the losses to the surroundings.** Proper insulation can reduce heat losses, but demands such as sensible fluid heating cannot be avoided.
- In terms of time and energy consumed, the **batch mode of starting a column is the best.** A pre-feed heat exchanger can be used to pre-heat the feed entering the system to improve the performance as it lowers the sensible heat demand and time to steady-state.
- In the case of varying power input, the **energy fraction for start-up comprises 1-6% of the total energy available, while the time fraction accounts for 1.5-6% of the total hours of power available.** These fractions are dependent on the power input and thus vary in the long-term depending on seasonal changes.
- The steady-state **operation window is >90% of the total operating window**.

Operation Criteria

The criteria for operation is as follows:

- With sufficient power to overcome stripper heat losses and the pumping power needs of the DAC system, only then a start-up is possible. In case the power supply cannot overcome these prerequisites, the column is shut down.
- During steady-state operation, when the energy demand per mol of CO_2 produced exceeds 450 kJ, the column is shut down. This is a design condition that ZEF has identified.
- If the buffer tanks are full, the desorption column is shut down temporarily till the levels inside the tank return to base levels.

Kinetics

Qualitative analysis of the TEPA-PEG200 sorbent indicates that the desorption of CO_2 is diffusion-limited.

- At higher temperatures, vigorous boiling decreases the effective diffusion length. This improves the mass transfer characteristics, and lower lean loadings are possible. But operating at higher temperatures also means – lower sorbent lifetimes and greater energy consumption.
- Reducing the liquid hold-up itself lowers the liquid column's height and thus better mass transfer and improved desorption.

7.1.3 Dynamic response of the Integrated DAC model

Absorber

- The absorber area has a significant impact on the sorbent composition. **A larger surface area allows the sorbent to achieve rich loadings faster since the space-time yield remains unchanged.** The optimum size needs to be matched with the rate at which the desorption column is operating and returning the lean sorbent to ensure the absorber outlet composition does not drop too low.
- Absorber sump size offers a dampening effect. **It minimizes the impact of the ambient conditions on the sorbent composition by maintaining a composition within acceptable limits throughout the operation window.** The larger the sump, the higher is the dampening effect.

Desorption Column

- The top ratios and the production of CO_2 and water fluctuate significantly due to the varying inputs. **Adjusting the system temperature and pressure to reign in the top ratio within ZEFs specification proved to be a good option.** From the design perspective, it was found that increasing the number of stages in the column will lower the top ratios, but this is a rigid method.
- The water loading of the sorbent influences the energy consumption of the column. Higher levels of water loading result in greater sensible heating demand. The system takes a hit during arid conditions (water loading<10 molH_2O/kgTEPA), lower partial pressures of H_2O simply not a lot of CO_2 is being desorbed thus, higher consumption of energy.
- Accumulation in the buffer depends on the stripper production. Since the top ratios are off from spec, one of the products is being produced in excess. During the dry spells, not enough water is being captured, and thus it leads to a depletion in the buffer tank.

- The temperature inside the column is a function of the mass flow rate, sorbent composition and power input. The sorbent composition varies on longer time scales than the power input. Thus to maintain the top ratio of the products, we need to maintain the temperature inside the system following the power input. It calls for an adjustable mass flow rate.
- **For a hot and dry climate (Sahara), the production is limited by the water loading of the sorbent**. Lower water loadings reduce the P_{H_2O} , therefore leading to insufficient water production and lower cyclic capacities.
- **For a cool and wet climate (Mediterranean), the production is limited by the availability of consistent sunlight outside the summer months**, thereby leading to poor PV panel performance. With a lack of energy available, despite adequate sorbent loadings, higher throughput cannot be achieved.

Control Scheme for the Desorption column

- **Mass flow control:** Although the temperature remains constant, **variations in the water loading determine the top ratio.** A varying temperature setpoint is needed based on the top ratio to cope with the varying inputs.
- **Mass-Temperature control:** A reasonable control of the top ratio is possible using a cascade control that adjusts the primary temperature setpoint depending on the top ratio. **Not suitable for extremely wet conditions when the temperature cannot be lowered below 100 to maintain lower partial pressures of water.**
- **Mass-Temperature Pressure Control: Dynamic adjustments of the temperature and pressure of the system is seen to be the best option to maintain the top ratio** since in cases where the temperature controller limit is reached, the pressure controller takes over.

7.2 Recommendations

7.2.1 Absorption

- **The effect of sorbent viscosity on the space-time yield needs to be investigated**. This work uses STY curves that account for the VLE and current loading conditions. A change in viscosity significantly alters the diffusion characteristics of the sorbent, and these changes in viscosity are observed under regular operation. Thus incorporating this effect will improve the dynamic model behaviour of the absorber.
- **Similarly, the effect of ambient temperature on the absorption of CO_2 and H_2O** needs to be incorporated for a complete picture of absorption characteristics.
- **The use of different ratios of the TEPA-PEG200 sorbent for different climatic conditions would be beneficial for the system's performance**. Depending on the humidity conditions, the amount of diluent can be altered to allow more amine sites to be present. Moreover, adjusting diluent also changes the amount of water absorbed, especially in highly wet conditions like the Mediterranean.
- **The mass transfer model developed by Matteis [40] needs to be modified to incorporate the behaviour of newer sorbents.** This mass transfer model can then be coupled with the absorber model to provide accurate predictions of rich loadings of the sorbent.

7.2.2 Kinetics

- **The effect of increased nucleation sites on the effective diffusion length needs to be studied in more detail** This can be achieved by embedding nano-particles on the inner surface of the reboiler, having an ultrasonic probe submerged in the reboiler to generate cavitation bubbles.
- **Alternate reboiler designs with lower liquid hold-up need to be investigated.** Flat or horizontal designs, perhaps in the domain of microfluidics, can be looked at. These designs should be geared towards improving the mass transfer characteristics of the process.

Note: Additional results from the kinetics experiments are presented in section D.5.

7.2.3 Desorption Column

- **Investigate the possibility of using sorbent as a heat transfer liquid to cool the PV panels.** This serves two purposes; it will cool the panel allowing it to operate within optimal conditions for production. On the other hand, the pre-heated sorbent can then enter the desorption column, lowering the sensible heat demand of the process.
- **Heat recovery from the column during shut-down.** Since the column operates at high temperatures, this stored energy is lost to the surroundings during shut down. Methods to minimize these losses or recover the heat need to be investigated. Investigate the feasibility of a warm start between operations via waste heat recovery.
- **A dynamic analysis of FM and AEC is needed to develop a global control scheme for the ZEF micro-plant.** Currently, the dynamic nature of the DAC output has been understood, but the response of subsystems downstream to fluctuating inputs needs to be investigated. Only then can a sequence of operations for plant-wide start-up and shut-down can be chalked out.
- **Possibility of ramping up production of FM and AEC while the buffer tanks are full.** In such cases, despite the availability of power, the desorption column is shut down. FM and AEC downstream should use the surplus to increase their production, thereby returning the buffer to nominal levels.
- **Compare the cost of purging excess CO_2 H_2O to the cost of increasing the buffer tank volume.** The former affects the operating cost of the system, while the latter dents the capital expenditure. Quantifying which one is larger and at which point equilibrium is reached will be crucial in sizing the buffer and developing a robust control philosophy.
- **Systematic analysis of utilizing a constant power source (Battery) to drive the DAC subsystem will prove helpful. Compare the costs of the battery (CAPEX) to the gain in revenue due to the increased operation window and thus increased production.** Alternatively, design a smaller plant that meets the original production criteria. Figure 7.1 depicts the change in the production period while using a battery to power the process. **For the same rated power , a battery performs better in terms of production and increasing the operation window as compared to a process driven by a PV panel.**

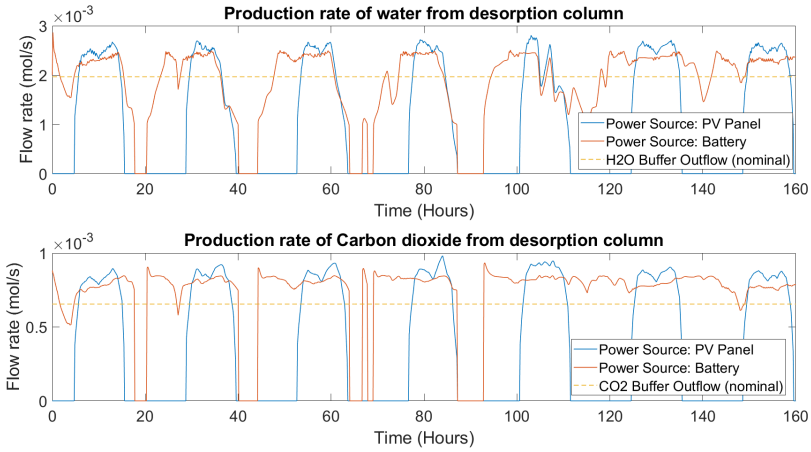

Figure 7.1: Comparing the effect of using a PV panel against a constant power source such as a battery on the CO_2 & H_2O production. Simulation carried out for the month of March, 2016 in Bechar, Algeria (Sahara Climate).

Note: Additional results for the battery case are provided in section D.4.

- **For dry climates, shift the operating window towards the earlier hours of the morning.** Since the absolute humidity is higher in the mornings, leading to adequate water loading of the sorbent, thereby reducing the need to operate DAC in the afternoon when the atmosphere is arid. **The shift in operation window can be accommodated with a battery** that supplies power in the mornings during PV panel downtime and charges in the afternoon during DAC downtime.
- **For cool and wet climates with *inconsistent sunlight*, alternative power sources are recommended.** The summer months generate an energy surplus, as compared to winter. Investigate the possibilities of storing surplus energy in the long term to be used in the winter. Appropriate sizing and costing of the battery is needed.
- **In wet conditions or early hours of morning** allow the system to operate at **higher top ratios (>3**. This ensures a greater amount of water is produced by the desorption column, while it is available in the atmosphere. This philosophy compensates for the drier conditions during the later portion of the day. Once the buffer tanks are approaching full capacity, the operating ratio can be adjusted accordingly.

Appendix A

Appendix A: Relevant Theory

A.1 Carbon Capture Route

A.1.1 Adsorption

Adsorption involves separation of a fluid from a mixture, by adsorbing onto the surface of a solid adsorbent. Adsorption is a surface phenomenon. Primary advantage of CO_2 capture via adsorption is the lower energy demands and material losses, compared to absorption based capture [19]. Depending on the nature of bonds formed between the adsorbate and adsorbent, it can broadly be classified into physical and chemical adsorption. The following table highlights the major differences between the two.

Table A.1: Difference between physical and chemical adsorption [19]

Type	**Physical adsorption**	**Chemical adsorption**
Principle	van der Waals	Chemical bonds
Temperature	High adsorption at low temperature	Occurs at relatively high temperature
Adsorbate	Non-selective	Selective
Heat of adsorption	Low range (8-20 kJ/mol)	High range, equal to heat of reaction (40-800kJ/mol)
Reversibility	Reversible	Can be irreversible, depends on the chemical reaction
Adsorbtion rate	Fast	Slower, requires energy of activation

A.1.2 Membrane separation

It involves mass transfer of a particular species across a semi-permeable membrane due to a pressure gradient. Osmosis is an example of a membrane based mass transfer process, through which plants take in water and nutrients from the soil.
In the case of carbon capture, the cost of membrane separation depends on two major components: the membrane module itself and the cost of the vacuum pump required to establish a strong pressure gradient across the membrane from the permeate side [19]. Different types of membranes have been developed.

- **Polymeric membranes:** Glassy polymers made from cellulose acetate and polyimide can be used for selectively separating CO_2 from flue gas mixtures. But they do not fare to well at high partial pressures due to CO_2 induced plasticization.

- **Inorganic membranes:** These membranes have appropriately sized pores that can selectively trap molecules from a fluid mixture depending on the size of the molecule. They act as molecular sieves.
- **Ionic Liquid membranes:** High selectivity for CO_2 and stability at relatively high temperatures.

A.2 Solid Sorbent Systems

Absorption and desorption are often carried out in the same unit in the plant via temperature or pressure swing methods. The absorber or desorber here is a porous solid matrix structure, made up of the sorbent material. Like liquid absorbent systems, ambient air is made to flow through the porous absorber, where the CO_2 in the incoming air reacts with the sorbent and bonds with it.[43].

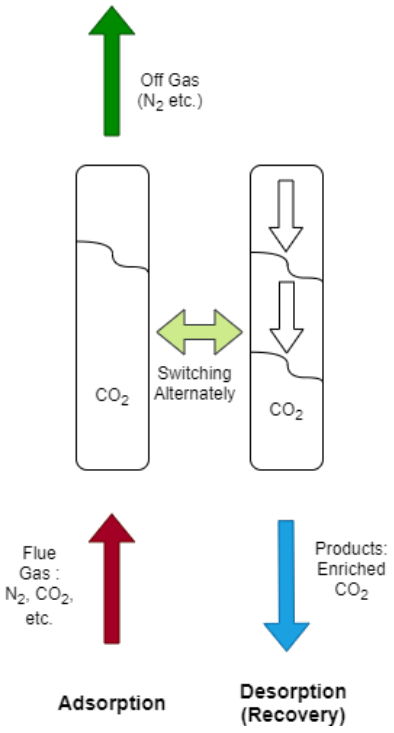

Figure A.1: Schematic illustration of a solid sorbent carbon capture process. The vertical columns represent absorption & desorption columns

Once the material is saturated with CO_2, the airflow is stopped, and the material is heated to initiate the desorption. Zeolites have been considered as prime candidates as solid sorbents for carbon capture. These micro-porous aluminosilicates are incredibly efficient at capturing CO_2 from the air due to their high selectivity due to their pore size, which matches the size of a CO_2 molecule.

A.2.1 Solid Amine Sorbents

These are essentially porous solid supports impregnated with amines. Depending on the type of bonds formed between the amine molecules and the support they are classified into three categories [44].

- **Class 1:** Here the amines are impregnated into the pores of the support, and are held in place by physical forces such as hydrogen bonds.

- **Class 2:** These are a class of sorbents, where the amines are covalently bonded to the walls of the support.
- **Class 3:** In this case the amine monomers have undergone polymerisation inside the support structure, resulting in polyamine structures that are tethered to the surfaces of the support.

Solid amine sorbents have lower heat of regeneration for the sorbent, since sensible heating loads are lower. Moreover, the complexity of constructing the absorption/desorption column is complex, since both the processes need to occur in the same place. Unfortunately, the repeated cycles of temperature changes during absorption and desorption have a negative impact on the structural integrity of the support [44].

Advantages:

- Solid sorbents usually have lower regeneration temperatures, lowering the energy costs involved.
- Designing an absorber with solid stacks of sorbents is more manageable than working with liquid sorbents [43].

Disadvantages:

- Manufacturing zeolites with custom-sized pores is challenging and expensive.
- Most solid matrices cannot withstand the repeated temperature swings needed for desorption, and they lose their structural integrity quite soon decreasing life cycle time and increasing costs [45].
- Chemical reaction kinetics are also slower for solid sorbents as compared to liquid sorbents.

A.3 Amine: Performance characteristics

A.3.1 Heat of Regeneration

The energy demand for regeneration can be separated into three components:

$$E_{regeneration} = E_{sensible} + E_{absorption} + E_{vaporisation} \tag{A.1}$$

- **Sensible Heat:**The sensible heat component is the amount of heat energy needed to raise the temperature of incoming feed to the desorption temperature. The sensible heat component depends on the mass flow rate, the composition of the loaded amine and also the desorption temperature [46].
- **Heat of Vaporisation :**The latent heat of vaporisation is also quite significant since it refers to the energy needed to expel the H_2O from the amine into the vapour phase. The heat of vaporisation for amine-water blends has been found to be higher than that of pure water, and this can be ascribed to the presence of hydrogen bonds between the amine and H_2O molecules formed during mixing [46].
- **Heat of Absorption :**The heat of absorption refers to the amount of energy liberated due to chemical bond formation when the CO_2 reacts with amines to form carbamates or bicarbonates. This is an exothermic reaction, thus to reverse the reaction to liberate the absorbed CO_2 and water, we need to supply thermal energy to break these chemical bonds. In the case of MEA, research reveals that 50-60% of the regeneration energy is basically the heat of absorption. Thus, to reduce energy demands in the stripper column, it is desirable to have amines with lower heat of absorption [46].

$$\ln\left(\frac{P_2}{P_1}\right) = \frac{\Delta \mathrm{H}_{absorption}}{R}\left(\frac{1}{T_2} - \frac{1}{T_1}\right) \tag{A.2}$$

Usually, the Clausius-Clapeyryon equation Equation A.2 is used to evaluate the desorption temperature of the sorbent, while taking absorption temperature, pressure and the heat of absorption as the inputs.This results in a high desorption temperature, since literature shows that sorbents like MEA and TEPA have absorption enthalpies in the range of 70-80kJ/mol of CO_2 [27].
But, Dowling et al. [25] utilised the Clausius-Clapeyron equation to evaluate the heat of absorption of TEPA, using the data obtained from the Specific Interaction Theory (SIT) model and VLE experiments. In this case the inputs were absorption and desorption pressures and temperatures using isotherms from experimental data.
Another possibility is novel sorbents, with low regeneration temperatures. Using the same Clausius-Clapeyron equation, while taking the inputs as the desorption pressure, ambient partial pressure of CO_2, absorption and *desired* regeneration temperature, in such cases it is seen that the heat of absorption comes out to be higher than the conventional amines.
Naturally, this raises concerns, since on the surface a higher heat of absorption will increase the energy demand of the desorption column, but, with lower regeneration temperatures, the sensible heating load on the desorption column will also be significantly lesser. Further investigation is necessary to evaluate whether the drop in sensible heat load outweighs the increase in the heat of absorption. If it does, there is motive to develop such sorbents.

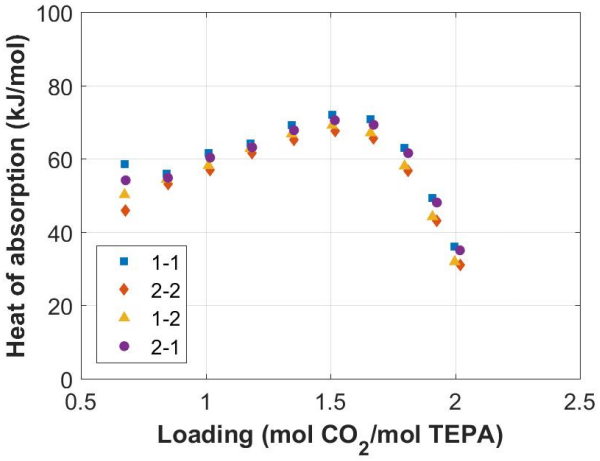

Figure A.2: Heat of absorption calculated using the Clausius Clapeyron equation and the CO_2 absorption isotherms. [25]

A.3.2 Stripper: Quantifying Energy Consumption

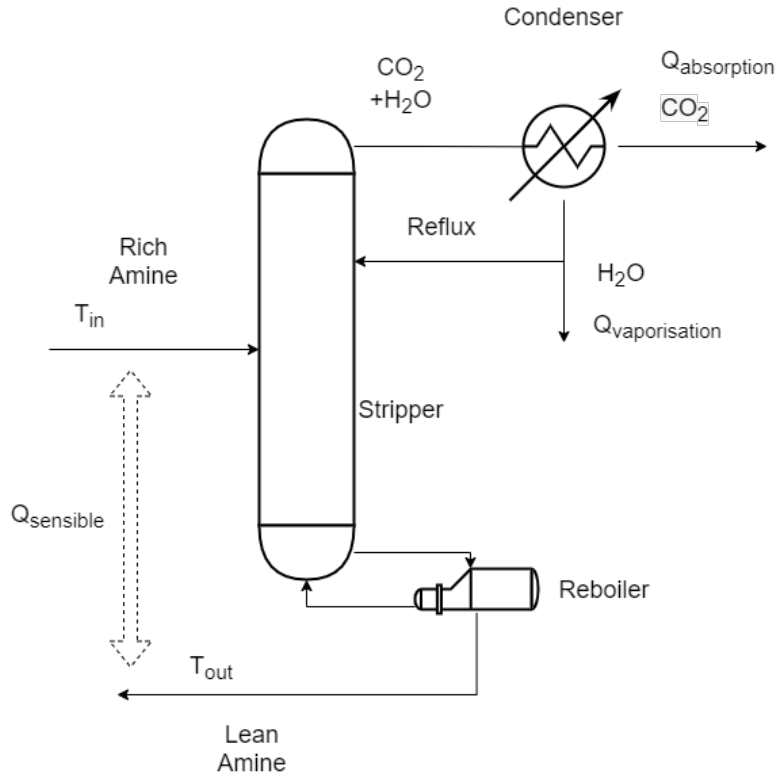

Figure A.3: Schematic of a stripper column, depicting the energy requirements [19].

The first step towards optimising the cost of the process and plant would be to quantify energy consumption and identify areas where the plant or system design changes can improve efficiency. But, changes in plant design only address part of the issue, drastic changes in energy consumption depend on the nature of the sorbent used.
Goto et al. [47] utilised a 2-(isopropylamine) ethanol-based solvent (IPAE-based solvent) in a pilot plant study for post-combustion capture. The plant produced around 10 tonnes of CO_2 per day. The flue gas stream had a relatively high concentration of CO_2, approximately 12-13%. The treated flue gas was made to interact with the IPAE based sorbent (45% wt. concentration, aqueous amine solution). This sorbent was chosen due to its low heat of absorption and large CO_2 capture capacity. The plant's operating conditions were varied, especially the liquid-gas ratio in the absorption column and the steam regeneration rate in the desorption column. It was discovered that steam regeneration rates were proportional to the amount of CO_2 recovered, and the energy costs. On the other hand, lower liquid-gas ratios was ideal for lower energy requirements. Through the study, for an optimised run, they calculated an energy requirement of approximately 3.0 GJ per tonne of CO_2 with a 90% recovery rate [47].

Table A.2: Compilation of important results from the pilot plant study [47].

	Run 3	**Run 4**	**Run 5**
L/G [kg/Nm^3]	5	2.5	2.5
Reboiler steam feed rate [GJ/h]	1.2	1	1.4
CO_2 recovery [%]	78	76	92
Energy Requirement [GJ/tonne CO_2]	3.4	2.9	3.1

Dowling et al. [25] developed a steady state model for the DAC unit at ZEF, which was used to evaluate the energy consumption of the stripper unit under various conditions of operation the results are presented in the Relevant theory section.

A.4 TEPA: Absorption & Desorption

A.4.1 TEPA:Absorption

Research shows that the addition of water to TEPA has a significant positive impact on the CO_2 absorption rate [27]. This can probably be ascribed to the lower viscosity of the mixture with increasing water content, allowing for better mass transfer rates due to faster surface renewal at the sorbent air interface.

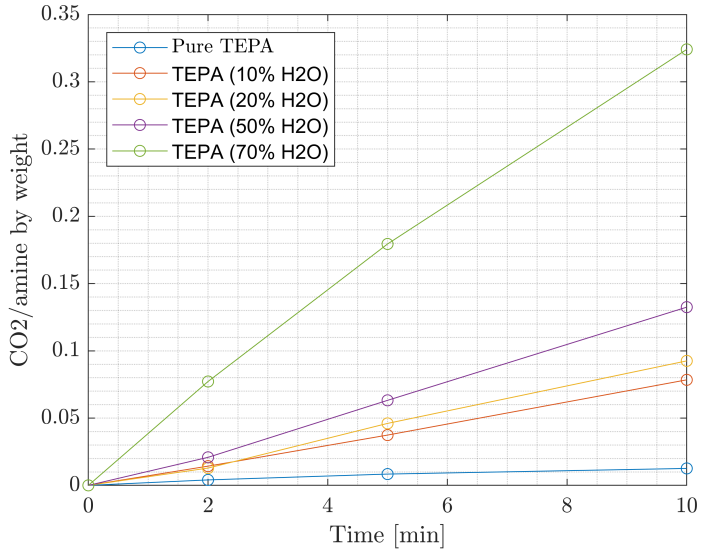

Figure A.4: Variation of CO_2 loading with change in water concentration in TEPA-H_2O mixture [27]

A.4.2 TEPA:Desorption

Desorption of the ternary mixture is carried out at high temperatures ideally between 100-140°C. Beyond 135°C, the amine undergoes severe thermal degradation, which is undesirable [48],[25]. Ideally, for desorption, high temperatures and lower pressures are necessary to expunge the absorbed CO_2 and water from the H_2O. In the case of ZEF, the system pressure is usually fixed depending upon the desired cyclic loading and the ratio of the products. Thus, the only variable left for varying in desorption is the temperature. Nevertheless, experiments by Bart Ovaa [45] showed that with increasing temperatures and lower pressures, more desorption took place from the same initial rich loading.

A.5 Design of Desorption column

A.5.1 Design of Stripping Columns

As discussed earlier, desorption columns come in various configurations, but the most commonly used ones are briefly discussed below:

Trayed Columns

Essentially a cylindrical, vertical column, divided up into sections via trays. Inside the column, the rich sorbent and stripping gas flow counter currently and come into intimate contact over plates or

trays, which enhances the rate of mass transfer. Trays come in different configurations, but in the most common cases, it is essentially a perforated plate with a weir and downcomer [20].

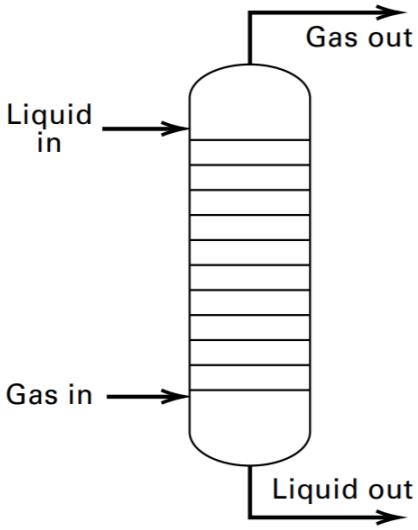

Figure A.5: Schematic of a trayed column [20]

The liquid forms a thick film over the plate and flows over the weir into a downcomer. The influence of gravity further leads it to the next tray. The stripping gas bubbles up from below and comes into contact with the liquid film on the tray through holes. Lockett identified different two-phase regimes [49] on these trays, which have been elaborated in the relevant theory section.

Trays can also further be classified into sieve, valve and bubble cap trays, elaborated in relevant theory.

Table A.3: Comparison of types of trays [20]

	Sieve Trays	**Valve Trays**	**Bubble-Cap trays**
Relative Cost	1.0	1.2	2.0
Pressure Drop	Lowest	Intermedieate	Highest
Efficiency	Lowest	Highest	Highest

Packed Columns

Packed Columns are vertical pressure vessels with one or more sections of packing material. The liquid sorbent is flowing downward through the packing, as the vapour phase flows upward. As they are brought into intimate contact, the mass transfer occurs. The packing material is classified as random or structured packing depending on the arrangement. As the name suggests, random packing is tiny pellets of the material randomly poured into the column. Structured packing, on the other hand, has well-defined pathways that are manufactured through extrusion or embossing, which are designed to maximise the mass transfer efficiency [20].

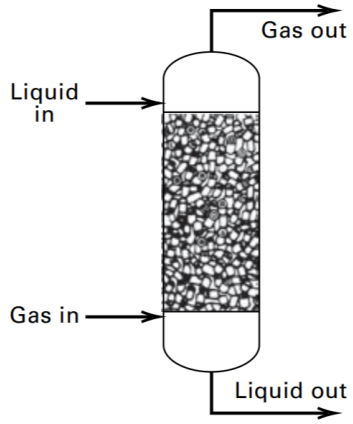

Figure A.6: Schematic of a packed column [20]

Table A.4: Differences between tray and plate columns [20]

Tray Columns	**Packed Columns**
Suitable for a wide range of liquid and vapour loads. Especially for low liquid rates.	Suited for medium to high flow rates of liquid and vapour loads.
Maintenance of damaged or dirty trays is easier. Modular approach possible.	Modular packings are available, but cost of manufacturing and replacing these is quite high and time consuming.
Better equipped for larger diameter columns.	Suitable for smaller diameter columns <0.6m
High liquid residence time, better mass transfer but higher pressure drop.	Low liquid entrainment and hold-up, lower pressure drop.

A.5.2 Desorption column: Reboiler

In the industry, the type of reboiler used depends on the application and size of the column.

- For large use cases, external reboilers are used, such as a fired heater, forced circulation boiler, kettle reboiler, thermosyphon reboiler.
- For smaller use cases, generally, the reboiler is integrated into the design of the column itself in the bottom [20].
- Most reboilers are essentially shell and tube heat exchangers, with the bottoms product usually flowing on the shell side, and steam is usually the heating fluid but can vary depending on the application.

A.5.3 Tray Froth regimes

- **Froth regime:** ideally favoured regime, the liquid phase is continuous with the gas passing through the film in a stream of tiny bubbles or jets [49].
- **Spray regime:** Here, the gas phase is continuous, which occurs for low liquid flow rates [49].
- **Bubble regime:** For low gas flow rates, the liquid sorbent is quite calm, while large bubbles rise up in swarms to interact with the liquid [49].

Ideally, the liquid sorbent doesn't carry any vapour bubbles to the next stage (occlusion), and the vapour phase doesn't entrain any liquid sorbent particles to the next stage. Moreover, there is no

weeping, i.e. flow of the liquid through the holes in the tray [20].

A.5.4 Types of Trays

- **Sieve tray:** the simplest of all trays, with holes or perforations on the tray, diameter varies depending on the application. Economical, and do not cause any significant pressure drop across each stage [20].

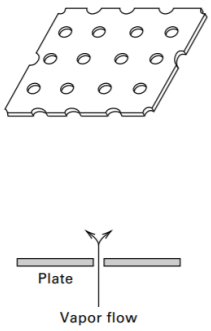

Figure A.7: Schematic of a sieve tray [20]

- **Valve tray:** Similar to a sieve tray, but the size of the holes can vary due to the presence of a valve cap that overlays the hole while sitting on a couple of legs. As the gas flow rate increases, it pushes the cap upwards, increasing the size of the opening and vice versa—higher pressure drop than sieve trays, but also more efficient in terms of mass transfer [20].

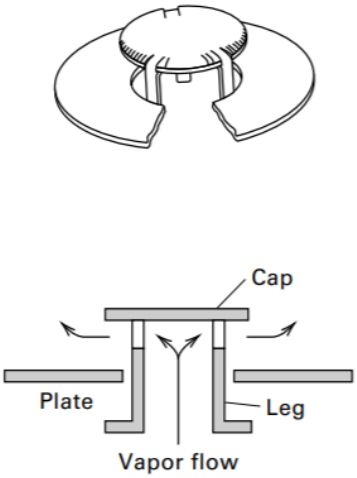

Figure A.8: Schematic of a valve tray [20]

- **Bubble cap tray:** Consists of a larger diameter cap that sits on top of a smaller concentric riser. The cap has triangular or rectangular slots for the vapour to pass through. The vapour enters the riser from the stage below, passes through the passage between the cap and riser and passes out of the slots in the cap, creating a froth at the base of the cap. Highest efficiency as compared to sieve and valve tray, but causes a high-pressure drop across stages and is also costly [20].

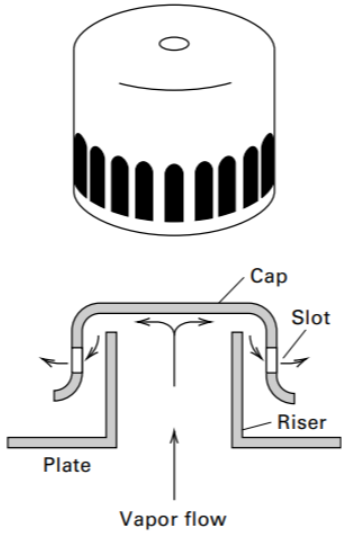

Figure A.9: Schematic of a bubble cap tray [20]

In addition to the structural aspects of a stripping column, the equipment design is heavily influenced by a load of other variables, such as [20]:

- Feed composition, flow rate temperature and pressure and quality.
- Column operating temperature and pressure.
- Desired composition of top and bottoms product.
- Number of equilibrium stages, stage efficiency.
- Choice of stripping gas or absorbent.
- Analysis of essential heating and cooling requirements.
- Dimensions of the column, i.e., the height and diameter.

A.6 Stripper: Energy Quantification

Table A.5: Operating Conditions tested by Dowling et al. [25]

Operating Conditions	**Temperature (Celsius)**	**Relative Humidity (%)**
Dry & cold (1)	20	25
Humid & cold (2)	20	75
Dry & hot (3)	40	25
Humid & hot (4)	40	75

Some of the learnings from the research are listed below:

- A cyclic capacity of 1 mole of CO_2 per kg TEPA is assumed constant. A dry and cold climate could not meet the H_2O requirement of ZEF. But if the climate is too humid, the enthalpy of vaporisation increases sharply, overwhelming the energy consumption and costs. In the latter case, since the partial pressure of water in the desorption column will be higher than required, a reflux stream will be needed to ensure the desired amount of CO_2 is delivered as product. Naturally, the additional reflux also increases the thermal load on the stripper.

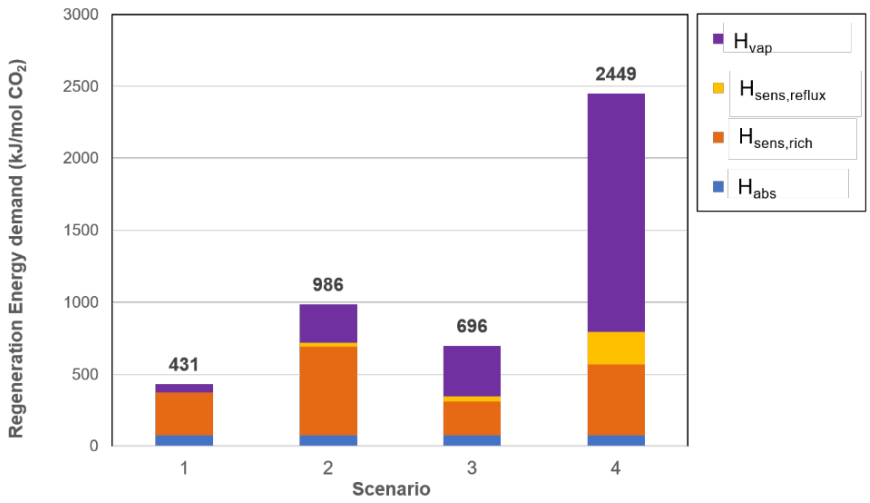

Figure A.10: Energy demand of the stripping column for different scenarios highlighted in Table A.5 [25]

- The cyclic capacity was then varied, while keeping the ambient conditions constant to understand the influence of the former on the energy requirements. It was noticed that increasing the cyclic capacity of the DAC unit, decreased the sorbent flow rate for the desired output of Carbon dioxide and water (Ambient temperature of 20°C and 50% relative humidity). Increasing the cyclic capacity, decreases the amount of water and CO_2 in the lean stream, implies the drop in partial pressure inside the desorption column. The drop in the CO_2 partial pressure is sharper than the water partial pressure, thus the reflux ratio increases resulting in an increase in the heat of vaporisation. Since, a lower flow rate of TEPA is needed , the sensible heating demand goes down, thus the overall energy demand depends on the balance between the reflux ratio and feed flow rate.

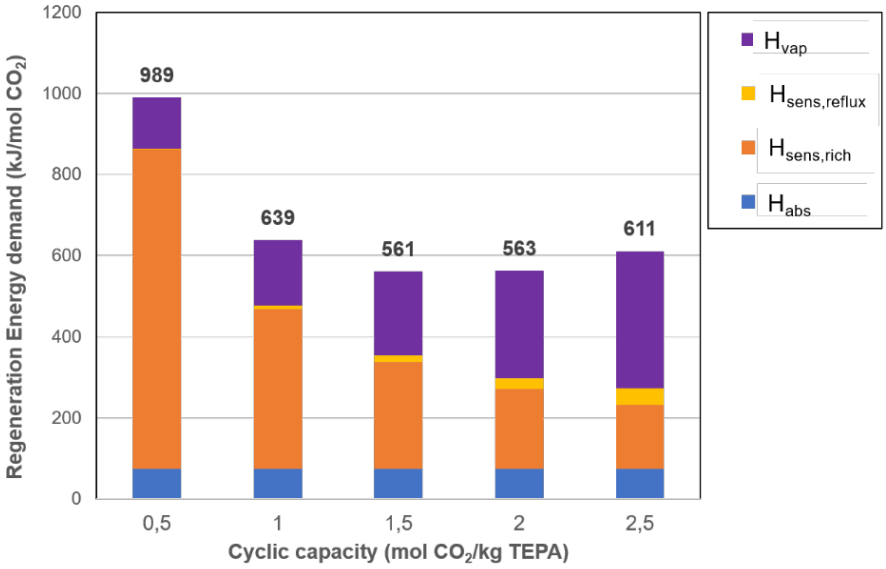

Figure A.11: Energy demand of the stripping column for different cyclic capacities [25]

- Finally, the stripping temperature was varied, while keeping the ambient conditions (20°C & 50% relative humidity) and cyclic capacity (1.5) constant. Increasing the stripper temperature, increases the overall pressure in the column, but the increase in CO_2 partial pressure is sharper

than H_2O, thus a lower reflux ratio is needed to obtain the desired output. Naturally, the sensible heating load will be larger with increasing stripping temperature, but, the heat of vaporisation will be lower, due to lower reflux ratios. An extremely high temperature cannot be used, although it favours better CO_2 removal since it reduces the life span of the sorbent.

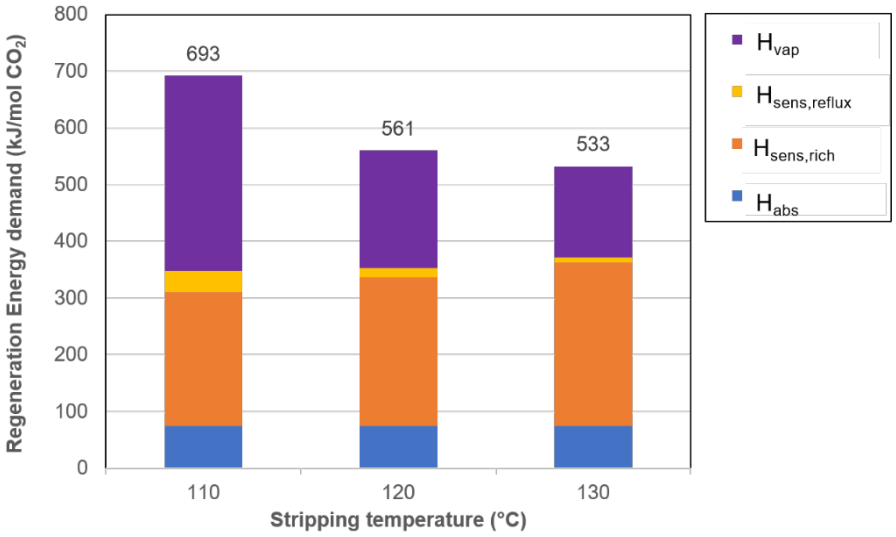

Figure A.12: Energy demand of the stripping column for different stripping temperatures [25]

Based on these findings, the ideal scenario for ZEF was identified to be a dry and hot climate, with a stripping temperature of 130°C for TEPA and a cyclic loading of 1.5 mole of CO_2 per kg TEPA.This puts the stripper energy demand at 533 kJ/mole CO_2 [25], as compared to 172kJ/mol CO_2 for MEA [50]. Thus, a sorbent with better regeneration characteristics than TEPA, and process optimisation is needed to lower the overall energy demand of the stripper.

A.7 Stripper: Chemical Kinetics

A.7.1 Chemical Kinetics

From the two-film theory [20], it is clear that there are several processes occurring sequentially for the carbon dioxide to be absorbed into the amine. Two important steps that play a role in the overall mass transfer rate is the diffusion of the gas into the amine across the interface and the chemical reaction leading to the formation of carbamates, as explained earlier.

$$k = A \cdot \exp \frac{-E_a}{RT} \tag{A.3}$$

To determine the rate-limiting step, a non-dimensional number is introduced: the Hatta number, it is used to compare the rate of reaction in a film to the rate of diffusion of species through the same film. It is similar to the Thiele modulus, which was developed to compare the reaction and diffusion rates in catalyst induced reactions. Larger values of the Hatta number imply the reaction is diffusion-limited, and vice versa. In the case of liquid amine-based carbon capture, the Hatta number ranges between 10 to 35 [51], which means the reaction rates are instantaneous, but the mass transfer is diffusion-limited.

$$Ha = \frac{1}{k_L}\sqrt{D_{CO_{2,am}} k_2 C_{a\,\min e}} \tag{A.4}$$

Similarly, the second Damkohler number is a ratio of the chemical reaction rate to the diffusive mass transfer rate [52].

$$Da_{II} = \frac{L^2 r}{DC} \tag{A.5}$$

A.8 VLE: Fundamentals

A.8.1 Concept of Phases

A phase means any equilibrium state of a macroscopic system that is homogenous with respect to its physical properties and chemical composition. Since a phase corresponds to an equilibrium state, it is intrinsically stable. But this state is defined within certain ranges of temperatures and pressures, beyond which the system ceases to be intrinsically unstable and splits into homogenous subsystems corresponding to different phases. This is called a phase transition. In addition to the conditions of thermal and mechanical equilibrium, the two phases should also have the same values for chemical potentials for them to coexist. This is called the phase rule [53].
For multi-component mixtures, regions of phase coexistence become more complex, to simplify the process of understanding the degrees of freedom associated with the mixture a nifty equation can be used:

$$F = C - P + 2 \tag{A.6}$$

This is referred to as the Gibbs phase rule. It specifies the number of independent intensive parameters in the system that can be changed without violation of the phase rule [53].

A.8.2 Vapour-Liquid Equilibrium

When vapour and liquid phases of a pure substance or a mixture of components coexist under particular conditions of temperature and pressure, it is called vapour-liquid equilibrium (VLE). Since the phase coexistence of the vapour and liquid is a function of temperature, pressure and composition of the mixture, it is possible to establish mathematical relationships that can be used to extract information regarding one unknown quantity provided the other two are known. Utilising pressure vs mole fraction or temperature vs mole fraction, VLE diagrams can be used to accurately understand the behaviour of a mixture or pure substance over a wide range of temperatures, pressures and compositions [53]. VLE data for a particular species is a crucial input for designing the desorption process. For example, depending on the desired composition, it is possible to quantify the variation in temperature and pressure needed to shift the VLE to obtain the desired separation.
For mixtures, the condition for equilibrium between phases can be represented by the *iso-fugacity* condition.

$$f_i^V = f_i^L \tag{A.7}$$

This should hold for every component in the mixture. Ideally, we would like to establish a relationship between the fugacity of each component with the composition of the mixture.Thus, the fugacity coefficient of components in the gaseous or vapour phase is defined as:

$$\phi_i^V = \frac{f_i^V}{y_i P_{total}} = \frac{f_i^V}{p_i} \tag{A.8}$$

The fugacity of a component in the gas phase can be considered as the ”effective partial pressure” exerted by that component in a non-ideal gas mixture. And the fugacity coefficient is the ratio of fugacity to the partial pressure of the component. For ideal gas mixtures, fugacity of the component is equal to the partial pressure. Thus the fugacity coefficient is a measure of the deviation of a real gas from ideal gas behaviour in a mixture.
For liquid components in a mixture, the fugacity of a component is related to the activity of that component in the mixture through its mole fraction. The activity of a component can be defined as

the "effective concentration" of that component in the mixture. The activity coefficient is a measure of the deviation from ideal solution behaviour. For an ideal solution, the activity of a component is equal to its mole fraction, and the activity coefficient is 1.

$$\gamma_i = \frac{a_i}{x_i} = \frac{f_i}{x_i f_i^0} \tag{A.9}$$

The concepts of activity and fugacity are analogous to each other; as such, they represent the respective "corrected" quantities for real liquid and gaseous mixtures. The $f_i{}^0$, in the second term, is the standard state fugacity of component i. Usually, for convenience, the standard state is that of the pure liquid at system temperature and pressure [53]. This can be calculated:

$$f_i^0(T, P, x_i = 1) = P^*_{i,vap}(T)\phi^s_i(T) \exp \int_{P^*_{i,vap}}^{P} \frac{V_i^L(T,P)}{RT} dP \tag{A.10}$$

where $P_{i,vap}{}^*$ is the pure component saturation vapour pressure and $_s$ i is the pure component fugacity coefficient. The exponential term is called the Poynting factor, which can be usually neglected, as a liquid is nearly incompressible [53]. Putting all these formulas together into the iso-fugacity condition results in the well-known VLE relation for each component:

$$y_i P_{total} = \gamma_i x_i P^*_{i,vap} \frac{\phi^s_i}{\phi_i} \exp \int_{P^*_{i,vap}}^{P_{total}} \frac{V_i^L}{RT} dP = \gamma_i x_i P^*_{i,vap} F \tag{A.11}$$

Often, this relation is simplified by assuming the correction factor F equal to unity, which is justified at low to moderate pressures. This relation is then called the modified Raoult's law.

$$y_i P_{total} = \gamma_i x_i P^*_{i,vap} \tag{A.12}$$

For ideal solutions, since the activity coefficient is unity, the equation further simplifies to :

$$y_i P_{total} = x_i P^*_{vap} \tag{A.13}$$

Raoult's law applies to ideal solutions in the liquid phase in equilibrium with the gaseous phase treated as a mixture of ideal gases. According to Raoult's law, the partial pressure of a given component in the vapour above the solution is proportional to the molar fraction of that component in the solution.

A.8.3 Separation using Vapour-Liquid Equilibria

Existing literature and software packages can provide a litany of data for binary mixtures, unfortunately for multicomponent mixtures (more than 2), significantly lesser data is available due to the practical difficulties associated with data collection. But it is possible to circumvent this by using other methods, to gain insight into the possibilities of separation of a particular mixture. Distribution coefficient or the K value is the ratio of mole fractions of a species in the vapour and liquid phases in equilibrium.

$$K_i = \frac{y_i}{x_i} \tag{A.14}$$

Where y_i represents the mole fraction in the vapour phase, and x_i represents the mole fraction in the liquid phase. This depends on the temperature, pressure and for real mixtures the nature of the species in the mixture. It gives us a measure of the proclivity that a particular species has to move towards a certain phase. For example, if K>1, it implies that for a given temperature and pressure, species i will have a higher mole fraction in the vapour phase than in the liquid phase. Taking this

one step further, to compare the feasibility of separating components, we evaluate the ratio of the respective K values. This is called the relative selectivity. Larger the value of alpha, easier is the separation.

$$\alpha_{i,j} = \frac{K_i}{K_j} \tag{A.15}$$

In an ideal system, the liquid phase behaves, according to Raoult's Law and the vapour phase according to the ideal gas law. For a certain system, the K value is given by:

$$K_i = \frac{y_i}{x_i} = \frac{P^*_{i,vap}}{P_{total}} \tag{A.16}$$

For a non-ideal system, the K value is also depending on the composition of the mixture:

$$K_i = \frac{\gamma_i^L}{\phi_i^V} \cdot \frac{P^*_{i,vap}}{P_{total}} \tag{A.17}$$

A.9 Modelling

A.9.1 Controller Types

- **Proportional Control:** The simplest mode of control, wherein the control action or the adjustment made to the manipulated variable is proportional to the error. The nature of the controller depends on the gain; one should take care not to have high controller gains as this can induce instabilities in the system. One major drawback of proportional control is its inability to achieve zero steady-state offsets. The integral action of the controller rectifies the former.
- **P & Integral Control:** To eliminate the steady-state offset observed in proportional control, integral mode tries to sum up the errors up until the current time step and adjusts the manipulated variable accordingly. Proportional model takes into account the error at the current time instant while integral control takes into account the cumulative error build up till that time instant. A drawback with integral only control is the slower response times. A smaller integral time results in an aggressive response that can induce oscillations in the system.
- **PI & Derivative Control:** To overcome the slower response times experienced due to the addition of integral mode, derivative control is introduced. The latter tries to anticipate the rate of change of error and thus adjusts the manipulated variable before the error becomes too large, thereby improving the transient response. Derivative control is not used by itself, but it is combined with P or P&I control.

Appendix B

Appendix B:Experimental Procedures & Equipment

B.1 Sorbent Loading

Performance evaluation of a desorption column calls for a supply of loaded sorbent with a known composition of CO_2 and H_2O. To maintain parity across experiments, the sorbent composition is maintained at similar levels across different batches prepared, within limits of experimental error. A mixture of TEPA: PEG200 in a 1:2.5 ratio was used to prepare the masterbatches with inputs from the sorbent selection team. The method of loading the sorbent is explained in

B.1.1 Sorbent Loading: Setup

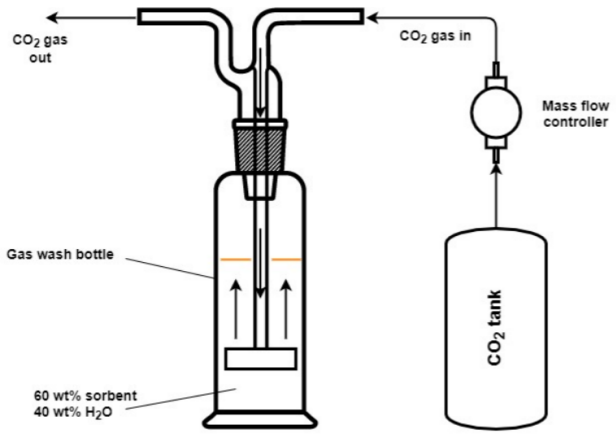

Figure B.1: Schematic representation of the sorbent loading setup

This setup enables the loading of a sorbent artificially. It consists of a pair of 500ml gas wash flasks, pair of bottle heads with a diffuser, a pressurized carbon dioxide tank, a magnetic stirrer, and a flow regulator. The first flask is for the sorbent loading; the second is partially filled with water and acts as a buffer between the CO_2 tank and the first flask. A buffer flask is used to prevent the backflow of sorbent into the CO_2 feed tank under any circumstances. A flow regulator is used to control the flow rate of gas as it flows from the tank into the buffer flask, bubbles through the sorbent solution and is eventually expelled into the fume hood. The sorbent flask is placed on a lab heater with a magnetic stirrer that mixes the sorbent during loading, thus enhancing the absorption rate. A moderate flow

rate of gas is maintained. Smaller bubbles are preferable due to the higher specific surface area in contact with the sorbent. It also prevents the vigorous frothing of sorbent, which can tip the flask if it isn't secured correctly.

B.1.2 Sorbent Loading: Procedure

The preparation of a masterbatch is split into two phases: making the lean sorbent followed by loading it with CO_2. One can achieve this via the following steps:

- To prepare 500grams of lean sorbent with 30% H2O, add 100g of pure TEPA and 250g of PEG200 (1:2.5) to the gas wash flask, followed by 150g of water. Stir the mixture thoroughly for a couple of minutes using the magnetic stirrer. The sorbent will release some amount of heat of absorption due to the reaction between TEPA and water.
- After obtaining a homogenous mixture, close the sorbent flask by inserting the bottle head attached with a diffuser. Fill in some water into the buffer flask, close it and connect the outlet to the sorbent flask.
- Set the magnetic stirrer at a speed of 500rpm; since the addition of PEG200 and water, the sorbent viscosity is low enough to allow the rotation of the stirrer without the need for heating it.
- Open the regulating valve gradually till tiny bubbles appear in the buffer flask, followed by the sorbent flask. Let the gas bubble through the sorbent for 45 minutes. With time the sorbent becomes more viscous due to CO_2 loading. It may offer more resistance to the flow of gas near the diffuser, do not increase the flow rate under such circumstances since the pressure drop across the line can be dangerous.
- The appearance of the sorbent changes at higher loadings; it turns visibly more viscous and opaquer. Shut off the gas flow, turn off the magnetic stirrer and disengage the buffer flask from the sorbent flask.
- Transfer the contents to a bigger storage flask and repeat the loading procedure with fresh lean sorbent until the desired amount of loaded sorbent is ready.
- Thoroughly mix the contents of the larger storage flask to get rid of stratification. Once a homogenous mixture is obtained, perform an FTIR to evaluate the CO_2 and H_2O concentrations.

B.2 Desorption Column: Setup

Figure B.2 shows the complete desorption column setup used for the start-up and shut-down experiments. Different parts of the setup are highlighted in the figure. The main components of the setup are the stripper column, flash tank & condenser.

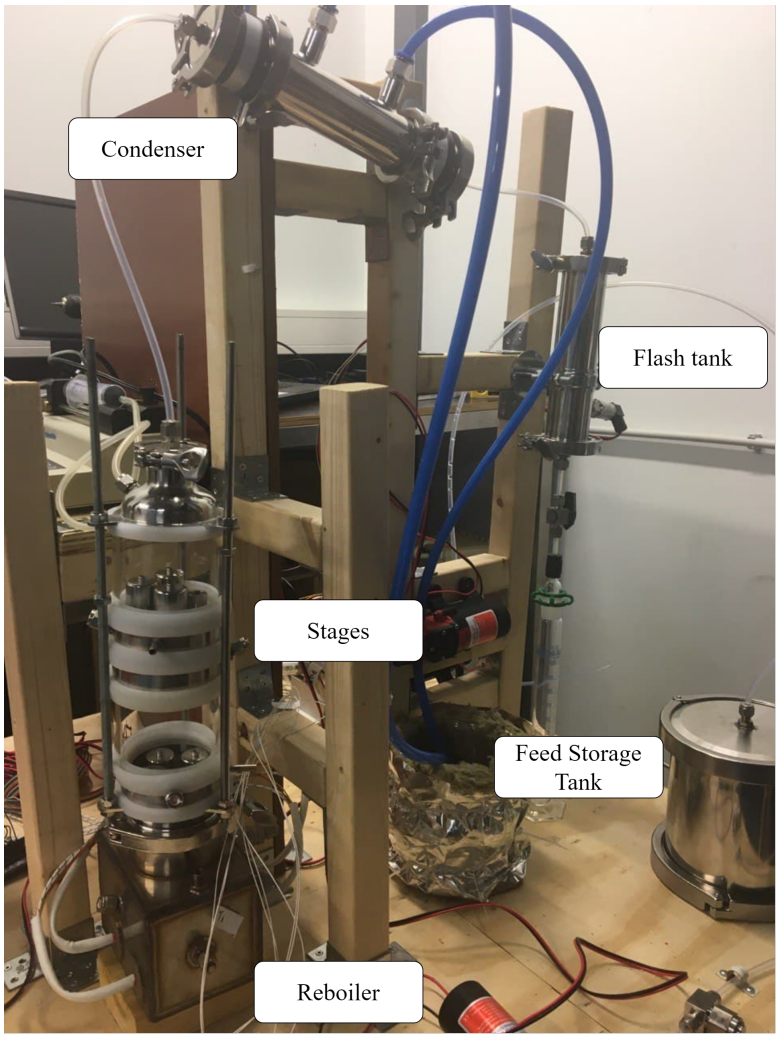

Figure B.2: Complete desorption column setup used for the start-up and shut-down experiments.

B.2.1 Stripping Column

The stripping column is comprises a number of stages (interchangeable) and a reboiler. The reboiler is provided with immersion heaters, which provide the energy to heat up the column and for desorption. The feed enters the column from the middle stage through the feed port, which is connected to the feed storage tank via a series of pipes and a pump.
The flow rate of the sorbent is controlled by altering the speed of the pump and fine tuning is achieved using a needle valve.The lean sorbent is collected in a separate lean storage tank.
The vapour leaving the top of the column enters the condenser, and is cooled with the aid of ice water. The entire setup is insulated with 1 inch thick glass wool to minimize the heat losses.

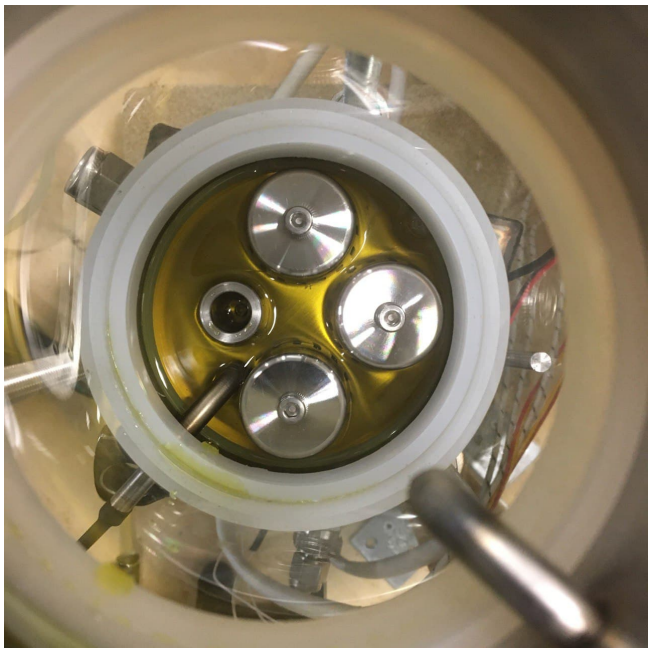

Figure B.3: Top view of a stage filled with the sorbent. The stainless steel objects are the bubble cap trays viewed from above.

Each stage in the stripping column is provided with a sampling port. The latter is used to collect liquid and vapour samples from each stage. Each stage also has a thermowell, that allows temperature measurements at the location using an NTC sensor. Bubble cap tray arrangement (Figure B.3) is used to improve mass transfer. It allows vapour from the bottom stage to bubble up through the liquid via the cavities in the bubble caps.

B.3 Measuring energy consumption of the desorption column

- The system's power demand is recorded with the help of a multi-meter that measures the current and voltage across the electrical load components in the setup, i.e., the immersion heaters and the pumps.
- The power consumed is then obtained as the product of the current and voltage.

$$Power = V \times I \ (Watts) \tag{B.1}$$

- The energy consumption is evaluated as the product of the average power and the time interval between two measurements. Since the power to the heaters has only minor fluctuations, +/- 5 Watts, the work assumes the power input to be constant throughout the experiment.

$$Electrical\,energy = P \times \Delta t \ (kJ) \tag{B.2}$$

  Once the system has operated in a steady state for a sufficient amount of time, the immersion heaters are switched off and shut down is initiated.

B.4 VLE Sample Analysis

Fourier-transform infrared spectroscopy (FTIR) is used to analyse the samples collected during the kinetics experiment. With the aid of FTIR it is possible to analyse the concentration of TEPA, PEG200, H_2O & CO_2 in the quaternary mixture. Via this method infrared radiation interacts with

the molecule. Certain wavelengths of the radiation are absorbed by the molecule, and the chemical bonds begin to vibrate. The result of an FTIR is an infrared spectrum, which is a plot of the intensity of the radiation against the wavenumber of the light.
The position of the peaks, the intensities and the width corresponds to the nature or type of chemical bonds present inside the molecule. An Agilent Cary 630 FTIR (Figure B.4) is used to analyse the samples collected in this work.

Figure B.4: FTIR setup being used at ZEF, to analyse the composition of loaded sorbent.

The spectrum from the FTIR is processed and analysed using a software tool - TQ Analyst. The tool has been calibrated using samples of known concentration and their spectra, and thus can be used as a tool to accurately estimate the compositions of samples of unknown concentrations and spectra.

Appendix C

Appendix C: Modelling Approach

C.1 Space-Time Yield CO_2

Based on the experimental data, a space-time yield curve for carbon dioxide was developed as shown in Figure C.1. The curve takes into account the current CO_2 loading of the sorbent, the loading at VLE. The driving force, i.e. the concentration of CO_2 in the atmosphere, is accounted for in the curve. The CO_2 concentration is assumed to be constant at 410 ppm. This assumption holds good considering the concentration of CO_2 remains unchanged over the time scales this thesis is concerned with. But a provision for different CO_2 concentrations has been included in the curve, which normalises the curve about the new concentration and delivers appropriate results.

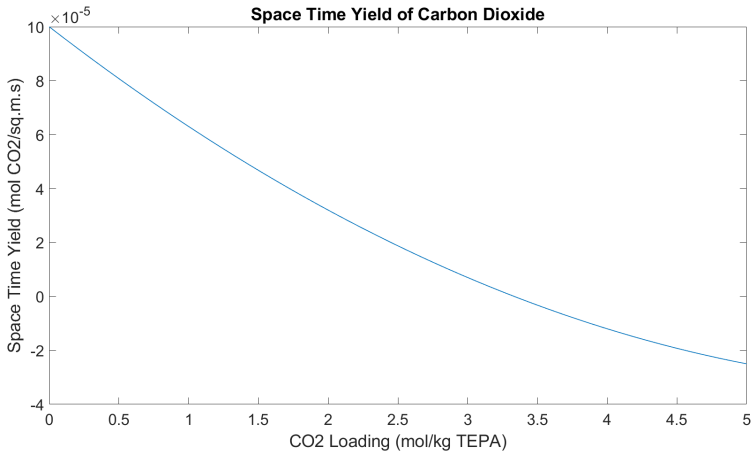

Figure C.1: The space time yield curves for CO_2

C.2 Space-Time Yield H_2O

Similar to the space-time yield curve for CO_2, the STY data for water is based on experimental data as shown in Figure C.2. It takes into account the current loading of water in the sorbent, and the loading at VLE. Unlike CO_2, the driving force for absorption, i.e. the concentration of water in the air (absolute humidity) varies significantly over the concerned time scales. Thus an accurate representation of the space-time yield of water is represented by a three dimensional surface. This takes into account the varying levels of water in the atmosphere depending on the time of day or year, and geographic location.

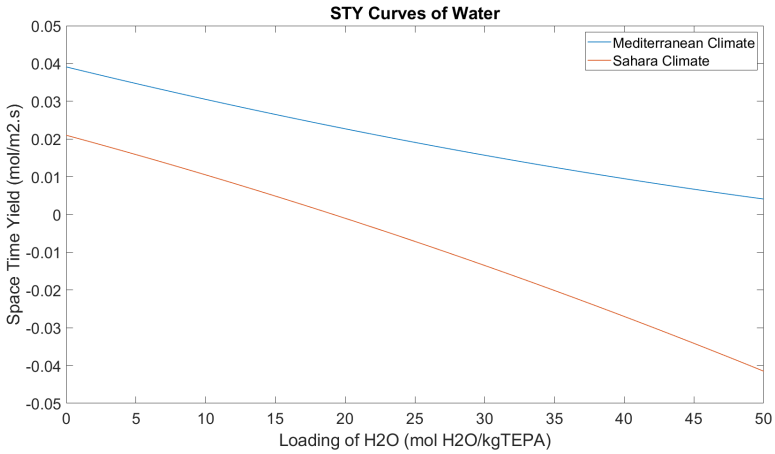

Figure C.2: The space time yield curves for water

Figure C.2 is based on experimental data for two different climatic conditions or values of absolute humidity. Naturally, the latter changes depending on the time and place, and thus the VLE loading of the sorbent is also expected to shift accordingly. Therefore, for the intermediate values of VLE loadings, interpolation is carried out to yield a 3 dimensional surface as shown in Figure C.3. The absorber model utilises this surface plot to identify the space time yield at every time step. The procedure is as follows :

- The absolute humidity is used to evaluate the equilibrium water loading of the sorbent using the following polynomial equation:

$$Loading_{VLE} = (171327 \times Absolute\,humidity^2) + (526.86 \times Absolute\,humidity) - 3e - 14 \quad \text{(C.1)}$$

- The VLE loading from Equation C.1, and the current water loading of the sorbent are used to calculate the space time yield of water with the polynomial equation that represents Figure C.3
- Following which the new water loading of the sorbent is updated and the process continues.

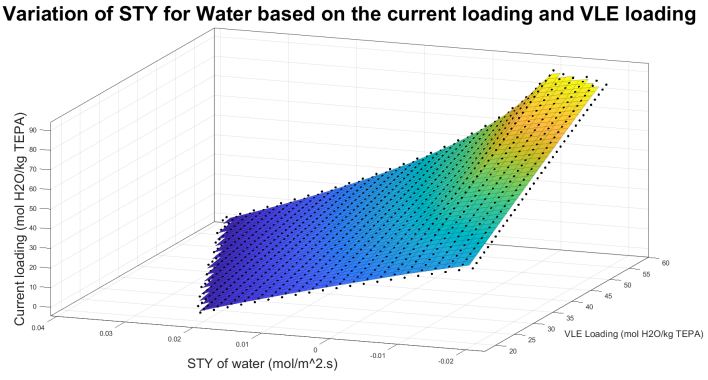

Figure C.3: The space time yield surface for water for different values of VLE loading of the sorbent. Applicable for a wide range of absolute humidity fluctuations.

From the space-time yield functions, it is possible to have negative yields. This is physically possible when external conditions such as absolute humidity change, which causes a shift in the VLE loadings, forcing a certain amount of CO_2 or water to be desorbed spontaneously in the absorber until a new equilibrium is established.

Appendix D

Appendix D: Additional Results

D.0.1 PV Panel

The photocurrent generated by the panel is proportional to the incident solar radiation on a PV cell. The relationship between the panel temperature and the potential difference across the cell is inverse. Semi-conductor devices usually have a negative temperature coefficient, considering the potential difference is developed based on the difference in energy levels of electrons in the ground state vs the excited state. Thus, at higher panel temperatures, the band-gap reduces, causing a lower potential difference to develop across the cell's terminals. Therefore, maximising the power output from a PV panel requires sunny and cool conditions.

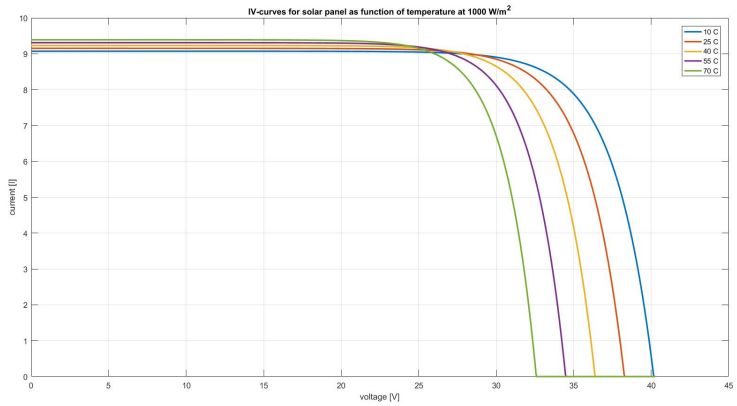

Figure D.1: Variation of I-V characteristics curves of a PV panel with variations in temperature

Within DAC, there are different electrical loads or energy consumers.

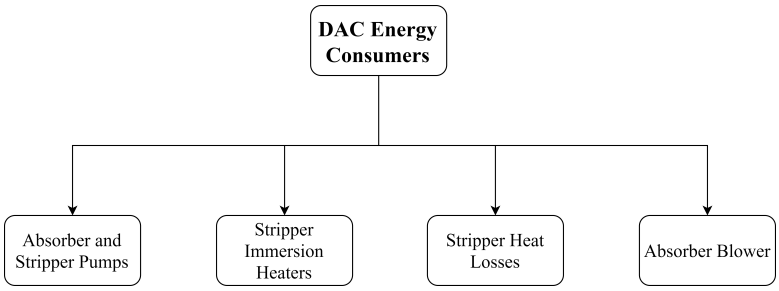

Figure D.2: Schematic representation of DAC components that consume energy

The largest fraction of the energy consumed by the immersion heaters inside the desorption column is required to heat the sorbent to very high temperatures. The auxiliary components such as the absorber stripper pumps and the absorber blower are crucial in circulating the sorbent and air. Thus, it is imperative to quantify the amount of energy consumed by these components.

D.0.2 Evaluating the Pump Power

The total dynamic head is calculated using the following equation, which considers the static head and the frictional losses. The latter is dealt with using the Darcy Weisbach equation.

$$Total\,Head = Static\,Head \; + \; Frictional\,Head \tag{D.1}$$

$$Total\,Head = \rho g H \; + \; \frac{128 H \mu Q}{\pi d^4} \tag{D.2}$$

The pumping power is then calculated using :

$$Pumping\,power = Total\,Head \times Q \tag{D.3}$$

These calculations assume the maximum viscosity for the loaded sorbent achieved in air farm experiments. The viscosity of the sorbent is dependent on the CO_2 and H_2O concentrations. Since these vary across different times scale, the viscosity of the sorbent can also fluctuate quite a bit. Naturally, this has an impact on the pumping power. Moreover, the mass flow rate of fluid being pumped also affects the pumping power. For this design the recycle flow rate has been kept constant, but the effect of increasing mass flow rate and varying viscosity is depicted in the figure below:

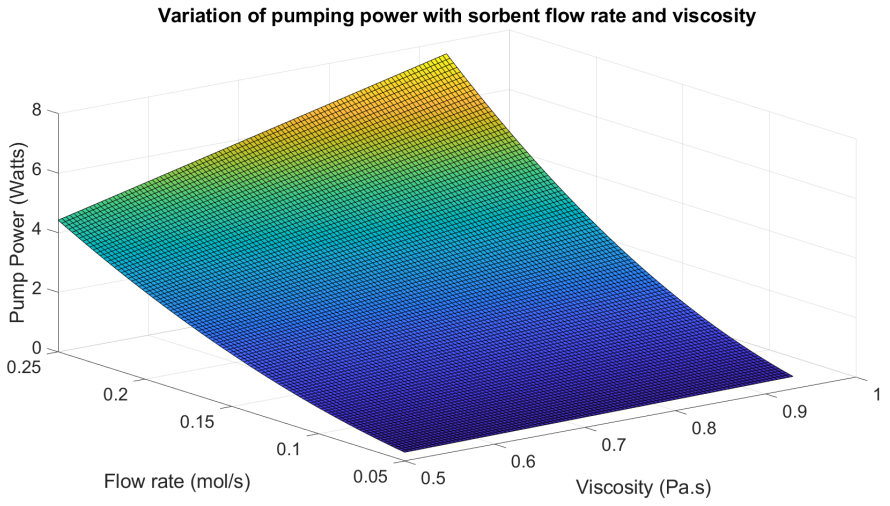

Figure D.3: Variation of pumping power as a function of sorbent mass flow rate and viscosity

D.0.3 Desorption Column: Heat Losses

Another cause of concern is the heat loss from the desorption column to the surroundings. These losses need to be overcome to maintain the temperature inside the desorption column, it also gives insights into the minimum condition for starting up and thus shutting down the column, which will be elaborated upon in later sections.

A simple analysis of the heat losses from the column is carried out. The assumptions of the model are listed below:

- The stripper and its contents are assumed to be at the same temperature, i.e. a lumped system.
- The column is modelled as a vertical cylinder covered in Rockwool insulation.
- The heat losses are assumed to be constant, although not entirely true, since during start-up and shut down, and the losses will be lower due to lower column temperatures. Still, the analysis aims to obtain the upper limits of losses possible while the column is operating in a steady state.

The design parameters used for evaluating the stripper heat losses are indicated in the table below:

Table D.1: Dimensions and related parameters of a typical desorption column based on the miniature plant at ZEF, for analysing the stripper heat losses.

Parameters	**Value**
Column height	0.4 m
Column diameter	0.05 m
Column temperature	120 Celsius
Ambient temperature	30 Celsius
Prandtl number (Air @ 30C)	0.72
Thermal conductivity	0.02 W/mk
Kinematic viscosity	1.749e-5 m2/s
Thermal conductivity (Rockwool)	0.035 W/mK
Heat Losses	15 Watts

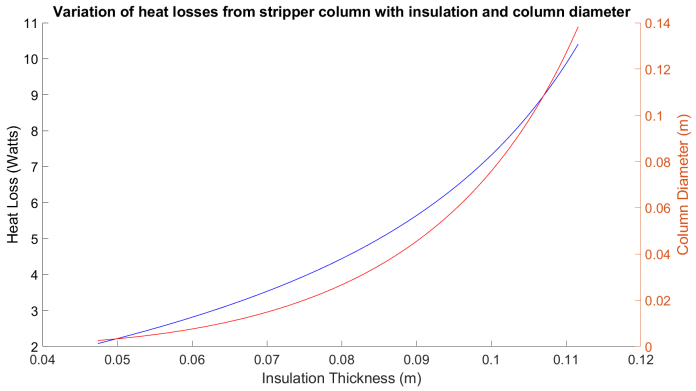

Figure D.4: Stripper heat losses as a function of the insulation thickness

insulation can minimise the stripper losses to the order of 10-15 W. To simplify the implementation of the integrated DAC model, the power input into the system is taken to be :

$$Model\ Power\ Input = PV\ Panel\ output - Stripper\ heat\ loss - pumping\ power \tag{D.4}$$

D.1 Experiment Phases:Start-up

- **Phase 1 (Start-up):** From t=0 to the time the temperatures in the desorption column reach a steady-state or stabilise is the time to start-up. The reboiler and its contents are heated via immersion heaters. The stages above the reboiler are heated by hot vapour rising from the sorbent present in the reboiler. Since the evolution of vapour is possible only after the reboiler crosses a threshold temperature, there is an initial delay in heating the stages above the reboiler. Once all the temperatures have stabilised, the column is hot enough to initiate the feed. A minimal amount of water and CO_2 is evolved during this phase.
- **Phase 2:** The mass flow is initiated, usually of the order of 0.1 to 0.05 g/s. There is an initial dip in the temperatures inside the reboiler. The temperature dip is due to the cold feed entering the system. Since the power is constant, it can only provide a fixed amount of enthalpy into the column. After a certain amount of time, a steady state is reached again, and the system begins to produce CO_2 and H_2O.
- **Phase 3:** Steady-state, continuous operation of the system. Steady puffs of CO_2 and condensed H_2O is collected during this part of the operation. Once the feed sorbent tank is almost depleted, the shut-down process is initiated.
- **Phase 4:** During shut-down, there isn't any evolution of CO_2 or H_2O. The temperatures in the system start to decline due to heat losses to the surroundings gradually. The pressure begins to dip since water in the vapour phase starts to condense and is reabsorbed in the sorbent.

D.2 Energy & Time fractions

- **Energy fraction:** Ratio of the energy required to start up the column to the total energy available per day.

$$Energy\,fraction = \frac{Energy\,consumed\,during\,Start-up}{Total\,energy\,available} \tag{D.5}$$

- **Time fraction:** Ratio of the time required to start up the column to the total time* available per day.

$$Time\,fraction = \frac{Time\,consumed\,during\,Start-up}{Total\,time\,available} \tag{D.6}$$

Note: The total time available refers to the average amount of time the PV panel produces power, corresponding to the average daylight hours available.

D.3 DAC System Engineering

D.3.1 Mass-flow control

Figure D.5 depicts the production of Carbon dioxide and water, while comparing the performance of the single loop mass control against the parallel control loop.

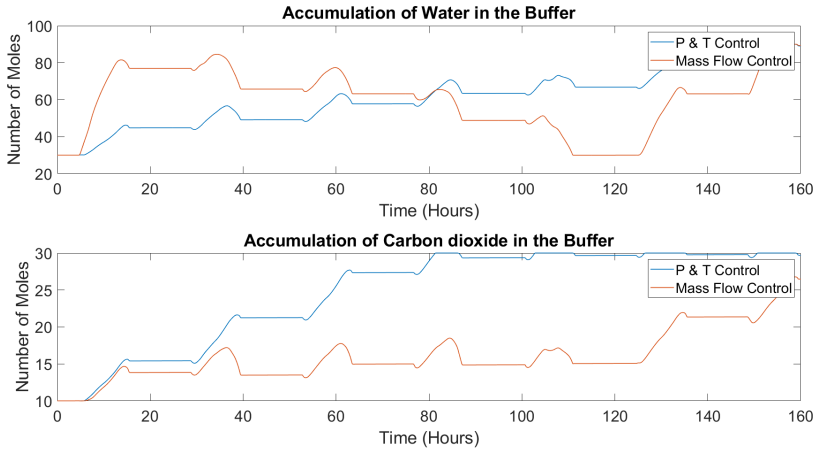

Figure D.6: Comparing the effect of single loop mass flow control against parallel control on the accumulation of H_2O & CO_2.Simulation carried out for the month of March, 2016 in Bechar, Algeria (Sahara Climate).

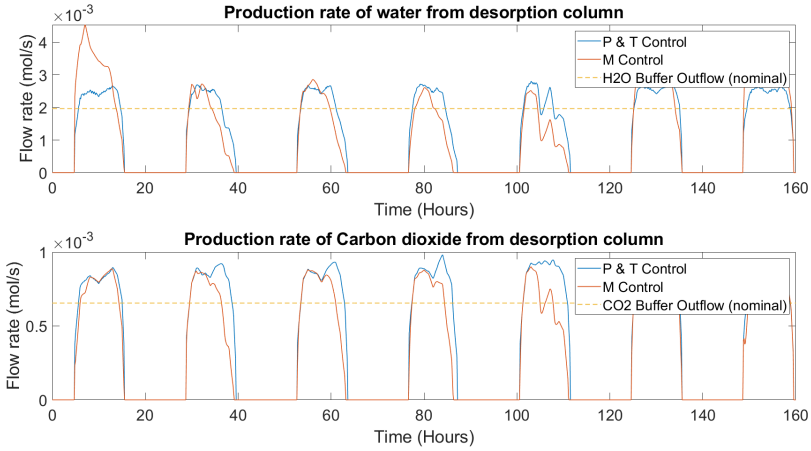

Figure D.5: Comparing the effect of single loop mass flow control against parallel control on the CO_2 & H_2O production. Simulation carried out for the month of March, 2016 in Bechar, Algeria (Sahara Climate).

Figure D.6 depicts the accumulation of Carbon dioxide and water, while comparing the performance of the single loop mass flow control against the parallel control loop.

D.3.2 Mass-flow & Temperature Control

Figure D.7 depicts the production of Carbon dioxide and water, while comparing the performance of the cascade control loop against the parallel control loop.

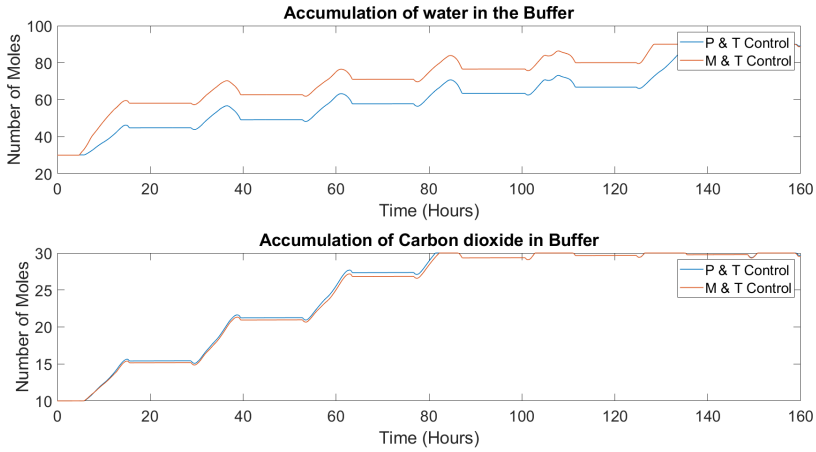

Figure D.8: Comparing the effect of cascade control against parallel control on the accumulation of H_2O & CO_2.Simulation carried out for the month of March, 2016 in Bechar, Algeria (Sahara Climate).

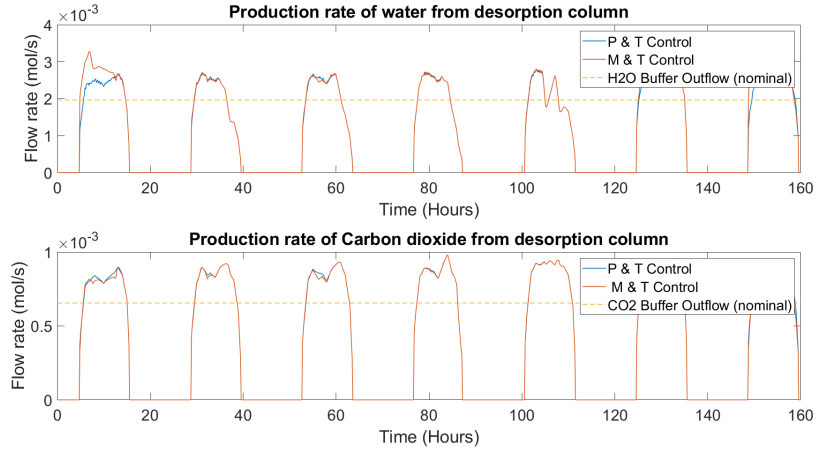

Figure D.7: Comparing the effect of cascade control against parallel control on the CO_2 & H_2O production. Simulation carried out for the month of March, 2016 in Bechar, Algeria (Sahara Climate).

Figure D.8 depicts the accumulation of Carbon dioxide and water, while comparing the performance of the cascade control loop against the parallel control loop.

D.3.3 Pressure Control

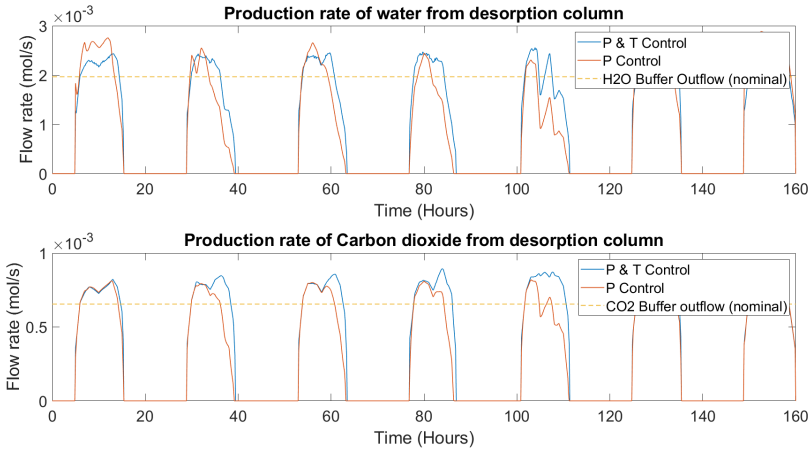

Figure D.9: Comparing the effect of single loop pressure control and the final control scheme, on the production of water and carbon dioxide.Simulation carried out for the month of March, 2016 in Bechar, Algeria (Sahara Climate).

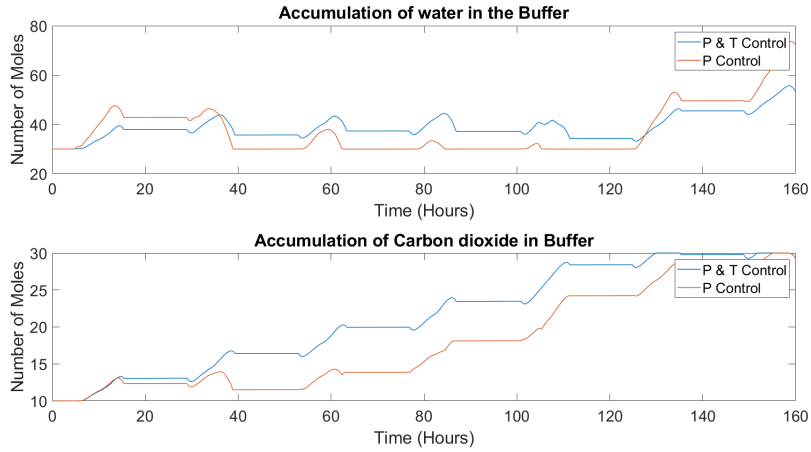

Figure D.10: Comparing the effect of single loop pressure control and the final control scheme, on the accumulation of water and carbon dioxide.Simulation carried out for the month of March, 2016 in Bechar, Algeria (Sahara Climate).

D.4 Battery Case

The battery case represents using a constant power source to drive the entire process of desorption. Figure D.11 and Figure D.12 indicate the performance of the desorption column in terms of accumulation of the products and the top ratio achieved.

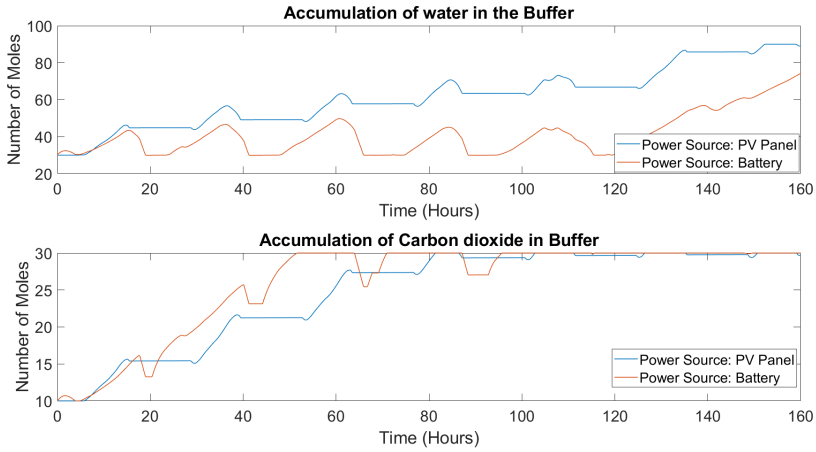

Figure D.11: Comparing the effect of using a PV panel against a constant power source such as a battery on the CO_2 & H_2O accumulation. Simulation carried out for the month of March, 2016 in Bechar, Algeria (Sahara Climate).

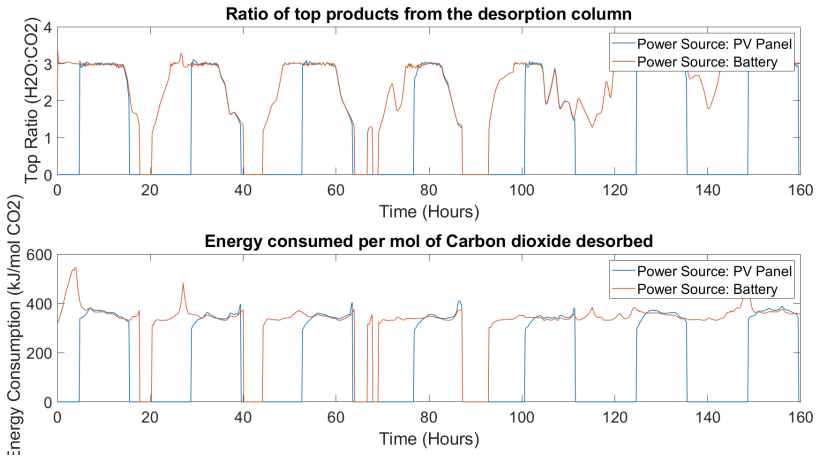

Figure D.12: Comparing the effect of using a PV panel against a constant power source such as a battery on the top ratio of products from the desortpion column. Simulation carried out for the month of March, 2016 in Bechar, Algeria (Sahara Climate).

It is observed that due to the wider operation window, the system powered with the battery accumulates a large excess of the products in a short period of time. This indicates, that the process can perhaps be driven by a batter of lower power rating to meet the nominal demand of the systems downstream.

D.5 Kinetics

D.5.1 Kinetics: Effect of Nucleation Sites

With an increase in the nucleation sites, bubbles will form with greater ease at lower temperatures, thus promoting mass transfer.

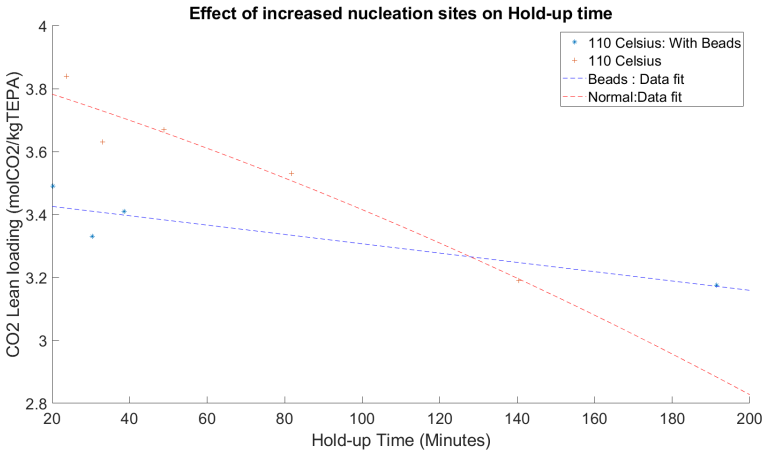

Figure D.13: Effect of nucleation sites in the reboiler on hold-up times

It is clear that with an increase in the nucleation sites, lower lean loadings are possible for the same temperature. This adds weight to the initial indication from existing research that the desorption of CO_2 is diffusion-limited. In this case, if the process were kinetically limited, the sorbent loading would have been unaffected by the presence of additional nucleation sites.
However, more research in this field is needed for conclusive results.

D.5.2 Kinetics: Effect of liquid hold-up

Lowering the liquid hold-up allows for better mass transfer, since the diffusion length is reduced. Naturally, we can expect lower lean loadings for the same hold up times and temperatures as seen in Figure D.14

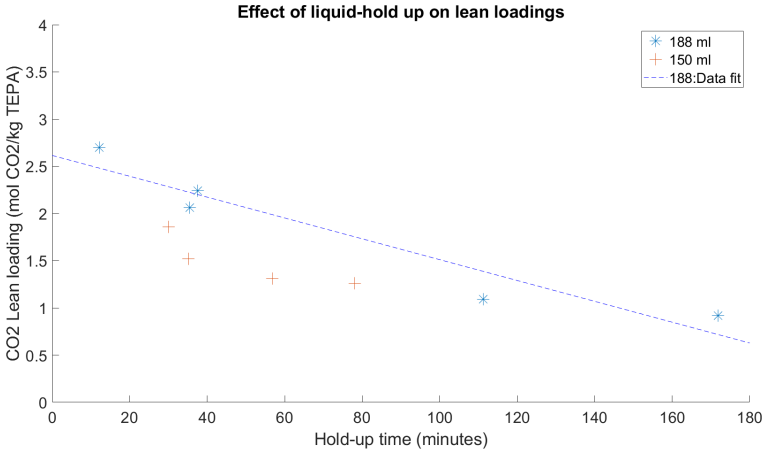

Figure D.14: Effect of liquid hold-up on the lean loadings.

Thus, one way to reduce the effective diffusion length and thereby improve the mass transfer characteristics is to:

- Add nucleation sites. Smaller the dimensions of the sites, sharper are the contact angles allowing the bubbles to detach from the surface with greater ease. This can be done by embedding micro-nano-sized particles on the inner surface of the reboiler to provide a rough surface finish.
- Decreasing the liquid hold up itself, lowering the height of the liquid column inside the reboiler reduces the diffusion length drastically. This will lead to better mass transfer and thus leaner

loadings for the exiting sorbent.

References

[1] P. Friedlingstein, M. Jones, M. O'sullivan, R. Andrew, J. Hauck, G. Peters, W. Peters, J. Pongratz, S. Sitch, C. Le Quéré, *et al.*, "Global carbon budget 2019," *Earth System Science Data*, vol. 11, no. 4, pp. 1783–1838, 2019.

[2] O. Gaffney and W. Steffen, "The anthropocene equation," *The Anthropocene Review*, vol. 4, no. 1, pp. 53–61, 2017.

[3] R. Lindsey, "Climate change: Atmospheric carbon dioxide," *National Oceanic and Atmospheric Administration: Copenhagen, Denmark*, 2020.

[4] J. Blunden and D. Arndt, "State of the climate in 2019," *Bulletin of the American Meteorological Society*, vol. 101, no. 8, S1–S429, 2020.

[5] C. A. Tracker, *Climate crisis demands more government action as emissions rise*, 2019.

[6] N. Saji and T. Yamagata, "Possible impacts of indian ocean dipole mode events on global climate," *Climate Research*, vol. 25, no. 2, pp. 151–169, 2003.

[7] P. Christoff, "The promissory note: Cop 21 and the paris climate agreement," *Environmental Politics*, vol. 25, no. 5, pp. 765–787, 2016.

[8] R. K. Pachauri, M. R. Allen, V. R. Barros, J. Broome, W. Cramer, R. Christ, J. A. Church, L. Clarke, Q. Dahe, P. Dasgupta, *et al.*, *Climate change 2014: synthesis report. Contribution of Working Groups I, II and III to the fifth assessment report of the Intergovernmental Panel on Climate Change*. Ipcc, 2014.

[9] I. R. E. A. (IRENA), *Global energy transformation. the remap transition pathway (background report to 2019 edition)*, 2019.

[10] F. Dalena, A. Senatore, A. Marino, A. Gordano, M. Basile, and A. Basile, "Methanol production and applications: An overview," in *Methanol*, Elsevier, 2018, pp. 3–28.

[11] K. Shah, A. Pan, V. Gandhi, and P. Chiang, "Photo-electrochemical reduction of co2 to solar fuel: A review," in *Photocatalytic Nanomaterials for Environmental Applications*, vol. 27, Materials Research Foundations. Materials Research Forum LLC, 2018, pp. 211–235.

[12] A. Irabien, M. Alvarez-Guerra, J. Albo, and A. Dominguez-Ramos, "Electrochemical conversion of co2 to value-added products," in *Electrochemical Water and Wastewater Treatment*, Elsevier, 2018, pp. 29–59.

[13] S. S. Araya, V. Liso, X. Cui, N. Li, J. Zhu, S. L. Sahlin, S. H. Jensen, M. P. Nielsen, and S. K. Kær, "A review of the methanol economy: The fuel cell route," *Energies*, vol. 13, no. 3, p. 596, 2020.

[14] E. I. Koytsoumpa, C. Bergins, and E. Kakaras, "The co2 economy: Review of co2 capture and reuse technologies," *The Journal of Supercritical Fluids*, vol. 132, pp. 3–16, 2018.

[15] M. M. Roggenkamp, "Re-using (nearly) depleted oil and gas fields in the north sea for co2 storage: Seizing or missing a window of opportunity?" In *The Law of the Seabed*, Brill Nijhoff, 2020, pp. 454–480.

[16] G. P. Hammond and J. Spargo, "The prospects for coal-fired power plants with carbon capture and storage: A uk perspective," *Energy Conversion and Management*, vol. 86, pp. 476–489, 2014.

[17] C. Madeddu, M. Errico, and R. Baratti, *CO2 Capture by Reactive Absorption-Stripping: Modeling, Analysis and Design*. Springer, 2018.

[18] C. A. T. Force. (). "What is post combustion capture," [Online]. Available: https://www.fossiltransition.org/pages/post_combustion_capture_/128.php.
[19] S.-i. Nakao, K. Yogo, K. Goto, T. Kai, and H. Yamada, *Advanced CO2 Capture Technologies: Absorption, Adsorption, and Membrane Separation Methods*. Springer, 2019.
[20] J. D. Seader, E. J. Henley, and D. K. Roper, *Separation process principles*. Wiley New York, 1998, vol. 25.
[21] H. Ritchie, *Food production is responsible for one-quarter of the world's greenhouse gas emissions—our world in data*, 2019.
[22] A. Kumar, D. G. Madden, M. Lusi, K.-J. Chen, E. A. Daniels, T. Curtin, J. J. Perry IV, and M. J. Zaworotko, "Direct air capture of co2 by physisorbent materials," *Angewandte Chemie International Edition*, vol. 54, no. 48, pp. 14 372–14 377, 2015.
[23] G. Puxty and M. Maeder, "The fundamentals of post-combustion capture," in *Absorption-based Post-combustion Capture of Carbon Dioxide*, Elsevier, 2016, pp. 13–33.
[24] P. Danckwerts, "The reaction of co2 with ethanolamines," *Chemical Engineering Science*, vol. 34, no. 4, pp. 443–446, 1979.
[25] R. Dowling, "An experimental and computational study of co2 absorption in aqueous solutions of tetraethylenepentamine," 2020.
[26] D. W. Keith, G. Holmes, D. S. Angelo, and K. Heidel, "A process for capturing co2 from the atmosphere," *Joule*, vol. 2, no. 8, pp. 1573–1594, 2018.
[27] M. Sinha, "Direct air capture: Characterization and design of a novel absorption process," 2019.
[28] P. Muchan, J. Narku-Tetteh, C. Saiwan, R. Idem, and T. Supap, "Effect of number of amine groups in aqueous polyamine solution on carbon dioxide (co2) capture activities," *Separation and Purification Technology*, vol. 184, pp. 128–134, 2017.
[29] V. Tyagi, *Essential Chemistry Xii*. Ratna Sagar, 2009.
[30] N. MacDowell, N. Florin, A. Buchard, J. Hallett, A. Galindo, G. Jackson, C. S. Adjiman, C. K. Williams, N. Shah, and P. Fennell, "An overview of co 2 capture technologies," *Energy & Environmental Science*, vol. 3, no. 11, pp. 1645–1669, 2010.
[31] N. El Hadri, D. V. Quang, E. L. Goetheer, and M. R. A. Zahra, "Aqueous amine solution characterization for post-combustion co2 capture process," *Applied Energy*, vol. 185, pp. 1433–1449, 2017.
[32] R. Littel, W. P. M. Van Swaaij, and G. Versteeg, "Kinetics of carbon dioxide with tertiary amines in aqueous solution," *AIChE journal*, vol. 36, no. 11, pp. 1633–1640, 1990.
[33] B. Zhang, A. Bogush, J. Wei, T. Zhang, J. Hu, F. Li, and Q. Yu, "Reversible carbon dioxide capture at high temperatures by tetraethylenepentamine acetic acid and polyethylene glycol mixtures with high capacity and low viscosity," *Energy & Fuels*, vol. 31, no. 4, pp. 4237–4244, 2017.
[34] O. Aschenbrenner and P. Styring, "Comparative study of solvent properties for carbon dioxide absorption," *Energy & Environmental Science*, vol. 3, no. 8, pp. 1106–1113, 2010.
[35] M. J. Moran, H. N. Shapiro, D. D. Boettner, and M. B. Bailey, *Fundamentals of engineering thermodynamics*. John Wiley & Sons, 2010.
[36] T. E. Marlin, "Process control," *Chemical Engineering Series, McGraw-Hill International Editions: New York*, 1995.
[37] N. van de Poll, "Characterization and design of a stripper for a continuous direct air capture system," 2021.
[38] K. M. Jamie Calvert, "Start-up and shut-down times of power ccus facilities," 2020.
[39] E. Kenig, R. Schneider, and A. Górak, "Reactive absorption: Optimal process design via optimal modelling," *Chemical engineering science*, vol. 56, no. 2, pp. 343–350, 2001.
[40] A. De Matteis, "Continuous direct air capture, understanding mass transfer in reactive absorption of carbon dioxide: Experimenting and modelling a novel dac absorption process," 2020.
[41] G. Mulder, "Characterization, optimization and design of the sorbent system for a continuous direct air capture system," 2021.

[42] A. Aggarwal, *Wunderground: Weather data*, https://www.wunderground.com/history, 2021.
[43] R. P. Lively and M. J. Realff, "On thermodynamic separation efficiency: Adsorption processes," *AIChE Journal*, vol. 62, no. 10, pp. 3699–3705, 2016.
[44] E. S. Sanz-Pérez, C. R. Murdock, S. A. Didas, and C. W. Jones, "Direct capture of co2 from ambient air," *Chemical reviews*, vol. 116, no. 19, pp. 11 840–11 876, 2016.
[45] B. Ovaa, "Desorption of CO2 and H2O out of amines," Ph.D. dissertation, TU Delft, 2019.
[46] J. Oexmann and A. Kather, "Minimising the regeneration heat duty of post-combustion co2 capture by wet chemical absorption: The misguided focus on low heat of absorption solvents," *International Journal of Greenhouse Gas Control*, vol. 4, no. 1, pp. 36–43, 2010.
[47] K. Goto, S. Kodama, T. Higashii, and H. Kitamura, "Evaluation of amine-based solvent for post-combustion capture of carbon dioxide," *Journal of Chemical Engineering of Japan*, vol. 47, no. 8, pp. 663–665, 2014.
[48] G. T. Rochelle, "Thermal degradation of amines for co2 capture," *Current Opinion in Chemical Engineering*, vol. 1, no. 2, pp. 183–190, 2012.
[49] M. J. Lockett, "Distillation tray fundamentals," 1986.
[50] W. Zhang, H. Liu, Y. Sun, J. Cakstins, C. Sun, and C. E. Snape, "Parametric study on the regeneration heat requirement of an amine-based solid adsorbent process for post-combustion carbon capture," *Applied energy*, vol. 168, pp. 394–405, 2016.
[51] H. Kierzkowska-Pawlak, "Carbon dioxide removal from flue gases by absorption/desorption in aqueous diethanolamine solutions," *Journal of the Air & Waste Management Association*, vol. 60, no. 8, pp. 925–931, 2010.
[52] H. S. Fogler, *Essentials of Chemical Reaction Engineering: Essenti Chemica Reactio Engi*. Pearson Education, 2010.
[53] R. Hołyst and A. Poniewierski, *Thermodynamics for chemists, physicists and engineers*. Springer Science & Business Media, 2012.

Technische Universiteit Delft

Z E F

Zero Emission Fuels